UNIVERSIDAD AUTÓNOMA DE MADRID

DOCTORAL THESIS

How genetic, social, and evolutionary interactions shape the many levels of biological complexity

Author:
Clara Beatriz MORENO FENOLL , Licenciada en Bioquímica

Supervisor:
Dr. Juan F. POYATOS

Programa de Doctorado en Biociencias Moleculares
Departamento de Biología Molecular

Logic of Genomic Systems Lab, Centro Nacional de Biotecnología
CNB-CSIC, Madrid

September 2017, Madrid

Certificate of Supervision

I, Dr. Juan F. POYATOS, certify that this thesis entitled "How genetic, social, and evolutionary interactions shape the many levels of biological complexity" and the work presented in it were done under my supervision.

Date:

_____

Acknowledgements

To my thesis advisor Juan F. Poyatos. To my colleagues in the Logic of Genomic Systems Lab and co-authors in the scientific publications produced in this thesis Dr. Djordje Bajić and Dr. Matteo Cavaliere. To the rest of my colleagues in the LoGS Lab. To the La Caixa Foundation for providing my funding. To Dr. Esteban Martínez-García from the Molecular Environmental Microbiology Laboratory (CNB-CSIC), co-author of one of the publications produced in this thesis. To Dr. Paul B. Rainey for hosting the research stay that produced some of the results presented in the second chapter of this thesis and the rest of the Laboratoire de Génetique de l'Evolution at ESPCI , especially to Dr. Maxime Ardré. To the UAM Erasmus program for providing the opportunity to visit Dr. Rainey's Lab. To Dr. Álex Couce for his contribution to the third chapter of this thesis. To my external reviewers Dr. Alberto Pascual García and Dr. Maxime Ardré. To the Spanish National Biotechnology Centre, its services and the Systems Biology Department. To my academic tutor Dr. Miguel A. Rodríguez Gabriel. To the Universidad Autónoma de Madrid and the doctoral program in Molecular Biosciences.

Resumen

Las interacciones entre genes, entre individuos sociales, y entre los resultados de historias evolutivas alternativas reflejan la organización y propiedades dependientes del contexto de cada respectivo nivel de complejidad biológica. Las interacciones genéticas modifican el efecto combinado de dos genes sobre las características de un organismo. Las interacciones sociales aparecen cuando algunos individuos de una población contribuyen a mantener un recurso común incurriendo en un coste personal. Las interacciones evolutivas ocurren cuando la adaptación a un ambiente particular altera la supervivencia de un organismo en otras condiciones diferentes. Estudiamos estos tres tipos de interacciones con una combinación de aproximaciones computacionales y experimentales en microbios. En **primer** lugar, evaluamos la estabilidad de las interacciones entre genes metabólicos bajo cambios en el fondo genético. Comparamos las redes de interacción genética de un modelo *in silico* de *Saccharomyces cereivisae* en dos tipos de contextos genéticos: deleciones simples y acumulación de mutationes neutrales. El reordenamiento de las redes genéticas se debe mayoritariamente a los genes catabólicos, revelando que pueden contribuir al crecimiento de un organismo en diferentes configuraciones de modo que se amortiguan las perturbaciones genéticas. Tras las deleciones neutrales se redujeron notablemente tanto esta capacidad de amortiguamiento genético como la capacidad del organismo de crecer utilizando fuentes de nutrientes alternativas, conectando la robustez genómica y ambiental. En **segundo** lugar, observamos la sostenibilidad de una comunidad microbiana en la que una interacción social de tipo cooperativo es esencial para su supervivencia. Individuos que no cooperan suelen aparecer y explotar a los cooperadores, poniendo en peligro este efecto colectivo. Utilizando una interacción social sintética construida con dos cepas de *Escherichia coli*, demostramos cómo *feedbacks* entre dinámicas poblacionales y evolutivas, combinadas con distribución espacial, pueden crear un contexto en el que la invasión de no cooperadores, contraintuitivamente, preserva el comportamiento social. Además, analizamos cómo la implementación molecular de una interacción social puede modificar estas dinámicas, tanto en el sistema sintético en *E. coli* como en un sistema natural, la producción de una molécula captadora de hierro por la bacteria *Pseudomonas fluorescens*. En **tercer** lugar, examinamos cómo de predecible es el efecto de la historia previa de un organismo sobre su reacción ante un ambiente nuevo. Contrastamos las redes interacción evolutiva generadas tras la adaptación de una cepa de laboratorio de *E. coli* a antibióticos de diferentes clases. La adquisición de resistencia a la misma droga puede, no obstante, resultar en diferentes respuestas a otro compuesto alternativo, incluyendo efectos opuestos en la supervivencia de la bacteria. Discutimos cómo la combinación de la arquitectura genómica y la contingencia histórica puede producir estos resultados tan variables.

Universidad Autónoma de Madrid

How genetic, social, and evolutionary interactions shape the many levels of biological complexity

by Clara Beatriz MORENO FENOLL

Abstract

Interactions between genes, between social individuals, and between the results of alternative evolutionary histories reflect the organization and context-dependent properties of each respective level of biological complexity. Genetic interactions modify the combined effect of two genes on the characteristics of an organism. Social interactions develop when some individuals of a population contribute to a common resource at a personal cost. Evolutionary interactions result when adaptation to a particular environment changes survival in unrelated conditions. We studied these three types of interactions with a combination of computational and experimental approaches using microbes. **First**, we evaluate the stability of interactions between metabolic genes upon changes in the genetic background. We compared the genetic interaction networks of an *in silico* model of *Saccharomyces cerevisiae* in two types of backgrounds: single deletions and accumulation of neutral mutations. Network rewiring was strongly associated to catabolic genes, revealing that they can add to an organism's growth in different configurations thus buffering genetic perturbations. Neutral deletion backgrounds greatly reduced both this genetic buffering and the ability to grow on alternative nutrients, connecting both environmental and genomic robustness. **Second**, we tracked the sustainability of a microbial community where a social cooperative interaction is essential for survival. Non-cooperative individuals tend to appear and threaten the collective effect by exploting cooperators. Using an engineered interaction between two strains of *Escherichia coli* we show how feedback between population and evolutionary dynamics, combined with spatial structure, can create a context where invasion by non-cooperators instead preserves the social behavior. We further analyze how the molecular implementation of a social interaction can modify such dynamics, on the synthetic *E. coli* system and in the natural production of an iron-scavenging molecule by *Pseudomonas fluorescens*. **Third**, we assessed the predictability of the effect of an organism's prior history on its reaction to a novel environment. We contrasted the evolutionary interaction networks associated to the adaptation of a laboratory strain of *E. coli* to different antibiotic classes. Acquiring resistance to the same drug could nevertheless result in different responses to an alternative compound, including opposite effects on survival. We discuss how a combination of genomic architecture and historical contingency can produce these contrasting outcomes.

x

Universidad Autónoma de Madrid

How genetic, social, and evolutionary interactions shape the many levels of biological complexity

by Clara Beatriz MORENO FENOLL

Contents

List of Figures

List of Tables

List of Abbreviations

AMK	amikacin
CTX	cefotaxime
COL	colistin
DFBM	**D**istribution of **F**itness effects of **B**eneficial **M**utations
DHFR	dihydrofolate reductase
DHPS	dihydropteroate synthase
FBA	**F**lux **B**alance **A**nalysis
FOS	fosfomycin
Gm	gentamicin
HGT	**H**orizontal **G**ene **T**ransfer
IMP	imipenem
Km	Kanamycin
LTEE	**L**ong **T**erm **E**volution **E**xperiment
MIC	**M**inimum **I**nhibitory **C**oncentration
MRSA	**M**ethicillin **R**esistant ***S****taphylococcus* ***a****ureus*
NFX	norfloxacin
PBP	**P**enicillin **B**inding **P**rotein
Pvd	pyoverdin
Sp	spectinomycin
SMX	sulfamethoxazole
S-T	**S**ulfamethoxazole -**T**rimethoprim
SGA	**S**ynthetic **G**enetic **A**rray
TMP	trimethoprim

Introduction

The term "interaction" very broadly refers to the reciprocal effect that two components of a system have on each other. In this thesis we use the concept of interaction to address questions at three levels of biological complexity: genetic, social, evolutionary. We selected this framework because, while at each level the term manifests as a precise effect on particular system components, it follows the logic of bridging the specific and the systemic. Thus, it emerges as a useful approach for the holistic understanding of biological entities in their full complexity.

The contribution of a gene to an organism's phenotype often depends on the accompanying genes, a phenomenon that is termed epistasis. In one individual epistatic interactions are a tractable abstraction of the genotype-phenotype map, revealing functional dependencies and redundancies [1]. One small change — such as deletion of one gene – provides information on two crucial features of a genotype: its robustness, i.e. how the individual components interact to buffer change and maintain a functioning system; and evolvability, i.e. how these individual components equally interact in alternative functional configurations that can give rise to new capabilities[2, 3].

Variability at this subcellular level combines to produce one or more phenotypes that again interact, translated into population-level properties [4, 5]. Population features can be roughly sorted into two classes: ecological (population structure) and evolutionary (genetic frequencies and their processes of change). It is becoming increasingly evident that even these two population properties cannot be considered separately, as each influences the other sequentially (e.g. Ecology acts on evolution via natural selection) and even simultaneously[6, 7]. In one type of individual-level interaction eco-evolutionary feedbacks impact in a clear manner: the production of a public good, i.e. a social interaction [8]. In a social interaction, the emergence of non-cooperative individuals exerts an effect on both evolution — as cheaters gain a fitness advantage by exploiting the public good — and ecology —as cheater invasion can disrupt the functionality of a community and lead to its decay [9]. Thus, feedbacks between ecological and evolutionary phenomena arising from individual interactions ultimately determine the fate of a population in a particular context [10].

Evolutionary histories can in turn interact, where previous adaptation modulates fitness in novel conditions [11, 12]. Adaptation in a particular eco-evolutionary backdrop proceeds with intrinsic variability, where a crucial shaping force is genomic architecture [13–15]. In this way, evolutionary interactions – placed at the highest level of complexity – connect back to genetic interactions.

Biological entities are thus defined by a combination of processes with some degree of hierarchical organization (i.e. the different levels of complexity) but multilayered, intertwined effects. Here, in order to address specific questions of systemic importance we select three particular types of interactions: between genes, between individuals and between evolutionary trajectories.

Furthermore, this thesis rests on two methodological approaches that ease the approximation to systemic topics: high-throughput genomic and computational tools [16, 17], and the use of microorganisms as "simulators" amenable for the study of general ecological and evolutionary processes [18, 19].

In **Chapter** 1 we study **genetic interactions**. Interactions between genes occur when two genes influence their respective effects on the organism, in a reflection of their underlying functional relationships [1]. Epistasis is often measured by comparing the expected and observed phenotypes of a double mutant given the respective single mutants. The development of high-throughput techniques for the generation and characterization of gene deletions allowed the examination of epistasis between all the genes of an organism (or a relevant subset) [20]. This renewed interest in epistasis as a system-level tool for genotype-phenotype mapping [16]. The stability of this mapping is coming under interrogation, i.e. what does it mean when an epistatic interaction network changes? [21] Another technology enables examination of genetic networks under a vast array of genetic and environmental conditions: metabolic reconstructions of microorganisms, that can be manipulated *in silico* to predict growth and flow through the different reactions [22]. We used the metabolic model of the yeast *Saccharomyces cerevisiae* [23] to evaluate genetic network stability under two types of genetic backgrounds: single deletion of active enzymes, and trajectories accumulating neutral mutations. We connect epistatic interaction changes to the logic of the different functional modules and the resulting metabolic robustness.

In **Chapter** 2 we study **social interactions**. Specifically, we focus on an interaction based on an essential public good in a synthetic bacterial community. At the microbial scale, public goods are often extracellular molecules synthesized at an individual cost but that can benefit the whole community [24]. With the use of a genetic

circuit we implemented in *Escherichia coli* an interaction where the public good enables survival to an antibiotic [25]. This type of cooperative interactions have a vulnerability: cheaters that do not contribute but reap the benefits of cooperation can invade the population and disrupt the collective effect. We set a scenario where we predict that eco-evolutionary feedbacks will translate instead cheater invasions into part of a cycle that preserves cooperation [26, 27]. A combination of simulations and experiments explore this feedback. Moreover, we examine how particular features of the biological system impact on the social dynamics by appraising the interacting effect of cellular growth stage [28] and the emergence of spontaneous mutants [29]. In this same avenue, we describe a novel phenotype linked, alternatively, to a natural system with social implications: the production of siderophores (iron-scavenging molecules) in *Pseudomonas fluorescens* [30]. We examine some aspects of a previously undescribed pattern of subcellular localization of this molecule and discuss its potential ecophysiological role.

In **Chapter** 3 we study **evolutionary interactions**. Adaptation to particular environment can indirectly modify the organisms suitability for a different one, this is what we term "evolutionary interaction". Specifically, the development of bacterial resistance to an antibiotic can alter its sensitivity to a different drug [31], an effect that can be used for the rational design of treatment protocols [32]. A topic of recent interest, evolutionary interactions between antibiotics have led to discoveries with great clinical potential involving the reciprocal development of increased vulnerability after adaptation to two antibiotic classes, β-lactams and aminoglycosides [33, 34]. Nevertheless, processes concerning the repeatability of evolution can introduce variability in the development of these collateral resistances and sensitivities [35]. Size and specificity of the genomic resistance determinants [36], hierarchies among the mutations amenable to selection [37], and epistasis between evolving alleles [38] can introduce diversity in adaptive trajectories. We evaluate the variability in the evolutionary interaction networks of *E.coli* clones adapted to a set of antimicrobials comprising a variety of classes and mechanisms. We emphasize the need for detailed consideration of evolutionary interactions between antibiotics that integrates the complex role of contingency in adaptive trajectories.

The work presented in Chapter 1 and the first three sections of the *Results* in Chapter 2 is already reflected in scientific publications, which can be found in Appendix A and Appendix B, respectively. The remaining content corresponds to work in progress.

Objectives

1. Using microbes to explore interactions at genetic, social, and evolutionary levels of complexity as a tool for the systemic understanding of biological systems.
2. Evaluating the stability of genetic interactions in metabolism and what it can reveal about the organization and robustness of a genomic system.
3. Understanding the interplay of ecological and evolutionary processes as they determine the population dynamics of a social interaction based on an essential public good.
4. Analyzing the effect of constraints associated to the molecular implementation of a social interaction on these dynamics.
5. Investigating the impact of variability in adaptive trajectories on the development of interactions between antimicrobial resistance patterns.

Chapter 1

Genetic Interactions

1.1 Introduction

The development of high-throughput techniques to manipulate and analyze genomes [39, 40] and the associated bioinformatic tools to sift and understand these high volumes of data [41] allowed us to start looking at molecular information with a systemic view [16]. Cellular and subcellular levels of biological complexity are increasingly amenable to the incorporation of specific details into global properties [20, 42, 43]. An essential system-level question is the assembly of the genetic components of an organism into particular traits concerning its ability to accommodate and assimilate perturbations [44]. Thorough mapping of these ecological and evolutionary characteristics integrating molecular functions and interdependencies is now a more feasible prospect.

Epistasis as a force defining genotype-phenotype mapping

The effects of all the genes in a genotype combine in a particular environment to ultimately produce a phenotype in ways that are not necessarily linear, i.e. the simple addition of all genes. This phenomenon whereby the effect of a gene on a phenotypic trait is dependent upon other genes is generally termed "epistasis". Genes can interact in a manner that either amplifies or masks their respective effects; in this way, analyzing epistatic interactions between genes is an abstract reflection of their functional relationships in the genotype-phenotype map [1]. At the cellular level, epistasis is usually measured as the deviation of the phenotype of a double mutant from the expected phenotype given the respective single mutants (if there were no interaction between the genes) [20]. In microbial cells, the type of organism utilized throughout this Thesis, the evaluated phenotype is commonly the growth rate of the cells as a proxy for organism fitness. Then, negative epistasis occurs when the double mutant exhibits greater fitness defects than expected and frequently reveals functional redundancies between the interacting genes. On the other hand, positive

epistasis arises when double mutant fitness is greater than expected, even equivalent to that of one of the single mutants. This type of genetic interaction is usually associated to functional dependencies, such as the subunits of a multiprotein complex (the positive interaction appears because inactivating one of the genes abolishes the associated pathway, such that successive perturbations cannot do further damage). Recently developed high-throughput technologies enabled the analysis of large genetic interaction networks, based on the systematic deletion or knock-down of a vast array of the genes of an organism [20, 45]. This type of high-throughput approach identified some features of large-scale epistatic interaction networks whose aggregated information was previously unavailable, such as the role as genetic hubs of some chromatin regulation processes in *Saccharomyces cerevisiae* and the worm *Caenorhabditis elegans* [20, 46] and the balanced distribution of weak and strong interactions [47].

In silico metabolic models of microbes and Flux Balance Analysis

Despite the substantial development of experimental techniques to measure genetic interactions, this approach remains highly labor-intensive and rapid advancement requires complementation by computational methods. Genome-scale metabolic reconstructions arose as a powerful tool to predict the growth rate, and other features such as the production of compounds of interest, of microbes under varying environments and genetic perturbations. A large collection of such models is now available, for a number of both prokaryotic and eukaryotic cells (`http://systemsbiology.ucsd.edu/InSilicoOrganisms/OtherOrganisms`) These models are built from the annotations of all the enzymatic genes of an organism in multiple steps including automated methods, manual curation, and complementation with additional information such as the subcellular compartment where a particular reaction takes place [48]. They contain all the known metabolic reactions of a given cellular type adjusted stoichiometrically, and can then be manipulated with a growing array of computational approaches. Flux balance analysis (FBA) is the basis of a family of constraint-based methods that can be applied to metabolic reconstruction models [49]. Using a steady-state assumption, FBA allows the prediction of flow through the many reactions of the metabolism that maximizes a given output, such as the synthesis of a particular molecule or organism growth. Prediction of cellular fitness is achieved by incorporating into the model a biomass reaction that rests on the production of essential metabolites. Additions to this basic approach include the integration of regulatory information, minimization of flux changes after perturbation [22], enzymatic constraints [50] or a restricted allocation of resources to different parts of the metabolism [51]. FBA methods were shown early on to produce

biologically realistic results in the prediction of growth features [52]. These reconstructions allow us to evaluate system-level properties of metabolisms through their performance across a wide range of genetic perturbation events and environmental changes. Analysis of *Escherichia coli* and *S. cerevisiae* models revealed a high degree of redundancy in metabolic pathways enabling biomass production in a vast array of random environments, which is likely preserved as evolutionary byproducts due to small differences in efficiency and pleiotropic effects [53]. Implementation of gene deletions necessary to appraise genetic interactions between all the enzymes in a metabolism is also straightforward (by restricting the flux through the associated reaction to 0). This approach uncovered some basic features of genetic networks, such as frequent, monochromatic (i.e. predominantly positive or negative) interaction between metabolic functional modules using the *S. cerevisiae* model [54], a result that was verified experimentally using a large-scale synthetic genetic array (SGA) that was also used to refine the model, adding to the frequent feedback between theory and experiments in the design and validation of metabolic reconstructions [55].

How stable is the epistatic genotype-phenotype map?

Conclusions about the features of a genome using the particular mapping of epistatic interaction networks tended to be based on static pictures, that is, of networks generated in constant conditions. However, understanding the full functional range of a genotype necessitates expanded evaluation, to include its resilience to perturbations and its potential for change (its robustness and its evolvability [3]). Relatedly, studies started emphasizing that genetic interaction networks were dependent on both genetic and environmental contexts, such as on the severity of mutations and the resource-richness of an environment (in a study performed *in silico* on phages [56]); or on the presence of toxins in the environment such as DNA-damaging agents (in studies carried out in *S.cerevisiae* [57–59]). That changes in epistatic interactions have evolutionary implications can be acknowledged by their conservation – and the lack thereof – in different species; as evidenced by comparing the networks of *S. cerevisiae* to another yeast, *Schizosaccharomyces pombe* [60–63]. The effect of environmental and genetic variables on the expression of a mutational phenotype was established specifically in the case of epistatic interactions [21], which given the pivotal role of epistasis in defining evolutionary trajectories [13, 64] (see Chapter 3 for further discussion) again ties this type of functionally abstract genotype to phenotype map to important evolutionary processes [2, 44].

We ask here how the genetic interaction network of a complete genomic subset fulfilling an essential cellular role, metabolism, is rewired in response to genetic and environmental perturbations. We carefully selected two types of genetic backgrounds

that reveal distinct but connected properties of the metabolism: single deletion of active enzymes, and accumulation of a large amount mutations with neutral effect on growth. The first type of background speaks to the built-in capability of metabolism to buffer changes and maintain a viable phenotype; the second reveals how a particular type of constraining evolutionary trajectory [65] will shape these plastic capabilities. The use of *in silico* models allowed us to directly connect changes in epistatic interactions at a broad phenotypic level (the growth rate of each mutant) with underlying rearrangements of fluxes through explicitly annotated metabolic reactions, and thus arrive at functional explanations at the detailed phenotypic level.

1.2 Materials and Methods

Model and genetic network assembly

We utilized as wild type the fully compartmentalized iND750 *S. cerevisiae* model. All simulations were performed using Flux Balance Analysis implemented in the COBRA Toolbox for Matlab (https://opencobra.github.io/cobratoolbox/latest/). The wild type growth conditions are glucose minimal medium and aerobiosis, implemented by setting flow through the glucose import reaction to a realistic $18.5\,\mathrm{mmol\,g^{-1}\,h^{-1}}$ and leaving the oxygen import reaction functionally unconstrained. Deletion mutants used to assemble the genetic networks and the different types of backgrounds are generated by constraining to 0 the flux through the associated reaction. Epistasis was calculated using a multiplicative model with scaling [54] with growth rates from the relevant sets of single and double mutants of each evaluated genotype. This model assumes that the fitness effects of genes combine in a multiplicative manner, such that the growth phenotype of a double mutant can be obtained by multiplying the respective single mutant fitnesses.Scaling defines interaction values between -1 and 1, which are further classed as synthetic lethal (SL), weak negative (WN), weak positive (WP) and strong positive (SP). Epistatic interactions are classified as SL when $\epsilon = -1$ and SP when $\epsilon = 1$. WN and WP comprise the remaining negative and positive interaction values, respectively. Epistasis values below $\epsilon < |0.01|$ are discarded. To simplify functional redundancies, genes coding for subunits of an enzymatic complex are considered as one interacting node in the network (eg. The ATPase complex containing 15 subunits, adding a significant volume of positive interactions with the same functional underpinning and patterns of change).

Genetic backgrounds

Single deletion backgrounds were generated by obtaining all the reactions with nonzero flux in the wild type conditions and systematically deleting them. Neutral deletion backgrounds were created by randomly deleting one of the model genes, re-measuring fitness in the glucose medium and fixing mutations with a neutral effect on the phenotype. This process is repeated until 100 neutral mutations have accumulated, following the logic of previous studies [65].

Network rewiring and metabolic analysis

When used for analysis, fluxes through reactions were normalized by the respective biomass production to enable direct comparison between genotypes. Background

dispersion was quantified as normalized Shannon entropy S_{MP} (MP denotes "module pair"). This is defined as $S_{MP} = \sum_{i=1}^{n} k_i \log k_i / \log N$ with n being the number of backgrounds with new interactions between the two modules, and k_i the number of interactions appearing in the background i (divided by the total number of interactions considering all backgrounds). This was normalized by $\log N$, where N is the total number of analyzed backgrounds where any new interaction appears between any two modules ($N = 37$).

Random environments

1000 random environments were generated by sampling from a nutrient pool containing 107 possible organic compounds, using an exponential distribution with mean = 0.1 to assign a probability of appearing in the environment to each nutrient source [53]. For each nutrient set, concentration was again randomly defined using a uniform distribution between 0 and $20\,\mathrm{mmol\,g^{-1}\,h^{-1}}$; in all cases oxygen remained unconstrained.

Experimental confirmation

Data on instability of interactions in response to environmental change were obtained from [59]. We considered nonsignificant epistasis values below 2 and above 2.5 (following the original reference). We defined SP interactions as those in the upper quartile among positive ones and similarly for negative ones. The instability of each category was quantified as the average number of treatments where the interaction changes or disappears (out of three). We quantified the functional similarity of the genes constituting an interaction as the ratio between the number of shared functional classes (biological process annotations in the original reference) and the minimal number of classes that one of the genes of the pair presents. Pairs with score greater than 0.1 were considered functionally "close" and "distant" otherwise. We considered an interaction "stable" if it remained within the same category (sign, strength) in all conditions and unstable otherwise. We downloaded from `http://www-sequence.stanford.edu/group/yeast_deletion_project/deletions3/` a list of yeast essential genes and used the genetic interaction data of yeast metabolism from [55]. For each module, we computed the ratio between the number of essential and the number of epistatic genes that we term θ.

1.3 Results

We interrogated the stability of the epistatic interaction networks of the metabolism of the yeast *S. cerevisiae* under different genetic backgrounds using an *in silico* reconstruction. *In silico* metabolisms are built from curated, annotated genes with stoichiometric fidelity, and are able to predict growth by optimizing biomass produced by incorporating essential metabolites. To assemble the interaction network of each individual genotype, we systematically generated all possible single and double mutants of the iND750 *S. cerevisiae* model [23] and assessed their associated fitness i.e. their growth rate. This single measurement already encompasses multiple phenotypic features, that is, the flux through the many reactions of the metabolic network as they combine to produce biomass. Epistatic interactions are then computed from these growth rates using a multiplicative model and scaled to range from -1 to 1 from synthetic lethality to complete masking, following previous studies [54] (*Materials and Methods*). The epistatic network emerges as an abstract representation of the relationship between metabolic genes as they yield organism growth. We then introduce genetic and environmental perturbations (in the form of gene deletion backgrounds and availability of different nutrients) and repeat the assembly of the genetic interaction network. Contrasting changes in phenotype – growth rate and metabolic fluxes – and epistasis allows us to assign functional relationships between these two levels of complexity in the genotype-phenotype map.

Rewiring of epistatic interactions after gene deletion reflects the differential organization of metabolic functional modules

The first type of genetic backgrounds evaluated was a set of single deletion mutants of the genes that were active under the established default growing conditions (glucose minimal medium, aerobiosis)(*Materials and Methods*). This set of epistatic interaction networks was characterized by connecting the genetic change to rearrangement of metabolic fluxes; analyzing the annotation, sign and strength of the involved interactions and the directions of change. The features of network rewiring reflect some fundamental properties of the organization of metabolism.

We first established that changes in the "lower" phenotypic level (i.e. incorporating more molecular detail) of metabolic flux rearrangements upon gene deletion were translated into meaningful changes in the "higher" level of genetic interaction networks. Rewiring of the epistatic network was computed by aggregating all the interactions that appear, disappear and change sign (Fig. 1.1A) and was found to be predictable by the change in metabolic fluxes (Fig. 1.1, Spearman's $\rho = 0.72, P < 10^{-8}$)

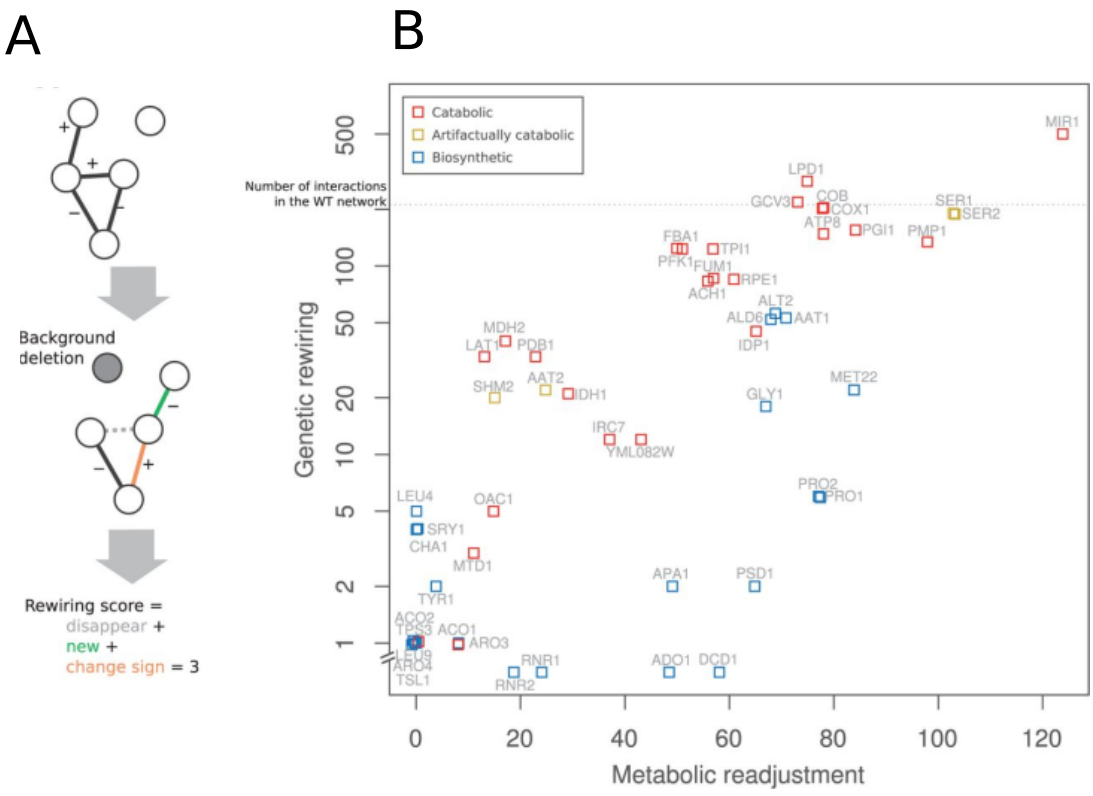

FIGURE 1.1: **Metabolic readjustment predicts network readjustment.** **A**) Rewiring is calculated using a simple metric that aggregates all the possible changes in an epistatic network after a gene is deleted. In a genetic network, nodes represent genes and links represent epistasis, positive (+) or negative (-) between them. After gene deletion interactions can disappear (dotted line), appear (green) or change sign (orange). **B**) Association between rewiring of a genetic network and rearrangement of metabolic fluxes (scored as number of reactions with altered relative flux) in the set of genotypes generated by single (active) gene deletion. The number of interactions in the *wild type* network (207) and the corresponding active metabolic reactions (277) are included for reference. Genetic backgrounds are represented with the name of the deleted gene, color shows the functional annotation of each gene (the rationale for the "artifactually catabolic" notation is explained in the main text)(data points are represented with some added noise to aid visualization and the y axis logarithmic scale is broken showing backgrounds with no genetic rewiring).

and particularly by qualitative change (that is, reactions switching on and off) (multiple linear regression $P < 10^{-8}$ compared to quantitative changes, $P = 0.97$). Changes in the genetic interaction network are then a reliable reflection of changes in the relevant phenotypic features determining fitness – in this case, in the flux through metabolic reactions contributing to biomass production. Adding further

detail, alterations in currency metabolites (such as NADH) and catabolic intermediates (from eg. glycolysis) were particularly tied to epistatic network rearrangement (*Appendix A*).

Catabolic genes soon emerged as central to genetic network rewiring, as backgrounds with catabolic genes deleted were also particularly unstable (it is worth noting that some genes associated to strong rewiring but annotated as non-catabolic were fulfilling an artifactually catabolic role in the model, discussed below; this if anything reinforces the general principle)(Fig 1.1.B)

Tracking the change of individual epistatic interactions (by noting the number of genetic backgrounds in which they were altered) revealed that the most unstable pairs comprised genes belonging to different functional modules i.e. to different "parts" of the metabolism (mean instability within the same group = 5.1, mean between groups = $7.8, P = 3.4 \times 10^{-5}$). Conversely, new interactions arose more readily between metabolic modules (90% of new interactions). Here, again, instability was largely found in catabolic functional groups (Fig. 1.2A), while biosynthetic genes showed fewer, more conserved interactions that varied only in specific backgrounds (Fig. 1.2B). Sign and strength of the interactions also emerged as a differential property of stable and unstable interactions. Strong interactions arise with unique and absolute functional dependencies: synthetic lethal (SL) interaction arises between two unique alternative pathways to contribute to fitness, while strong positive (SP) interactions take place between two steps in the same pathway (or subunits of a protein complex)(Fig. 1.3A, left). Weak interactions, respectively, occur when further alternative pathways of different efficiency exist (Fig. 1.3A, center), and when at least one of the interacting genes participates in another fitness-contributing function (Fig. 1.3A, right). In our set of backgrounds rewiring is stronger in weak interactions (Fig. 1.3B) and, among these, new interactions are more frequently weak negative (WN) arising anew (Fig. 1.3C) or transformed from weak positive (WP)(Fig. 1.3D). This would suggest that some proportion of the network changes is due to multifunctional genes switching between contributing to fitness in the same or different pathways.

That is, instability (measured in aggregate as appearing, disappearing or changing sign and/or strength) is greater in inter-module interactions that intra-module; greater in positive interactions compared to negative, and greater in weak interactions compared to positive. Strength and sign of the interactions is in turn related to the functional annotation of the genes involved. In the *wild type* network (Fig. 1.4A), SL interactions are predominantly associated to biosynthetic genes, such as aminoacid synthesis. Some of these interactions are easily understood as they involve pairs of gene paralogs arising from gene duplication, eg. *LEU9-LEU4* in the leucine synthesis pathway (Fig.1.4B). The weak positive and negative component of the network is more closely associated to catabolism, related to processes such

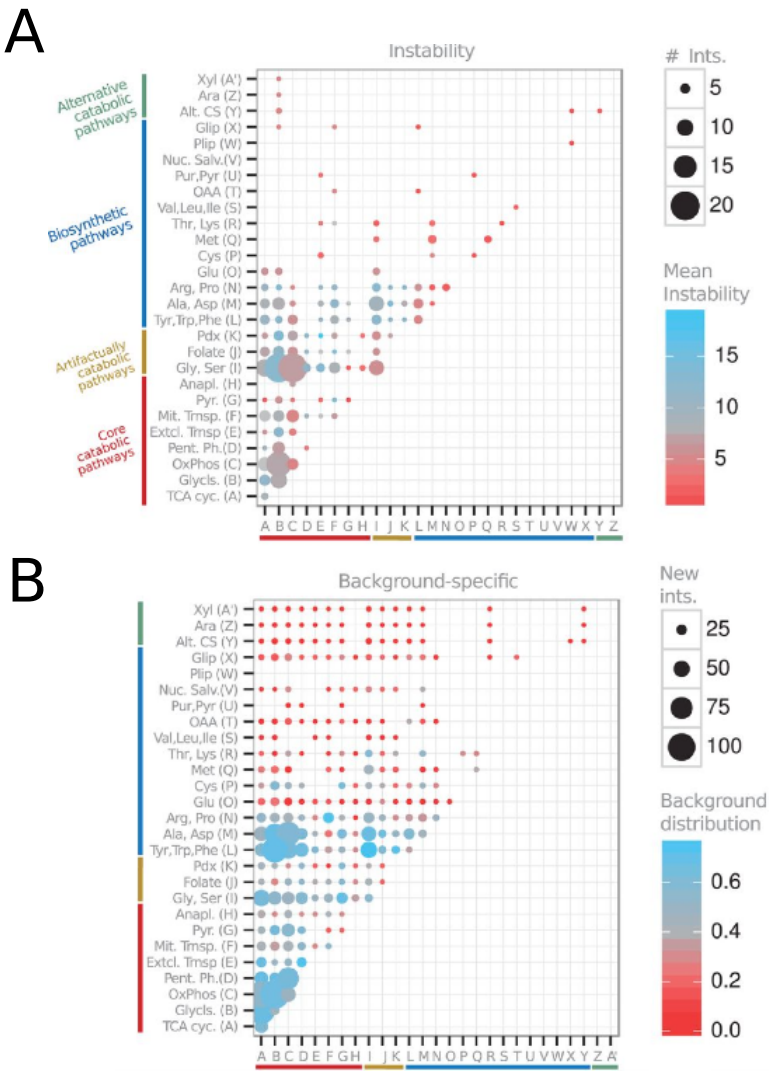

FIGURE 1.2: **Network rewiring varies with functional annotation.** **A**) Instability of *wild type* interactions between the different metabolic annotation groups. Dot size represents the number of interactions between a specific pair of modules, dot color represents the associated average instability as number of genetic backgrounds where an interaction disappears, changes sign or strength. **B**) New interactions (compared to the *wild type* network) between pairs of functional modules that appear in specific backgrounds. Dot size represents the number of new interactions, dot color represents their distribution among the set of single deletion backgrounds (normalized Shannon entropy, *Materials and Methods*).

as glycolysis (eg. *PGI1, PFK1, FBA1*), the tricarboxilic acid cycle (TCA)(eg. *IDH1, LPD1, SHD2*) and oxidative phosphorylation (*COX1, COB, ATP8*).(Fig. 1.4 C,D). We introduce the notation "artifactually catabolic" for a set of genes with different annotations (eg. *SER1, AGX1*) that act in concert in the model to produce ATP via a sort of "glycine fermentation", which is not described for *S. cerevisiae* and is probably due

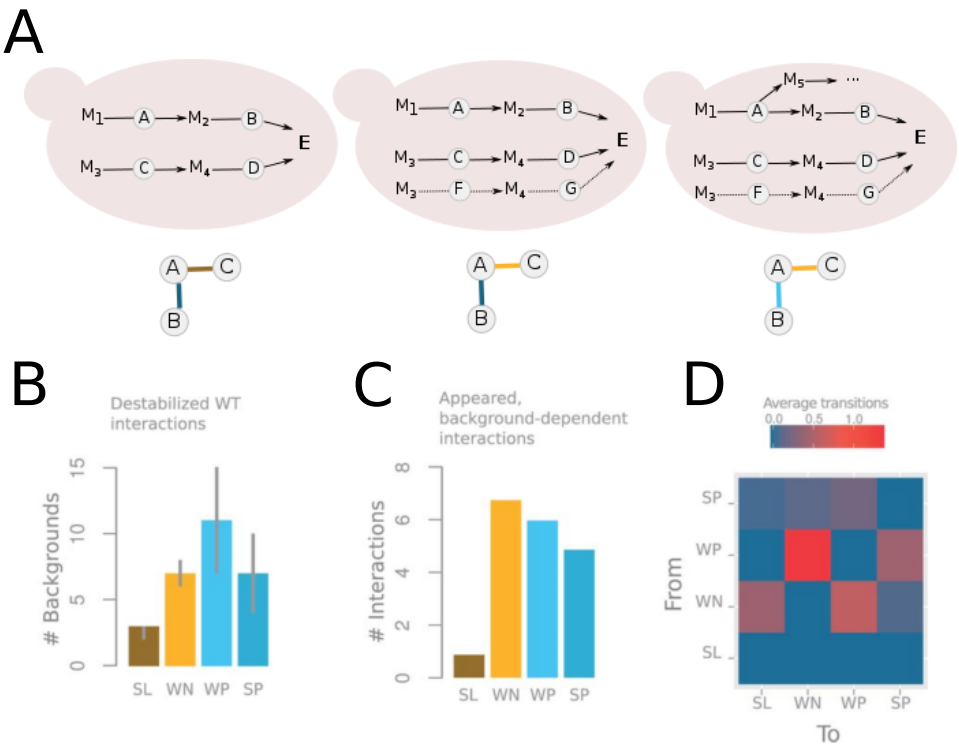

FIGURE 1.3: **Types of epistatic interactions and their instability.** **A**) Cartoons depicting the metabolic architecture underlying positive and negative, strong and weak epistasis. Circles represent genes (enzymes) as they transform metabolites feeding them into an essential function "**E**". *Left*: SP (strong positive epistasis) (dark blue) arises between the components of a pathway, while SL (synthetic lethal) (dark yellow) connects two unique pathway alternatives. *Center:* when a third, less efficient alternative pathway (dotted line) exists two genes providing the same function interact with WN (weak negative) epistasis (light yellow). *Right:* WP (weak positive) (light blue) connects genes acting on the same pathway when at least one of them performs additional functions in other pathway(s). **B**) Distribution of interactions in the *wild type network* that disappear in the set of single deletion backgrounds, grouped by interaction sign and strength (median with upper and lower quartile in gray line). **C**) Average number of new interactions appearing in the set of single deletion backgrounds, grouped by sign and strength. **D**) Expected number of transitions in an average background between interaction classes, grouped by sign and strength.

to an artifact of the model. Nonetheless these genes behave in concert with the truly catabolic ones in terms of network properties.

Catabolic genes exhibit a greater connectivity, comprising most of the genetic hubs linking catabolic modules with weak interactions (nodes with weak average epistasis $|\epsilon| < 0.5$ exhibit a mean of ~ 8 links; nodes with strong average epistasis $|\epsilon| > 0.5$ have ~ 3 links, Wilcoxon test $P = 0.003$)(Fig. 1.5A) . Deletion of one of these genes

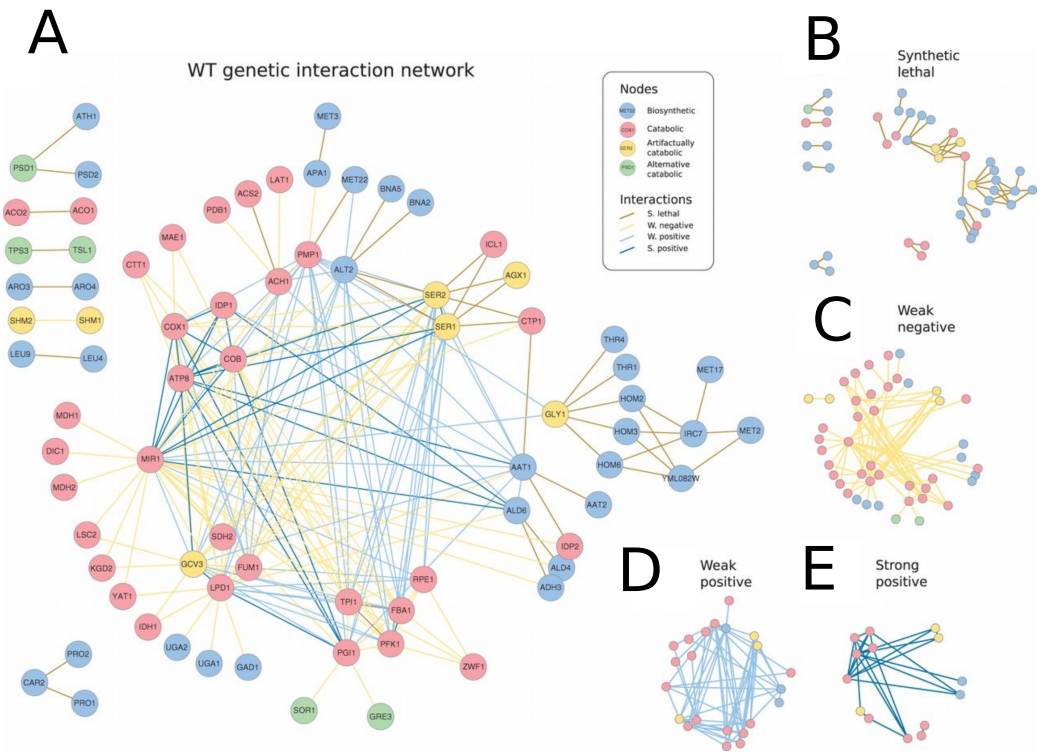

FIGURE 1.4: **Wild type network**. **A**) Epistatic interaction network of the *wild type S. cerevisiae*model. Nodes represent the genes in the model, color represents the corresponding functional annotation. Edges represent epistatic interactions, color represents sign and strength as in Fig. 1.3 and throughout the text. To emphasize the differential interaction patterns by functional modules the components of the network are shown separately, representing interactions of type **B**) SL, **C**) WN, **D**) WP, **E**) SP.

induces rewiring of these hubs, highlighting different means of achieving the necessary components for cellular growth (i.e. the necessary metabolites supplying the biomass reaction in the model). Take as an example the glycolitic gene *PFK1* (phosphofructokinase). Upon its deletion it is mostly other hubs such as *PGI1* and *FBA* that rearrange their epistatic links with other genes. In the case of FBA1 interactions disappear as this enzyme, connected with a SP interaction with *PFK1*, now becomes essential. On the other hand, new interactions appear with *PGI1*, an earlier glycolitic gene, and others such as the pentose-phosphate pathway gene *ZWF1* as initial processing of glucose is now diverted to this functional module (Fig. 1.5B) This pattern of hubs rewiring hubs holds for most of the genes with high interactivity (the exception is a biosynthetic hub, *IRC7*)(Fig. 1.5).

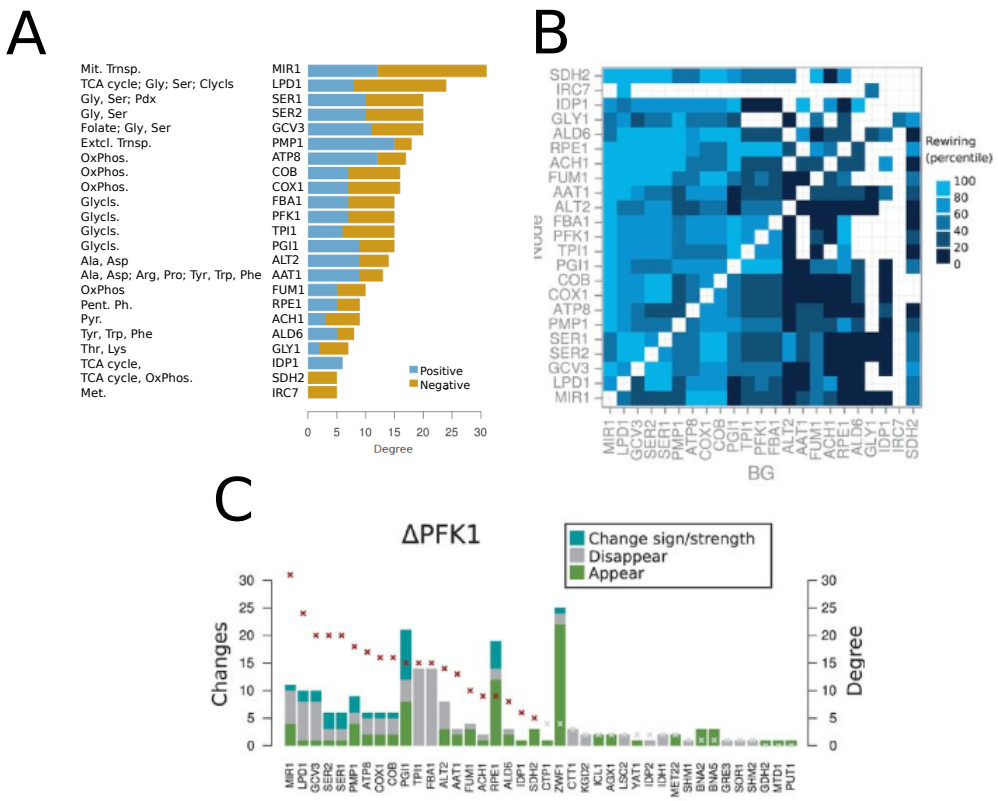

FIGURE 1.5: **Influence of the deletion and rewiring of hubs on epistatic network instability**. **A**) Genetic hubs in the *wild type* genetic network. Interaction degree and functional annotation of the 25 most connected genes in the *S. cerevisiae wild type* genetic network. **B**) Network rewiring after deletion of the hub *PFK1* as a function of the degree of the interacting genes (red crosses). Bars represent the number of modified interactions for each gene, colors represent the type of change (appear, disappear or change sign/strength in blue, gray and green respectively). **C**) Interaction rewiring of genetic hubs upon deletion of other hubs. Rewiring scores are normalized by the connectivity of each hub in the *wild type* network. Colors represent the percentiles of the normalized score (with percentiles [20 40 60 80 100] corresponding to a score of [0.22,0.4, 0.66,0.96, 5.6]; a value of 1 represents a case where the number of altered interactions matches the *wild type* connectivity; white denotes an absence of rewiring).

Catabolism then is a highly intertwined structure comprised of genes whose multifunctionality allows them to contribute to fitness and compensate each other in various configurations. The complexity of this organization based on functional versatility can be further understood taking as an example case the Δ*MIR1* background. *MIR1* is a carrier that imports inorganic phosphate into the mitochondria; hence its abundant SP interactions with oxidative phosphorilation genes in the *wild type* network (Fig. 1.4). It also presents numerous WN interactions with other genes that together can supply its function with lesser efficiency: upon deletion of *MIR1*,

phosphate must then be transported into the mitochondria coupled to the export of malate. This alternative pathway has far-reaching consequences on the homeostasis of the whole metabolism, such as redox imbalances that must be corrected through other mechanisms (Fig. 1.6A presents a simplified picture of these changes to illustrate the general mechanics of network rewiring, detailed changes are omitted; see *Appendix A*) This new pattern of metabolic fluxes and dependencies is translated into the network, inducing substantial rewiring (Fig. 1.6B, C).

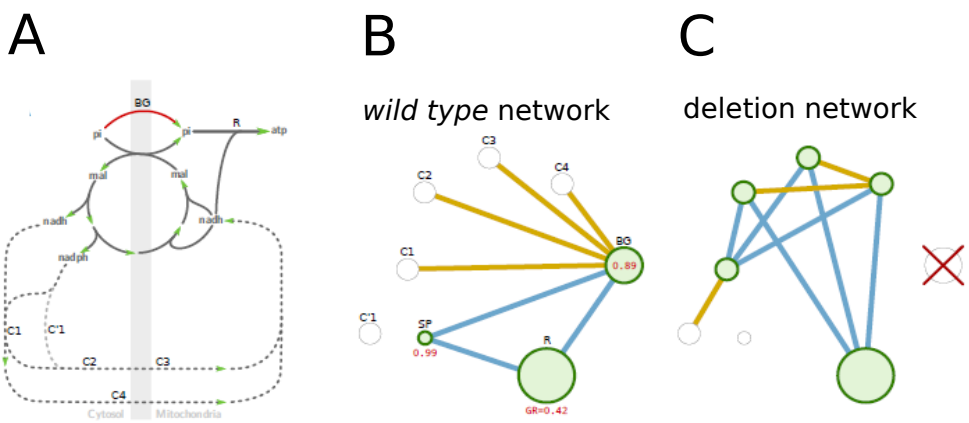

FIGURE 1.6: **Functional underpinnings of network rewiring. A**) Schematic representation of the metabolic reorganization that underlies the changes in the genetic network of a deletion genotype, based on the Δ*MIR1* background. Deletion of the background gene (*BG*, red) interrupts flow through a specific metabolic pathway . This induces the activation of a compensatory mechanism to fulfill its function (C1), which in turn usually generates metabolic imbalances that must be rectified through additional compensatory reactions (C2, C3, C4)(the exception being the deletion of a gene with a completely equivalent alternative, such as duplicated genes). In the case of *MIR1*, upon its deletion the main mechanism to import phosphate into the mitochondria is abolished (red). An alternative mechanism based on the antiport of malate is then activated, which necessitates correction of redox homeostasis. **B**) *Wild type* network of the *BG* gene. Green nodes represent active reactions, size of the node represents single fitness contributions. *BG* interacts positively with genes acting in the same pathway (R, denoting genes operating with *MIR1* to fulfill its main function of respiration) or otherwise dependent on it to function (SP), and negatively with the alternative and compensatory mechanisms (C1, C2, C3, C4). **C**) When the *BG* gene is deleted, the target function R develops instead positive interactions with the compensatory mechanisms, now acting in concert to maintain respiratory function. These genes can in turn interact with each other, positively or negatively depending on their functional relationships. Second order compensatory mechanisms can also be uncovered (C'1) and reflected in the new network.

Accumulation of neutral deletions significantly reduces the buffering and versatility of metabolisms

Single gene deletion backgrounds allowed us to connect network rewiring to the underlying metabolic structure, particularly the distributed robustness of catabolic modules. To explore this feature or metabolism, we generated an additional set of genetic backgrounds where neutral mutations accumulate (up to a total of 100 mutations per background, *Materials and Methods*). The resulting networks exhibit a reduction in the number of nodes (196 out of 200 are smaller in number of nodes compared to the *wild type*) combined with a tendency to increase the number of interactions per node (166/200 have, on average, more interactions). Negative interactions are mostly responsible for these changes: negatively interacting genes are deleted during the trajectory, and negative interactions undergo substantial rearrangement by disappearing, appearing and arising from previously positive interactions. Overall this, combined with an increase in essential genes (in 187/200 neutral genotypes), points to a restriction in buffering mechanisms. An example trajectory is examined in Fig. 1.7, tracking network change as neutral deletions accumulate. Here rewiring occurs in a stepwise manner, with some mutations leaving the network unaltered and others introducing extensive rearrangement (Fig. 1.7A); the latter are, not unexpectedly, particularly tied to the deletion of *wild type* hubs, an example being the early removal of *SDH2* which uncovers a new role as genetic hubs for other genes such as *FBP1* and disconnects others such as *IDP1* (Fig1.7.B) which will reconnect at a later step (Fig. 1.7D). The loss of buffering can be clearly observed looking at the glucose phosphorylation enzymes *HXK1*, *HXK2* and *GLK1*: after *HXK2* is deleted the remaining genes supplying this function, *HXK1* and *GLK1* develop a SL interaction (Fig. 1.7 C); later, *HXK1* is deleted as well and *GLK1* becomes essential (Fig. 1.7D). Note that because the remaining enzyme *GLK1* is only able to activate glucose, while the other two hexokinases can activate other sugars, catabolic versatility is reduced in combination with the observed network rearrangement.

Alterations in metabolic capabilities after neutral deletion accumulation should be further evident in the possibility of accommodating different nutrients to produce sufficient biomass for growth, as each individual source needs particular processing before being assimilated. To test this, we exposed our set of neutral mutation backgrounds to a collection of random environments ([53], *Materials and Methods*) and obtained the corresponding growth rates. The ensuing distribution encompassed a wide range of fitnesses i.e. varying capability of adaptation to new nutritional environments (Fig. 1.8A). We classified these backgrounds as high growth (HG) and low growth (LG) and compared the resulting genetic networks. Many network rewiring metrics were higher in LG backgrounds: they incurred greater change in the sign

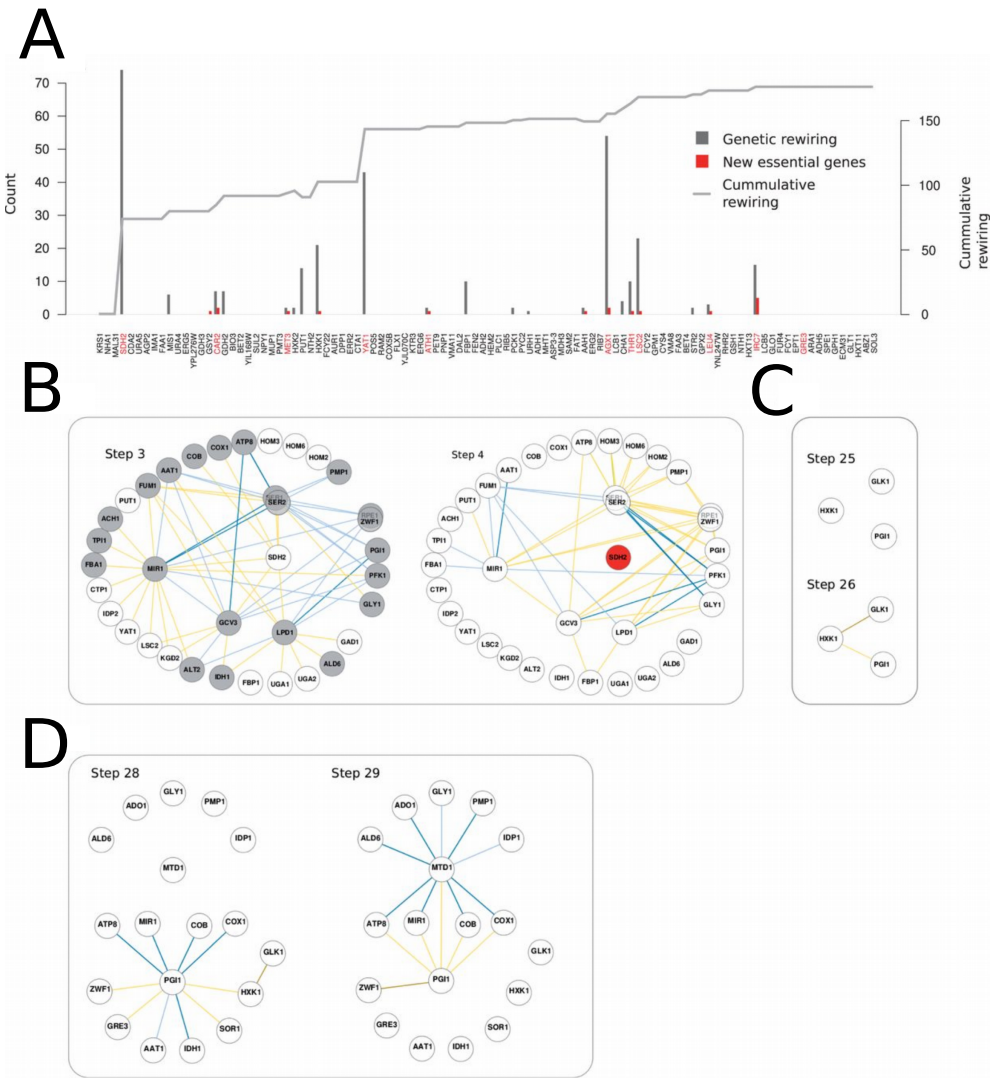

FIGURE 1.7: **Neutral background trajectory. A**)Trajectory of one neutral deletion backgrounds as mutations accumulate (*x* axis, genes colored in red are hubs in the *wild type* network) and the genetic network changes accordingly, showing the step-wise rewiring associated to each deletion and the cumulative rewiring over the trajectory. Rearrangement associated to three specific steps is shown in detail: **B**) In step 3 the catabolic hub *SDH2* is deleted, inducing substantial rewiring among other catabolic genes; **C**) Deletion of one of three genes able to perform the same function creates a SL link between the remaining genes; **D**) Additional deletion of one member of the remaining pair renders the last gene essential and further constrains the metabolism, rewiring of the local genetic network reflects these changes (see main text for further discussion of the functional implications)

.

and strength of interactions (Fig. 1.8B) (mean = 24.3 and 13.4 interactions per background in LG and HG, respectively) and these were particularly less conserved in

catabolic modules (i.e. less conserved weak and inter-module epistasis)(*Appendix A*). The final networks were smaller in number of edges and nodes, and contained more essential genes (Fig. 1.8C). LG epistatic networks were also proportionally more negative. While new interactions arose at a similar rate in HG and LG (mean = 60.6 and 61.0 respectively), in the latter they occurred in genes of particular significance: negative ones between the pentose-phosphate patwhay and other genes performing catabolic functions (Fig. 1.8).

The backgrounds accumulating neutral deletions, thus, incurred a variable but frequently significant reduction in compensatory mechanisms. The LG genotypes are particularly impaired in their ability to incorporate alternative carbon sources due to their notable loss of metabolic versatility and, particularly, of the pathways required to direct nutrients towards the later catabolic functions. This occurs because carbon sources other than glucose require initial transformation steps involving the pentose-phosphate pathway and gluconeogenesis to be then introduced into the common core of catabolism (at different stages of glycolisis or the TCA cycle). Deletion of many of these genes can be phenotypically neutral in glucose medium, but the metabolisms thus generated are harboring cryptic variability that is only exposed when challenged with varying environments or further genetic perturbations (as when assembling the genetic interaction network).

In silico results are consistent with experimental observations

The results described here are based on *in silico* metabolic reconstructions, but a quick assessment of experimental studies on this topic corroborate some of the features we describe. We confirmed some of our *in silico* predictions with other available experimental datasets. Using data from a previous study [62] we explicitly evaluated the comparative rewiring of genetic networks in *S. cerevisiae* and the distantly related yeast *S. pombe*, finding confirmation of the greater instability of weak interactions (with conservation rates of 4.9% compared to 8.7% for strong interactions, χ^2 test $P < 2,2 \times 10^{-16}$) and of positive interactions (0.8% of conservation while 5.4% of negative ones were conserved χ^2 test $P < 2,2 \times 10^{-16}$) (Fig. 1.9 A) (See*Discussion* for further examples).

The reflection of environmental plasticity on epistatic interaction rewiring was also apparent using data from genetic networks assembled by exposing yeast growing on rich media to three DNA-damaging agents: methyl methanosulfonate, camptothecin and zeozin [59]. Again, weak interactions show greater instability than strong ones, and positive interactions are less conserved than negative (comparing the untreated network to the three environmental alterations, Fig. 1.9 B). Functional relationships also define conservation status, as interactions among closely related genes are more

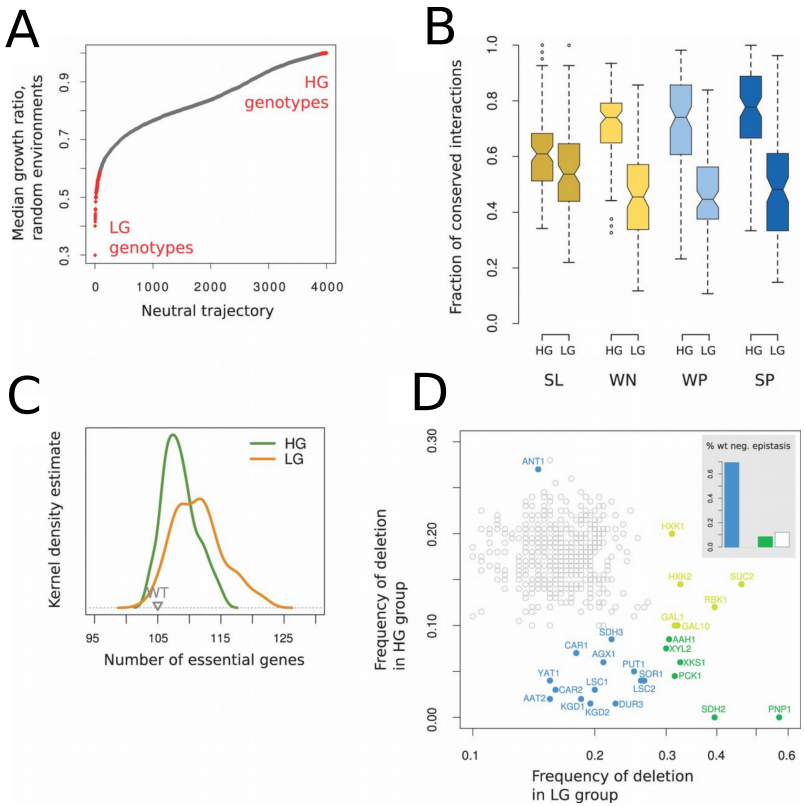

FIGURE 1.8: **Environmental plasticity of the neutral deletion backgrounds.** **A**) Fitness distribution, as the of a set of neutral deletion genotypes exposed to an array of random environments. Data points represent the median of the growth ratio between each background and the *wild type* for a given environment. 100 backgrounds with the highest and lowest growth were selected for further analysis (HG and LG respectively, highlighted in red). **B**) Instability of the genetic networks of HG and LG backgrounds as fraction of conserved interactions, grouped by interaction sign and strength. Boxes show the median (center) and first and third quartiles (lower and upper edges). **C**) Distribution of the number of essential genes in HG and LG genotypes. **D**) Enrichment/depletion of specific deleted genes in the LG or HG backgrounds. Colors represent genes found by a bootstrapping analysis to be significantly enriched or depleted in HG, LG or both (blue, yellow and green, respectively) ($P < 0.01$ accounting for multiple testing). **Inset**: proportion of genes from the significant groups that present interactions in the *wild type* genetic network.

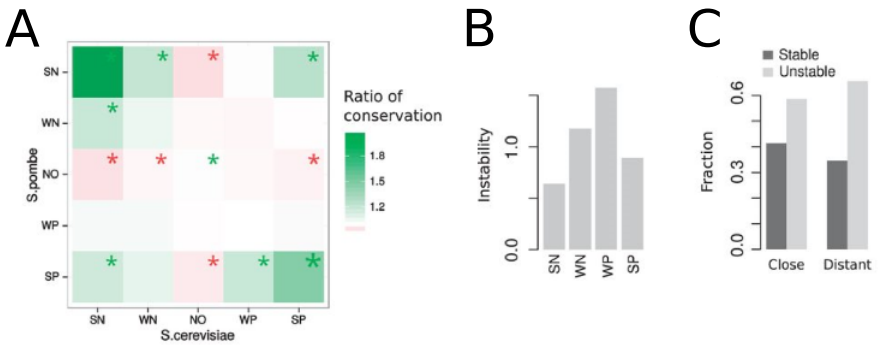

FIGURE 1.9: **Experimental support for the *in silico* conclusions.** **A**) Conservation of genetic interaction rewiring between two distant yeasts, *S. cerevisiae* and *S. pombe*, using data obtained from [62] considering direct orthologs. SN and SP defined as interactions belonging to the upper 30 percentile of all negative and positive interactions, respectively (WN and WP defined as the lower respective 70 percentile). NO indicates an absence of interactions. Box colors indicate ratios between the number of times that a transition is observed and the expected value (by random permutation 10000 times, stars indicate significance at $P < 10^{-4}$). **B**) Stability of interactions in response to environmental change, consisting of the addition of three DNA damaging agents to yeast cells growing in rich media. Data obtained from [59] (*Materials and Methods*). Unstable interactions grouped by sign and strength. **C**) Instability of the interactions in the dataset as in **B**, in relation to the functional distance between genes defined by the proportion of shared biological process annotation in the original reference.

stable than between more distant functional classes (Fig. 1.9C). Furthermore, weak epistatic interactions specific to each treatment also tend to arise between functionally distant genes (92% as opposed to 87% in the untreated genetic network, χ^2 test $P = 3 \times 10^{-15}$).

1.4 Discussion

Systematic deletion of metabolically active genes in one specific, realistic growth condition for yeast (glucose minimal medium and aerobiosis) allowed us to connect the stability of the respective genetic networks to the functionality of the deleted genes and their position within metabolic architecture. Interaction sign and strength are reflections of the way in which each gene contributes to the observable phenotype (Fig. 1.3A). Instability of the epistatic interaction network is mostly associated to weak interactions compared to strong; and to positive compared to negative interactions. Furthermore, network change is mostly tied to catabolic genes (a category to which most of the genetic hubs belong, Fig. 1.5 A), and to between-module interactions (Fig. 1.2A); most of the background-specific interactions are likewise encompassed in this classification (Fig. 1.2B). All this information converges on the distributed and versatile nature of catabolic processing, whose potentiality is already reflected in the *wild type* network (Fig. 1.4). Biosynthetic functional modules exhibit the opposite pattern: a greater proportion of conserved SL interactions, connected to a more linearized mode of operation.

While this study was entirely performed *in silico*, experimental observations reinforce our conclusions. Some of these studies are discussed in *Results* (Fig. 1.9); other studies in various genomic subsets report high conservation of SL and within-module interactions, compared to the rearrangement of between-module interactions [60, 61]. All these experimental studies are consistent with our predictions of rewiring being largely associated to weak and positive epistatic interactions. Sign changes that we identified in catabolic hubs could likewise be indicative of functional repurposing [63]. Comparable results are observed in the yeast genetic interaction dataset from [55], where we computed the ratio of essential and epistatically interacting genes (θ) finding a significantly larger ratio for biosynthetic modules ($\theta = 0.18, \theta = 0.94$ for catabolic and biosynthetic genes, respectively; Wilcoxon-Mann-Whitney test $P = 0.01$).

After examining another set of mutational backgrounds defined by neutral adaptive trajectories [65, 66], the functional underpinnings of genetic network rewiring are emphasized. In some cases (LG) catabolism has been "pared down" so that much of the distributed buffering is lost and functions are carried out by as few genes as possible; this causes an enrichment in essential genes, negative interactions and a notable decrease in environmental plasticity (Fig. 1.8).

In sum, the cell typically will respond to genetic and environmental stresses in ways that will necessitate the compensation of metabolites related to energy and/or redox balance. Catabolism is the fraction of metabolic reactions suited to these means, due

its distributed compensation mechanisms associated to high pleiotropy and interconnection between subfunctions. Once homeostasis is achieved and precursors are produced, biosynthesis of different cellular components proceeds through more linearized pathways with simple redundancy. This different organization is reflected in the patterns of genetic networks and their change (Fig. 1.10).

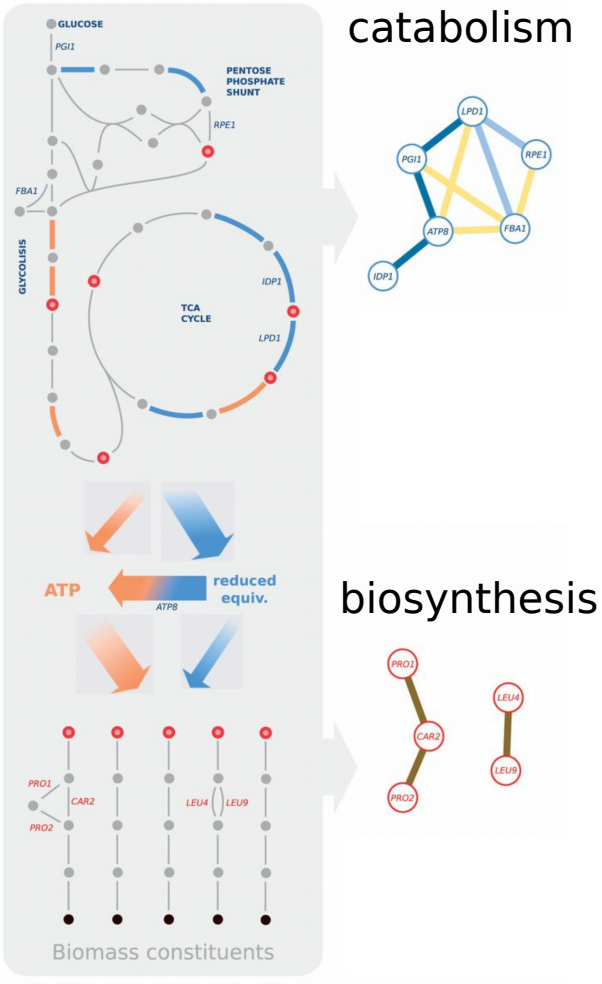

FIGURE 1.10: **Summary of the main conclusions obtained in this study.** The organization of metabolic functional modules (left) is reflected in the associated genetic network and its stability (right). Catabolism contributes the essential currency metabolites ATP and NAD(P)H (energy and reductive power)(reactions marked in blue and orange, respectively) and biosynthetic precursors (red). Degeneracy of catabolism leads to distributed robustness, manifested as unstable weak and positive interactions among functionally diverse genes (interaction sign and strength coded by color as in previous figures). Mutational and environmental robustness are linked in the rearrangement of the epistatic network (top). Biosynthesis is composed mostly of independent pathways in which robustness is mostly due to simple redundancy, leading stable synthetic lethal genetic interactions (bottom).

Chapter 2

Social Interactions

2.1 Introduction

Bacteria were traditionally studied under the framework of their antagonistic effect on human health -a view that focused on individual species acting in an isolated manner to cause infections. However,the complexity and versatility of microbial organisms is increasingly being recognized [67]. Interest in communities of microbes has been propelled by advances in metagenomics and other high-throughput techniques [68, 69], and they have emerged as useful experimental tools in Ecology and Evolutionary Biology [12, 19] and mediators in human health states [70, 71]. Microbial communities are shaped by social interactions between its members [72], and thus the understanding of microbial social dynamics emerges as central to the full comprehension of their natural lives and potential applications [73]. This understanding comprises rigorous assessment of all the interacting system variables determining the dynamics of a population at different levels of biological organization (biophysical, molecular, physiological), including ecological and evolutionary processes acting on similar time scales in an integrated manner.

Social dynamics in bacterial communities

Social interactions at the microbial scale often manifest as external molecules secreted into the medium, which act as public goods. In a broad sense a "public good" is a common resource maintained by the members of a community [9], and they are integral to the functioning of microbial populations [24]. They can supply information to individuals about the state of the collective, as in the case of quorum-sensing molecules that implement cell-cell communication between bacteria [74]. They can enable the degradation of nutrient sources too large to be individually processed, such as the case of the enzyme invertase which allows *Saccharomyces cerevisiae* to break down sucrose in the medium that can then be internalized [75]; or nutrients otherwise inaccessible, such us free iron scavenged by siderophores in

Pseudomonas aeruginosa and related species [76]. The formation of biofilms is fundamentally based on the sharing of external molecules, i.e. secreted polymers that construct a protective layer around the community; this category includes highly organized biofilms that are a regular part of a microbe's lifestyle, such as those formed by *Bacillus subtilis* [77], or structures quickly arising *de novo* in particular selective pressures, such as the mats created by *Pseudomonas fluorescens* in response to oxygen deprivation in static culture [78]. Public goods are also used by microbes to coordinate complex population-level behaviors, such as the induction of virulence in *Salmonella typhimurium* [79]. A common vulnerability threatens systems based on public goods: their exploitation by individuals, cheaters, that do not contribute to the shared resource but nevertheless reap its benefits. By avoiding the cost of cooperation, cheaters retain a fitness advantage that can lead them to invade the population, damaging the collective effort and in some cases ultimately causing population decay in what has been termed "The tragedy of the commons" [9] (Fig. 2.1, see [78] for a clear experimental example in the mats of *P. fluorescens*).

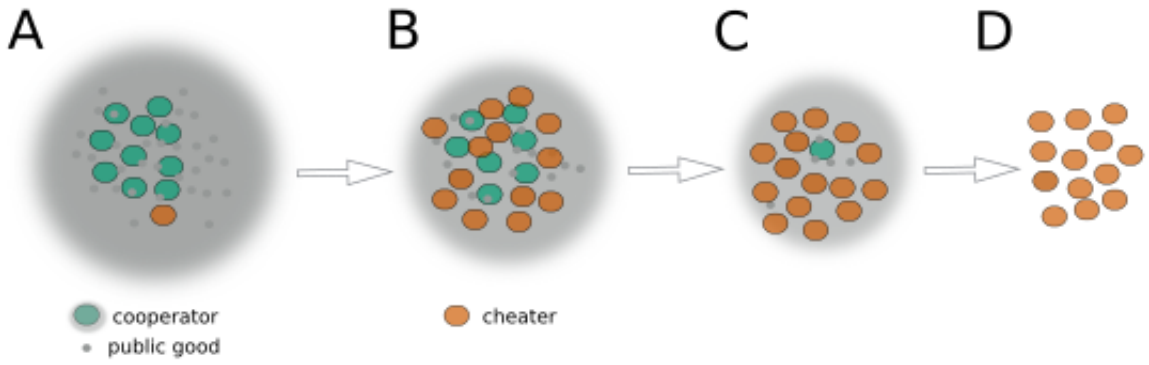

FIGURE 2.1: **Dynamics of a cooperative interaction in a microbial community.** **A**) Interactions based on public goods can be essential for the functioning of microbial communities, relying on the production of a shared resource (the public good, gray) by cooperators (green) at an individual cost. **B**) Public goods are inherently unstable. Cheaters (red) that do not contribute to the common resource but reap its benefits tend to appear. **C**) Because cheaters avoid paying the cost of producing the public good, they grow faster and invade the population. **D**) Cheater invasions can compromise or even destroy the collective effect.

Preservation of a social interaction mediated by public goods, then, necessitates additional features or mechanisms of control. The theoretical discussion on this topic is extensive [80] but we will focus on the many specific experimental examples that can be found in microbes. The general underlying principle is the assortment of cooperators, that is, the preferential interaction of cooperator among themselves and/or with the public good molecule. Implementation of this general strategy can entail

specific genetic mechanisms, such as the recognition of cooperators among themselves the exclusion of cheaters by what has been termed a "green beard" gene, or an indirect cost to cheating associated to pleiotropy in the cooperative gene [81, 82]. It can also involve, for example, the partial privatization of the public good, such as the case of invertase (described above) where cooperator yeast cells retain a small but sufficient percentage of the produced glucose to outcompete cheaters in conditions of scarcity [75].

Physiological, ecological and evolutionary constraints shape public good-based interactions

Nevertheless, disentangling the contribution of tangential factors to the social interaction to the sustainability of a collective effect is necessary to rigorously discuss the evolution and dynamics of cooperative behaviors; such as fitness tradeoffs [83], or the biochemical details of public good production and distribution [75]. This ties into the idea that a given molecule or cellular process might only display the characteristics of a public good in a certain context [30], and that the social interaction might be modulated by other factors of similar impact on ecological and evolutionary dynamics. Thus, detailed knowledge of the cellular and cell-environment interactions is required to fully comprehend the social aspect [10].

Deepening our understanding of the social features of microbial communities requires precise knowledge of the natural living conditions of the species, and detailed characterization of the processes involved from the ecological to the subcellular level. An important part of this discussion involved the production of siderophores by *P. aeruginosa* and other related strains, mentioned above but enumerated here in greater detail as an example of the complexity of public goods in their complete regulatory context.

The production of pyoverdin by some *Pseudomonas* spp. is one of the most widely used as a bacterial public good model system [72]. Pyoverdin is a water-soluble iron-chelating molecule synthesized as a response to iron scarcity, and exported into the periplasm and then the external medium through dedicated transporters [84]. After binding iron in the specific ionic state ferripyoverdin is again imported into the cell through another set of transporter proteins. There, iron is released to be used in cellular processes and pyoverdin is recycled and secreted again [85]. Because pyoverdin molecules present in the extracellular medium can be used by any neighboring cell with the appropriate receptors, regardless of its origin, it has frequently been described as a public good. However, many regulatory and environmental factors create a more complex picture. In an ecological context where multiple bacterial

strains interact, siderophore production could be tuned by a combination of competitive and cooperative dynamics [86]. The culture medium and the presence of spatial constraints (which can create an oxygen gradient that affects the ionic state of iron and thus its bioavailability) define the functionality of pyoverdin as a public good or a neutral or even deleterous product [30, 87]. Spatial effects observed at the subcellular level can further influence pyoverdin dynamics: in microcolonies of *P. aeruginosa* observed under epifluorescent microscopy, pyoverdin diffused preferentially between the periplasmic spaces of adjacent cells, reducing its loss into the external medium and the possibility of exploitation by cheats [88]. The siderophore, thus, potentially transitions from behaving as a public to private good. These environmental and single-cell level variables combine to determine varying population dynamics.

A novel framework connects ecological and evolutionary dynamics

Ecological and evolutionary processes were typically thought to occur over separate timescales, with ecology being considered "fast" and evolution "slow". The effect of ecology on evolution has been established for a long time in the form of natural selection, that is, the change in the distribution of heritable traits in response to the environment. Increased attention is being placed on the reverse phenomenon: the possibility that evolution can in turn influence ecology [6]. In a simple scenario, for instance, natural selection – ecology acting on evolution – can increase the growth rate of a population – evolution acting on ecology – ; recent discussions attempt to tease apart more complex scenarios where multifaceted aspects of ecology and evolution interact simultaneously [7]. Part of this framework shift originates from the recognition that evolution can be fast [89], and the possibility that rapid evolution can rescue a decaying population has become ever more relevant under the environmental alterations brought by global climate change [90, 91]. Within this novel framework microbes are a particularly suitable model and subject of study, given their fast life cycles and experimental amenability. Specifically, interactions between microbes emerge as a type of biological feature where eco-evolutionary feedbacks exert a clear influence.

One recent study tracked the development of an interaction between species that had previously not met in their natural ecological context: the yeast *S. cerevisiae* and the nitrogen-fixing bacteria *Rhizobium etli* [92]. *S. cerevisiae* produces molecules that affect bacterial growth, including both growth-promoting factors and an inhibitor. When co-culturing these two species in mixed conditions, an early commensal relationship develops through the growth factors, until their depletion and the rise of bacteria resistant to the inhibitor leads the prokaryotes to compete for resources. The

interaction then turns antagonistic. This study portrays how an eco-evolutionary process –specifically, the evolutionary rescue mentioned above – can quickly shape an interaction between unrelated species.

Eco-evolutionary feedbacks and constraints ultimately determine the fate of public good-based systems

Feedbacks between evolution and ecology also result from the social conflict between cooperators and cheaters of the same species, as a study in the invertase system of *S. cerevisiae* demonstrated. Here, a density-dependent effect (as cooperator retain a small fraction of the public good that gives them an advantage at lower densities) produces a distinct spiraling pattern in the population dynamics that couples the evolutionary spread of the cheating allele and growth of the population enabled by the public good [8].

Other strategies can connect ecological constraints (such as population size) to the sustainability of cooperation, such as stochastic contribution to a public good, or plasticity based on the sensing of population-wide cooperation levels [93]. We focused on a particular scenario where eco-evolutionary feedbacks in a social system can produce counter-intuitive effects: invasion by cheaters can be part of a mechanism that preserves cooperation, instead of necessarily leading to its collapse. This is one of a few contexts where a positive role for cheating individuals has been suggested; others include their potential role in the development of life cycles [94] or phenotypic cheating protecting cooperative alleles from genotypic cheating [79]. We analyze, both with a computational model and experimentally, how these paradoxical dynamics are mediated by synergy between eco-evolutionary processes and the effect of spatial structure. Previous theoretical studies have explored this issue [27], but experimental implementation in a synthetic bacterial system (two strains of *E. coli* engineered to display a social interaction) allows us to additionally assess the effect of other features of the bacterial system on the social dilemma. As part of the effort to rigorously contextualize microbial public goods in their interplay with biophysical to ecological variables, we additionally characterize a previously undescribed subcellular localization pattern of a natural bacterial product tied to social dynamics, the siderophore pyoverdin in *P. fluorescens* SBW25.

2.2 Materials and Methods

Culture media and reagents

For the eco-evolutionary feedbacks experiments. Strains were grown in LB broth $10\,\mathrm{g\,L^{-1}}$casein peptone, $5\,\mathrm{g\,L^{-1}}$ yeast extract, and $5\,\mathrm{g\,L^{-1}}$ NaCl) at $30\,^{\circ}\mathrm{C}$ with constant shaking. Overnight cultures were grown aerobically in flasks (170 rpm) at $30\,^{\circ}\mathrm{C}$, and experiments were performed in 96-well plates (Thermo Scientific, Denmark), with $200\,\mu\mathrm{L}$ of medium, $50\,\mu\mathrm{L}$ of mineral oil (Sigma-Aldrich, MO, USA), and shaking at 10000 rpm and $30\,^{\circ}\mathrm{C}$. Where indicated, antibiotics were added to the liquid medium or plate at final concentrations: kanamycin (Km) $50\,\mu\mathrm{g\,mL^{-1}}$, spectinomycin (Sp) $50\,\mu\mathrm{g\,mL^{-1}}$ in the construction of strains and $25\,\mu\mathrm{g\,mL^{-1}}$ in experiments, and/or gentamicin (gm) with concentration as noted in the experiments. The synthetic quorum-sensing molecule N-butyryl-L-homoserine lactone (C4-HSL) was purchased from Cayman Chemical (Mi, USA). Cell dilutions were done in PBS

(pH 7.4, Na_2HPO_4 80.6 mM, KH_2PO_4 19.4 mM, KCl 27mM, NaCl 1.37 M at 10X, USB Corporation, OH, USA).

For the subcellular localization of a public good experiments. Strains were grown overnight in LB broth at $28\,^{\circ}\mathrm{C}$ with constant shaking (180 rpm), then centrifuged 4 min at 6000 rpm and resuspended in succinate minimal medium (SMM) K_2HPO_4 6 g, KH_2PO_4 3 g, NH_4SO_4 2 g, $MgSO_4$ 0.2 g, NaOH 3 mM, sodium succinate 4 g)(Sigma-Aldrich, MO, USA) and incubated an additional 24 h before preparation of the microscope sample.

Strains

For the eco-evolutionary feedbacks experiments. The different *E. coli* strains were derivatives of JC1080 (BW25113 Δ*sdi::FRT*) [25]. The parental strain was constructed by integrating the cassette T0-SpR-rhlRPlacIq-PrhlGmRLAA-T1 into the λattachment site (attB) of *E. coli* JC1080 with the helper plasmid pLDR8, that bears the λintegrase, as described [95, 96]. The plasmid pZS4int-rhIL-GmLAA plasmid was constructed by adding the *aacC1* gene (GmR), from pSEVA611 plasmid [97], replacing the catLVA resistance marker from pZS4int-rhl-catLVA [25]. The final pZS4int-rhIL-GFP plasmid was assembled by replacing GmRLAA cassette for a GFP fluorescent reporter (from the lab collection). The pZS*2R-mCherry (ori-SC101*, PRGFP-rhlI, KmR) plasmid was constructed by swapping the GFP-rhlI cassette for the mCherry gene (lab collection). Then, the quorum-sensing reporter strain, "biosensor", was constructed by introducing into the λ attachment site (attB) of *E. coli* JC1080 the cassette T0-SpR-rhlRPlacIq-Prhlgfp-T1 as described above. The plasmid

pZS*2R-GFP-rhlI (ori-SC101*, PRGFP-rhlI, KmR) was obtained from [25](for further details see *Appendix B*).

For the subcellular localization of a public good experiments The strains used were *P. fluorescens* SBW25 *wild type* and a derived mutant defective in PvdS and tagged with mCherry under IPTG induction. Isolation and construction of these strains is thoroughly described in the cited literature [30, 78].

Simulation of eco-evolutionary dynamics

We used a model first described in [26] to simulate the dynamics of a population whose growth is based on an essential public good. It is based on a one-shot public good game [98] in which agents can contribute (cooperators) or not (cheaters) to the public good in groups of size N. Contributing implies a cost c to the agents. Group contributions are then summed, multiplied by a reward factor r (that determines the efficiency of the investments and the attractiveness of the public good) and redistributed to all group members, irrespective of their contribution. . The life cycle of the computational model is characterized by two distinct stages. In stage I the population is structured in evenly sized randomly formed groups in which the public good game is played. In stage II , each individual replicates according to the group composition (and payoff) experienced in stage I (see *Appendix B* for more details).

Experimental eco-evolutionary dynamics

To engineer the initial conditions, initial populations were prepared by mixing cooperators and cheaters at a defined population density (10^4 cells/well for high initial density experiments and 1-10 cell/well for low initial density experiments) and cooperator frequency. Overnight cultures of producers and nonproducers were washed twice with PBS by centrifugation for 15 min at 3800 rpm and room temperature. Then, OD600 was adjusted to 0.15. We assembled populations at the desired P frequency in a fixed final volume ($2.5\,\mathrm{mL}$), which was then serially diluted to the required cell density. This dilution was done in large volumes of medium ($20\,\mathrm{mL}$) and applying low dilution factor ($1/4$) each step to minimize the introduction of error in strain frequencies. Initial dilution steps were performed in PBS and the final 3 steps were performed in LB with Km, Sp.

Populations with a given initial cell density and cooperator frequency were prepared, distributed into a 96-multiwell plate and incubated for 15.5 h (T_1). Then, $1/10$ of each well was transferred into a new 96-multiwell plate with LB, Km, Sp and the specified gm concentration. This plate is again incubated for 8.5h (T_2). At the end of T_2 we plated whole well contents were spread onto 1.5% (w/v) LB agar

plates with five 3 mm glass beads for 30 s, and are incubated at $30\,^{\circ}\mathrm{C}$ for 48 h (or otherwise indicated). Then, to quantify the cell number of a population we counted colony forming units (CFU) under blue light illumination (LED transilluminator, Safe Imager^{TM} 2.0, Invitrogen, Waltham MA USA). The OD600 of cultures was measured in a VICTOR2x 2030 Multilabel Reader machine (Perkin Elmer, Waltham, MA, USA) with intermittent orbital shaking. For experiments with P and nP strains, Km and Sp were added to the media.

Characterization of the synthetic social interaction and biological constraints

To evaluate the invasion capability of nonproducers we prepared washed cultures of producers and nonproducers as described above . After adjusting OD600, to 0.15 we mixed both strains at the indicated frequency. Then, we inoculated three replica 50 ml Erlenmeyer flasks with 5 ml of LB, Km, Sp. After 24 h, we reseeded a new flask with a $1/100$ dilution and fresh medium. In order to estimate producer frequency in grown cultures, cells were $1/10$ serially diluted in PBS using a total of 10 ml of medium, plated onto LB agar plates, and colonies counted after 24h at $30\,^{\circ}\mathrm{C}$. We followed this process for 4 consecutive days. To determine antibiotic sensitivity overnight cultures were reseeded and grown for 4 h at $30\,^{\circ}\mathrm{C}$ to reach exponential phase. Aliquots of this culture containing $\sim 10^6$ cells were resuspended into a 96-multiwell plate with LB and a given dose of Gm, incubated for 2 h or 4 h, plated and counted. For experiments with the nP strain, Km and Sp were added to the LB medium. For experiments with cells in stationary phase, overnight cultures were used directly in the initial inoculation. We used additional wells without antibiotic in parallel to obtain a reference population size. We express the sensitivity to the antibiotic as "fraction surviving" (population size after exposure to antibiotic/reference population size without antibiotic). To measure the protective effect of the public good overnight cultures of nP were resuspended into LB with Km, Sp and the indicated concentrations of synthetic quorum-sensing molecule (C4-HSL). Then, we proceeded with the antibiotic sensitivity assay as described above.

Estimation of public good production

To estimate the concentration of the quorum sensing signal produced (C4-HSL), in different experimental conditions we used the reporter "biosensor" bacteria. We grew the "biosensor" strain overnight, adjusted the OD600nm to 0.1 and grew aerobically for 2.5 h at $30\,^{\circ}\mathrm{C}$. Then, the culture was aliquoted and purified supernatant from the experimental sample was added. We used known concentrations (0, $0.1\,\mu\mathrm{mol}$, $1\,\mu\mathrm{mol}$, $10\,\mu\mathrm{mol}$, $100\,\mu\mathrm{mol}$ of the commercial N-butyryl-L-homoserine

lactone (C4-HSL) to obtain a calibration curve. We grew these preparations aerobically for 3h, laid out $200\,\mu L$ of cultures in quadruplicates in a 96-well black/clear bottom microtiter plate (Sigma-Aldrich, MO, USA) and measured OD600 and GFP fluorescence (ex: 488nm; em: 520nm; cutoff: 495nm) in a SpectraMax M2e microplate reader (Molecular Devices, CA, USA). Supernatants were obtained from $200\,\mu L$ of overnight liquid cultures prepared following the predetermined protocol, centrifuged twice at room temperature to remove cells and used directly to induce growing cells of the reporter strain. Comparing observed supernatant fluorescence to the calibration curve approximated QS molecule quantities.

Mutation rate

We generated replica populations of the nP strain and initial density of ~ 1 cell/well. We distributed these cultures in 96-multiwell plates and allowed them to grow for 15.5h (T_1). We plated the whole well content on LB agar plates with the specified gm dosage and counted viable cells. From the distribution of Gm-resistant CFU observed in a set of replica populations the mutation rate was estimated with a maximum likelihood method as described in [99], using the online application "FALCOR: Fluctuation Analysis Calculator" (`http://www.keshavsingh.org/protocols/FALCOR.html`).

Microscope slides

To prepare the agarose pad, $220\,\mu L$ of agarose dissolved in SMM (2% w/v) were poured onto a microscope slide fitted with a sticky frame (Gene Frame,Fisher Scientific), pressed with a clean slide and allowed to dry for ~ 2 min. A small ~ 3 mm section of the pad and frame was cut across the slide to provide air for the growing cells. Growing cultures of SBW25 were again centrifuged 4 min at 6000 rpm and resuspended in fresh SMM. OD600nm was measured and additional dilutions were performed to adjust optical density to values previously determined by empirical means to result in an inoculum of 5-10 cells in this specific microscope field. $1.5\,\mu L$ of this preparation was inoculated on the agarose pad. After inoculating the pad,a clean coverslip was placed and carefully sealed onto the frame. Note that the only source of oxygen is the small channel cut across the agarose pad, which is liable to be depleted as cells closer to this channel grow into a thick lawn during extended culture time. To prepare the "liquid slides", the cultures were grown and OD adjusted as usual, and $140\,\mu L$ (using a single frame) or $410\,\mu L$(triple frame) of the liquid inoculum were placed on the frame and sealed with a coverslip. The "triple frame" conditions were used to produce an inoculum with a large proportion of cells in a polarized state, after 24 h of incubation, to be extracted with a syringe

and re-inoculated following the usual protocol. All experiments and incubations were carried out at $28\,^{\circ}\mathrm{C}$ unless otherwise indicated.

Time-lapse fluorescence microscopy and image analysis

Time-lapse fluorescence microscopy and image analysis The growing inoculated microcolonies were monitored by taking snapshots every 10 min for a typical total time of 18 using the microscope Axio Observer.Z1. Colonies were imaged under phase contrast (exposure: 30 ms) and Pvd using the fluorescence Source X-Cite 120 LED and the following filters: 390/40 BrightLine HC, Beamsplitter T 425 LPXR, 475/50 BrightLine HC (exposure: 30 ms, 12% intensity). Handling of the microscope, including the autofocus function for time-lapse imaging was achieved using the open source software MicroManager (with the plugin OughtaFocus) [100]. Images were taken with 63x and optovar 1.6x magnification. Visualization of the microscope output and image processing (such as background correction) was performed using the image analysis software Image J (https://imagej.nih.gov/ij/). Preliminary segmentation analysis was performed using the package for Matlab SuperSegger from the Wiggins Lab (http://mtshasta.phys.washington.edu/website/SuperSegger.php).

2.3 Results

Preservation of cooperation can be mediated by eco-evolutionary feedbacks in a simulated community that relies on an essential public good

We first analyzed the effect on eco-evolutionary dynamics of a social system with a constitutive, essential public good with a stylized *in silico* model [26]. In the model, a finite population of agents (representing bacteria) is transiently aggregated into groups of a given size. The model comprises two types of cells, cooperators that produce an essential public good incurring a fitness cost, and cheaters that arise from mutation and can use the public good avoiding the cost. In the groups the social interaction takes place, and individuals divide according to the payoff of the public good game [98] (Fig. 2.2A). This scenario produces characteristic dynamics, an example trajectory of which is depicted in Fig. 2.2B: by avoiding the fitness cost of cooperation, cheater agents multiply and invade the population.This, mediated by the essentiality of the public good, causes an overall demographic reduction that is translated into variability in the composition of the groups (Fig. 2.2C). Variability enables the isolation of cooperators that can then recover the population (Fig. 2.2D). The process of cheater invasion, population collapse, and cooperator recovery reoccurs cyclically, with some risk of population extinction. Thus, eco-evolutionary dynamics are sufficient to generate endogenous cycles of collapse and recovery of both population size and cooperator frequency. The conditions for recovery are set when initial population decay results in inter-group variability, in a process that resembles a statistical phenomenon known as Simpson's paradox [25]. Briefly, this phenomenon alludes to the contrast between a local (i.e. in a subpopulation or group) decrease in cooperators due to cheater invasion, and their global increase due to differential growth of cooperator-rich and cooperator-poor groups.

Experimental implementation of the social interaction confirms the eco-evolutionary feedbacks

We translated this conceptual framework into an experimental system. We engineered a synthetic social interaction between two strains of bacteria: a producer of a public good that is essential for population survival, and a nonproducer that does not contribute but can utilize this public good (Fig. 2.3A). Specifically, the cooperator/producer is an *Escherichia coli* strain modified to constitutively produce a molecule that freely diffuses in the medium; the molecule is the RhlI autoinducer from *P. aeruginosa*, which guarantees an absence of cross-talk with other bacterial systems. Both cooperators and cheaters/nonproducers are equipped with the cognate regulator RhlR, which in response to the autoinducer activates resistance

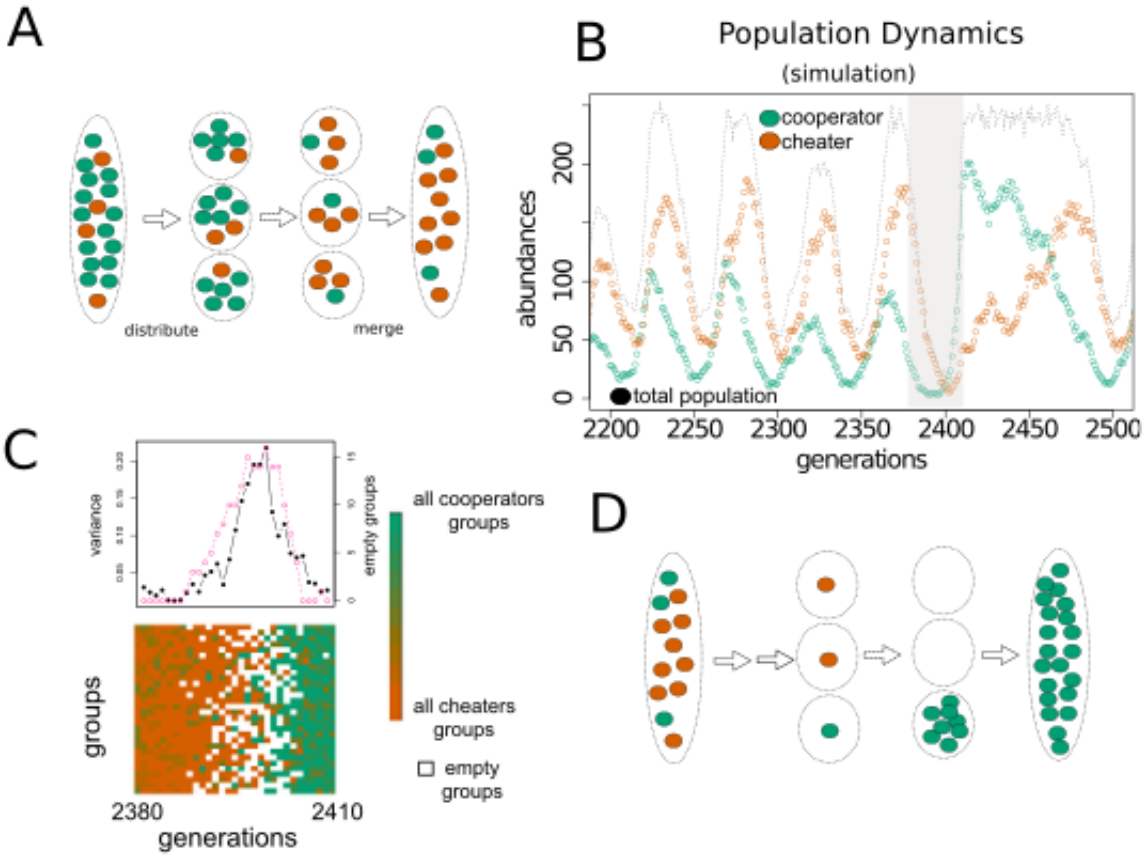

FIGURE 2.2: **Eco-evolutionary dynamics in a simulated social system where exploitation by cheaters contributes to the rescue of cooperation.** **A**) Cartoon depicting the *in silico* model of a microbial community which is organized as a transient metapopulation where cooperators (green) and cheaters (red, originating from cooperators by mutation) interact by means of a public good game (*Materials and Methods*). **B**) Typical population dynamics obtained with this model. Growth depends on an essential public good producer by cooperators. When cheaters invade, the decline in the amount of public good drives collapse of the population. This collapse paradoxically determines its subsequent revival. **C**) Revival is coupled to the endogenous emergence of variability in the composition of the groups when population is decaying. For the time window highlighted in **B** we display group composition (bottom; groups are colored according to their ratio of cooperators as indicated by the color gradient; white squares denote empty groups of a total of $N = 30$) and intergroup diversity (top, black curve, quantified as variance in group composition), number of empty groups (top, pink curve). **D**) Cartoon depicting the mechanism of cooperator recovery after cheater invasion, mediated by the assortment of cooperators into isolated groups enabled by the increase in intergroup variability measured in **C**.

to the antibiotic gentamicin (Gm). Resistance is implemented through a cytosolic antibiotic-modifying enzyme that inactivates the drug (Fig. 2.3B). We designed an additional "biosensor" strain where the public good induces green fluorescence, as

an instrument to measure public good production and its association to relevant population properties (*Materials and Methods)*.

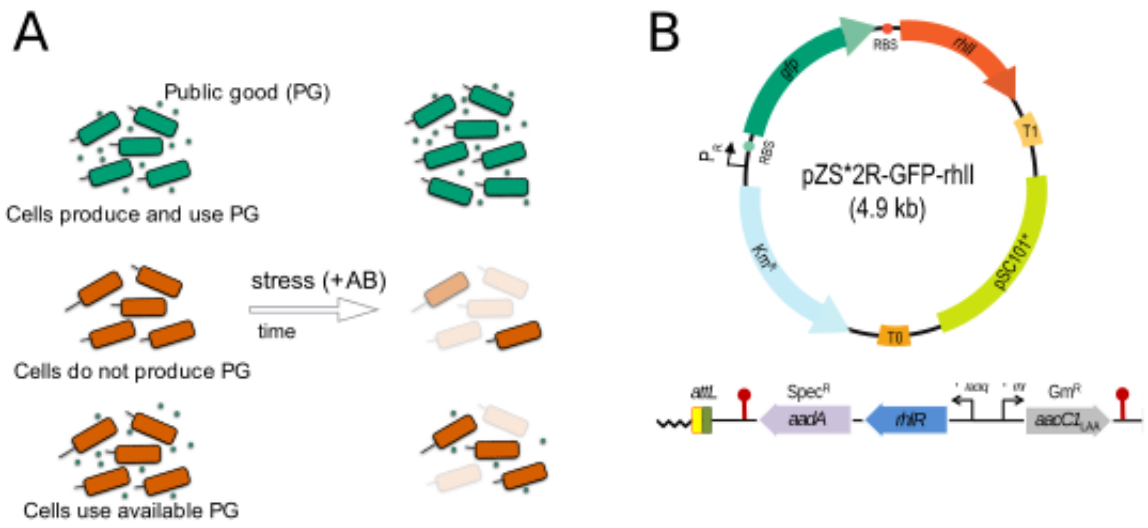

FIGURE 2.3: **Engineering of a bacterial synthetic social interaction**. **A**) We designed two types of strains, that can contribute (green) or not (red) to the production of a public good. A community that accumulates (top,cooperators) or obtains (bottom, cheaters) the public good in the environment is able to tolerate a bactericidal antibiotic stress, although the latter can survive least because the initial public good is spent. A community growing without public good would eventually collapse under stress (middle). **B**) Molecular implementation of the synthetic social interaction. The cooperator strain is equipped with a plasmid (top) carrying the necessary genes to synthesize the public good, the quorum-sensing (QS) molecule RhlI, and a GFP fluorescence tag allowing their phenotypic identification. In the cheater strain, the *rhlI* and *GFP* cassette is swapped with the alternative red fluorescence tag *mCherry* Both strains carry a genomic insert capacitating their use of the public good: the cognate receptor for the quorum-sensing molecule, RhlR, inducing the synthesis of the antibiotic resistance enzyme aacC1 which degrades the bactericidal gentamicin (Gm)(the system is based on a previous one [25], see *Materials and Methods* for construction details)

The synthetic social system thus designed allows us to ensure that public good production is constitutive (i.e. producers cannot avoid cooperating), the public good is equally available to cooperators and cheaters (the small autoinducer freely diffuses through cells), and it is properly essential (as the antibiotic is a bactericidal). Additionally, cooperators and cheaters are tagged with green and red fluorescence, respectively, which enables direct evaluation of their population frequencies. Synthesis of the public good molecule carries a fitness cost for producers, which manifests as a reduced growth rate. Then, the public good is required to tolerate a bactericidal stress (Fig. 2.4B) (note that it significantly increases population survival to a high

dosage of the antibiotic, for which a MIC of under an order of magnitude has been reported for *E. coli*, see http://mic.eucast.org/Eucast2/, but its presence is inherently unstable due to the fitness advantage of cheaters (Fig. 2.4A). It must be noted that, while in this case both the cooperator and cheater strain are engineered as is to ensure maximum control of the social interaction features, public good non-producers readily arise in natural settings [78].

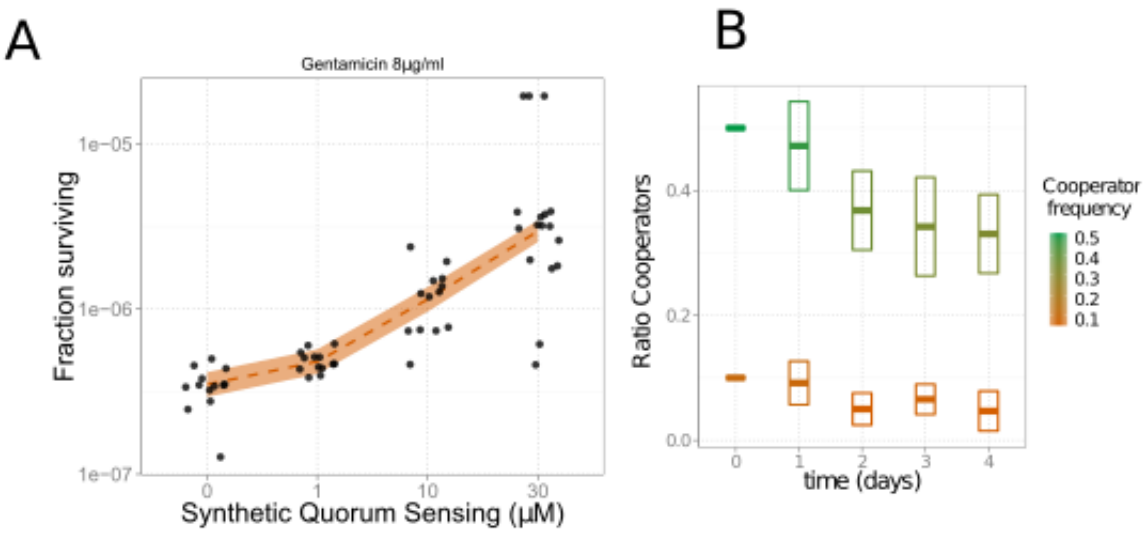

FIGURE 2.4: **Beneficial effect and vulnerability of the public good mediating the social interaction described in Fig. 2.3. A**) Survival to Gm of a population constituted only by cheaters increases when the essential QS (i.e. the public good) molecules are added to the pre-incubation medium, before being exposed to stress ($8\,\mu g\,mL^{-1}$ Gm, black dots represent $N = 17$ replicas per QS dosage, solid color represents 95% confidence interval of a local polynomial regression). **B**) Decay in the fraction of cooperators in a mixed population as cheaters, which do not pay the cost of synthesizing the public good, invade over time. Cheater invasion is independent of the initial fraction of cooperators (10% or 50%). Boxes indicate the standard deviation associated to the experimental estimation of ratios. (see *Materials and Methods* for protocol details).

We aimed to capture experimentally the fundamental features of the simulation: the population collapse induced by cheater invasions, and the subsequent recovery of cooperators. We designed a minimal experimental protocol to study the dynamics of the engineered bacterial interaction: we assembled a population with a specific frequency of our cooperator and cheater strains, and distributed it in a 96-well microtiter plate mimicking the transient division into groups. The social interaction occurs as bacteria are allowed first to grow for a time T_1 in which the public good molecule accumulates, and then exposed to the antibiotic stress for a second time

period T_2. Subpopulations are then plated and surviving cells are counted, merging the individual results into a population measurement. The outcome of one such experimental round can then become the initial conditions for a prospective next round (Fig. 2.5A). To test the effect on global resilience of cheater expansion we initially assembled populations with a high cell density ($\sim 10^4$ cells per subpopulation) and a range of producer frequencies i.e. varying degrees of cheater invasion (Fig. 2.4B). This array of populations was subjected to a level of antibiotic stress where we had corroborated that survival is closely tied to the presence of public good ($8\,\mu g\,mL^{-1}$, Fig. 2.4A). Nonproducer preponderance notably reduced the ability of the population to survive antibiotic stress (Fig. 2.5A), a reduction that was tied (as in the model) to the decreased global levels of public good (Fig. 2.5B inset). An additional feature of the experimental system is that the protective effect of the public good is dose-dependent: a greater antibiotic stress increases the demographic collapse of populations with the same ratio of cooperators (Fig. 2.5C). Furthermore, in this regime, the high initial cell density ensures group homogeneity (that is, every group behaves as the whole population). Cheater invasion, then, causes an overall demographic collapse, the extent of which depends on the amount of cooperators and the intensity of the stress. (Fig. 2.5B,C, respective right panels)

We continued tracking the dynamics of two populations with initial high cell density, 20% producers, and exposed to a medium and strong antibiotic dosages ($9.5\,\mu g\,mL^{-1}$ and $13\,\mu g\,mL^{-1}$, respectively) heretofore termed "pop1" and "pop2" (Fig. 2.5 C). After distributing populations assembled with the "pop1" and "pop2" characteristics population density and frequency (after the first experimental round cooperator frequency did not vary substantially, see *Appendix B*) we evaluated the variability in the composition of the subpopulation generated by the initial population collapse. Identification of a subpopulation as composed purely by cooperators or cheaters, or mixed, is easily achieved by simple phenotypic comparison of the colonies formed by a sample drop (as mixed populations exhibit a characteristic "striped" pattern created by a series of founder effects at the edge of the expanding colony [101]).We subjected these "pop1" and "pop2" populations to a subsequent round of the experimental protocol (Fig. 2.6A).

The two types of trajectories generate distinct distributions of subpopulations (Fig. 2.6B, pie charts depict the distribution of nonempty wells). While both exhibit increased variability in group composition compared to the initial conditions in Fig. 2.5C, the population originated from a greater initial demographic decay, "pop2", is characterized by a predominance of pure cheater groups and assortment of cooperators, which is the class best equipped to survive subsequent antibiotic stress. To comparatively evaluate the rates of recovery of "pop1" and "pop2" populations after the ensuing antibiotic stress, we chose to characterize the survival of pure

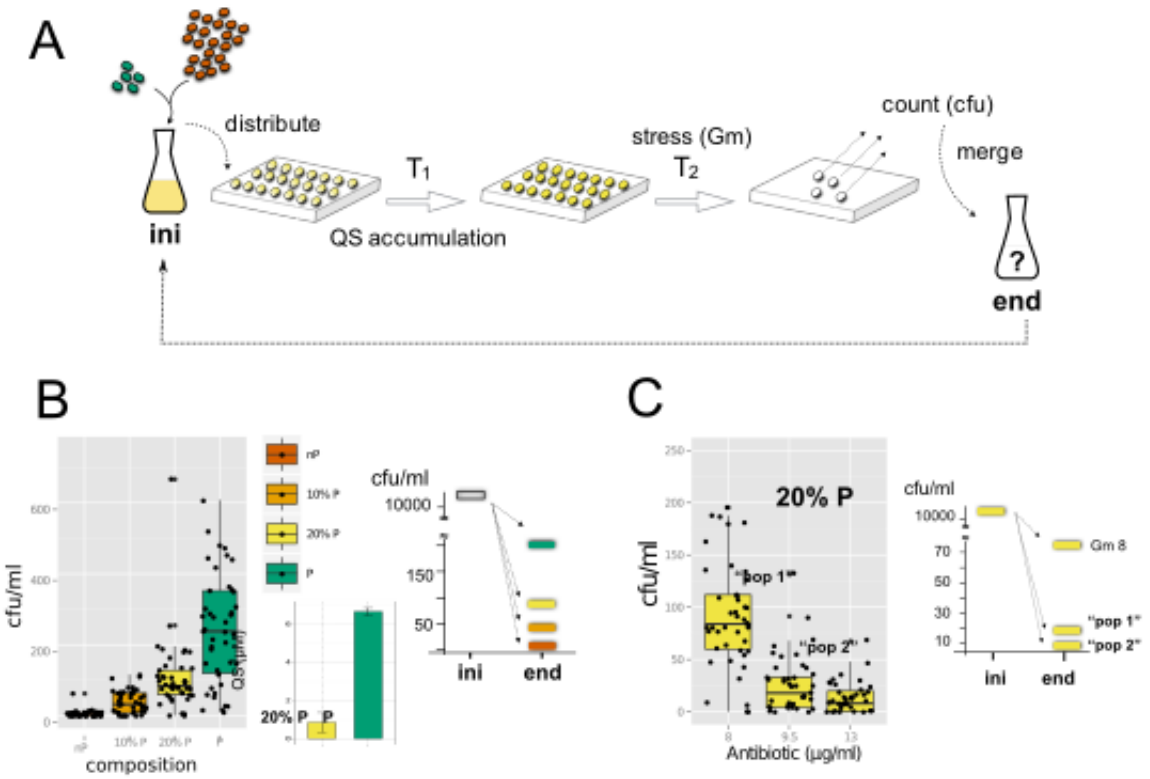

FIGURE 2.5: **Experimental test of the eco-evolutionary feedback: Collapse induced by cheater invasion. A**) An initial population (ini) with specific cell density and composition is distributed in a multiwell plate. Groups (wells) grow and accumulate quorum-sensing (QS) molecules (T_1, without antibiotic) and are reseeded into medium with gentamicin (Gm) (T_2). The final population is quantified by plating each well and merging the values to estimate the full population (end). The outcome of one experimental round can become the initial conditions for an ensuing round. **B**) Demographic collapse after exposure to $8\,\mu g\,mL^{-1}$ of Gm of populations with different composition(represented by colors). Dots represent the result of groups within a metapopulation, box plots represent associated statistical parameters ($N = 45$). Cooperators/cheaters labeled as producers (P)/ nonproducers (nP) of public good, respectively (left). Accumulation of QS at T_1 in groups constituted by 20% or all Ps (inset). Demographic decline of the full population as a function of composition (right). **C**) Demographic collapse under three Gm dosages of groups within a metapopulation from initial density as **B** and 20% Ps. Dots and box plots also as in **B** (left). Demographic collapse of the full population as a function of Gm. Population densities, and associated dosages of $9.5\,\mu g\,mL^{-1}$ and $13\,\mu g\,mL^{-1}$ are correspondingly termed as "pop 1" and "pop 2" conditions (right).

cooperator and pure cheater subpopulations under the respective regimes. This approach bypasses the uneven distribution of each type of group - cooperators, cheaters, and mixed- which would preclude characterization to statistical significance of the scarcer ones, combined with the variability in the specific frequencies

of each strain in mixed groups. Instead, it provides a range of statistically accessible recovery for "pop1" and "pop2" by defining the respective extremes (all cooperators for maximum recovery; all cheaters for the minimum). Recuperation of actual populations will then be found within this range, as mixed groups have been previously demonstrated to obtain intermediate rates of survival (Fig. 2.5B), and will further depend on the specific proportion of each type of subpopulation. In "pop2" trajectories subsistence of cooperator groups is most disproportionate, indicating not only a global demographic increase but a preservation of the public good producers when the populations are again pooled together (Fig. 2.6 B). We verified this statistical approach by measuring the subpopulation distribution and recovery of two actual "pop2" subpopulations, finding in both cases i) assortment of cooperator groups, at low frequency (4 out of 54 subpopulations and 9/53), ii) negligible recovery of non-producer and mixed groups, and, in contrast, iii) substantial recovery of isolated cooperators (Fig. 2.6C). These results confirm the phenomenon observed in the simulation, whereby feedback between ecological and evolutionary processes produce an endogenous mechanism for the preservation of cooperative genotypes: initial -and unavoidable- invasion by cheaters induces a demographic collapse which, mediated by inter-group composition variability, sets the conditions for cooperator assortment and recovery (Fig. 2.6D).

Constraints on the social system induce secondary effects on the dynamics

In an actual biological system – in contrast to the simulation described above – the many features of the organism are entangled with those of the specific social interaction of interest. Even in a synthetically implemented social interaction we found this to be the case. Particularly, we explored two features of the bacterial system that interact with the functionality of the public good i.e. with resistance to an antibiotic stress: cellular growth stage and the emergence of spontaneous mutants. Because antibiotics interfere with the normal growth processes of bacteria (such as targeting the ribosome, as is the case of the aminoglycoside antibiotic chosen here, gentamicin), entering a state of reduced growth can indirectly provide tolerance to a bactericidal. When bacterial cells grow to large numbers and thus close to exhausting the resources of the medium, they enter a stationary phase of reduced growth ; when exposed to fresh medium cells experience a certain delay before resuming division. This lag phase can protect bacteria from the antibiotic present in the medium in a way that is entirely independent of the available public good (Fig. 2.7A, right)[28]. Populations growing from a longer time, or starting from a higher initial cell density, would thus enter stationary phase and benefit from this effect. However, extended

growth can also have a detrimental impact on the stress-protecting social interaction (Fig. 2.7A, left): the metabolic changes associated with stationary phase produce changes in the medium that degrade the public good molecule (specifically, an increase in pH due to the switch from consuming sugars available in LB broth to aminoacids) [102]. Another aspect tied to growth dynamics of the populations is the appearance of spontaneous mutants that can resist the antibiotic [103], again through means tangential to the social interaction. These mutations can rescue a population that is directed towards decay due to lack of public good (such as an all-cheater subpopulation) thus deviating from the predictions of social theory. This type of rescue becomes more probable as population size increases (Fig. 2.7B,C), and more rare as the antibiotic dosage is strengthened [29]. All these effects arise from the particular features of the organism and combine with the social interaction to ultimately determine the destiny of the population. Of note, in "pop2" conditions the low initial cell density and high antibiotic dosage create conditions where these two discussed phenomena (protection due to lag phase and spontaneous mutation) have lesser impact; survival then is essentially mediated by the public good interaction.

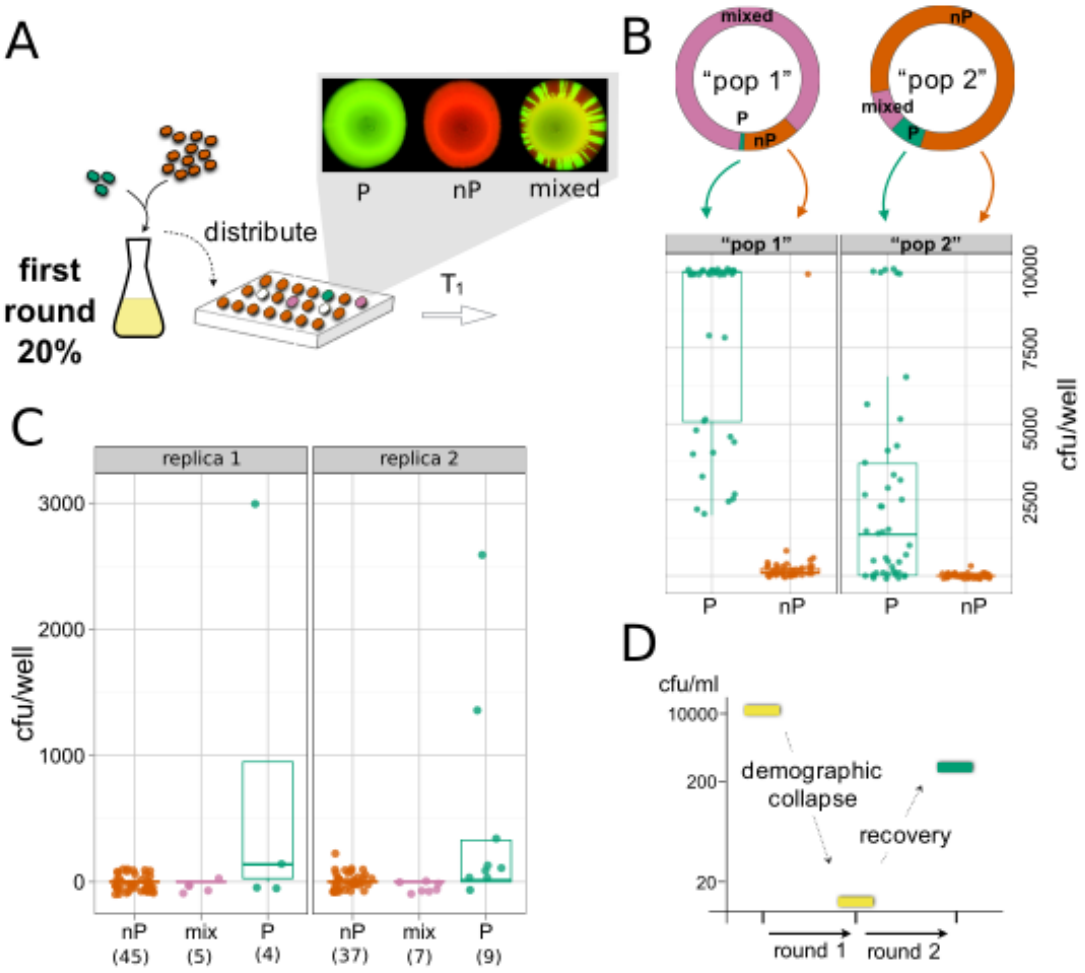

FIGURE 2.6: **Experimental test of the eco-evolutionary feedback: recovery of cooperators**. **A**) An ensuing round of the protocol implementing the eco-evolutionary dynamics of the model was prepared using as initial conditions the outcome of previous rounds with 20% initial Ps (Fig. 2.5C) termed "pop1" and "pop2". Resulting group variability was assessed by direct observation of the colonies arising from a sample of each subpopulation (top image), classifying the groups as pure cooperators (P, green), pure cheaters (nP, red) or mixed (striped) (see main text). **B**) Second round of the experimental protocol with initial conditions corresponding to those of either “pop 1” or “pop2” in Fig. 2.5C. The pie charts show the experimental distribution of nonempty wells determined as described in **A**. Quantification of the characteristic tolerance of groups of only Ps and only nPs is done by engineering replica populations with “pop 1” and “pop 2” cell densities, application of the protocol with correspondent Gm, and measurement of the recovery (dots represent a replica well, $N = 45$). A maximal value of 10000 cfu/well denotes strong recovery. **C**) Verification of the range of recovery rates determined in **B** in two replicate populations with "pop2" conditions, grouping the outcome of individual wells according to composition (the number of wells of each type is indicated below the x-axis). **D**) Summary of the experiments confirming the eco-evolutionary feedbacks that preserve cooperation. While the first round of the protocol causes a demographic collapse of the initial full population (20% Ps), it also generates a sufficient variance in the metapopulation, in a second round, to allow the recovery of cooperators (recovery is proportional to the characteristic growth of P wells and their abundance in a “pop 2” metapopulation, see *Materials and Methods*).

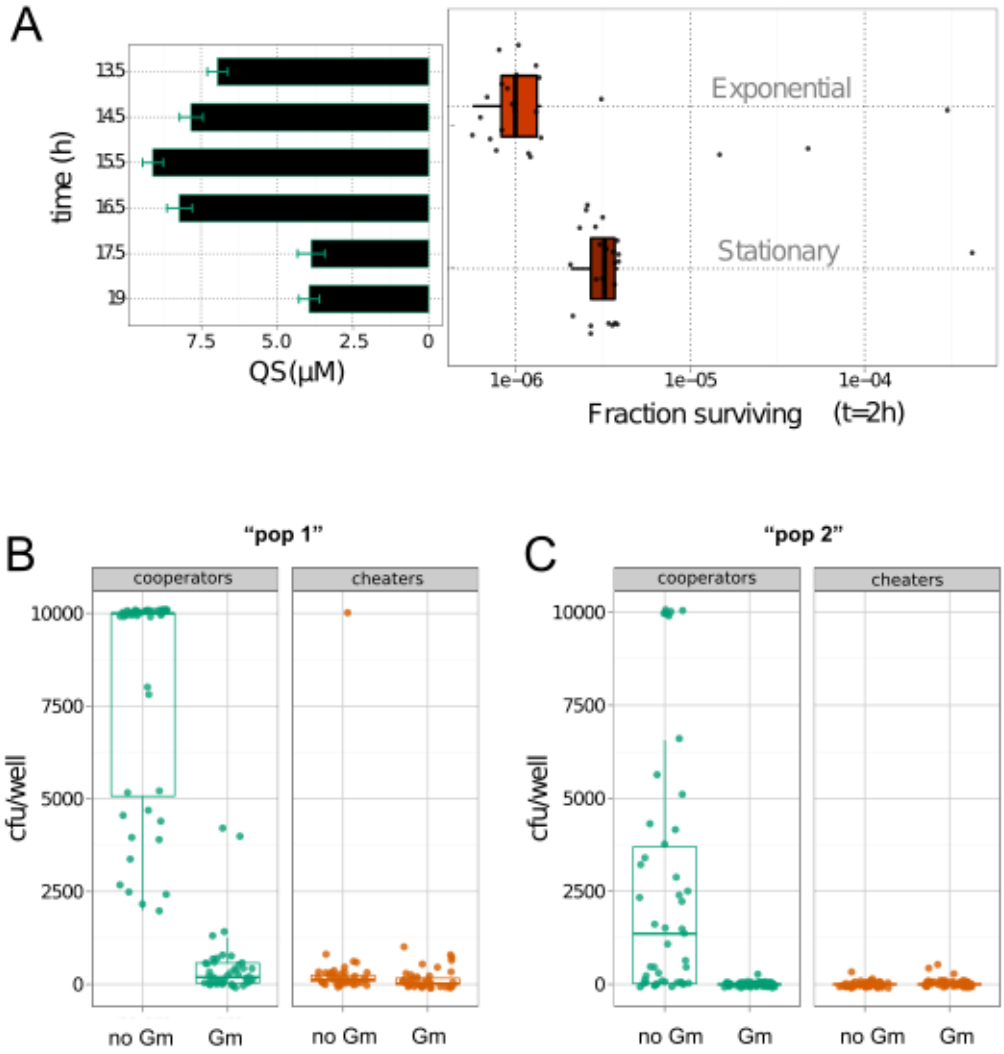

FIGURE 2.7: **Influence of secondary effects on the maintenance of public good-based communities under antibiotic stress**. **A**) Cheater cells in exponential or saturating phase were resuspended in medium with gentamicin (Gm) (*Materials and Methods*). Cells in exponential phase experienced less antibiotic tolerance (Gm = $12\,\mu g\,mL^{-1}$, dots correspond to $N = 45$ replicas, box plots indicate associated statistical parameters)(right). Concentration of quorum-sensing (QS) molecules decays as a function of time of growth [102], starting from an initial low-density of cooperators, i.e., "pop 2" density condition in Fig. 2.5C. Bars represent measurement errors associated to QS estimation (*Materials and Methods*) (letf). Starting from these "pop 2" initial densities, and after an accumulation time of 15.5 h (T_1), cells are in exponential phase, and the amount of QS is maximal. Recovery is thus strongly linked to the presence of the public good. **B,C**) Emergence of spontaneous mutants to Gm. Initial populations of cooperators and cheaters are subjected to an accumulation and stress protocol under the "pop 1" and "pop 2" conditions (same as Fig. 2.5C; black dots represent replicas, $N = 45$; box plots represent statistical parameters). We repeated the experiment for each strain and dosage, so that one can quantify the typical resulting population, and also the mutant subpopulation (by plating with Gm and without Gm; the specific plating dosage of antibiotic corresponds to that of the matching growing conditions). Emergence of spontaneous mutants is reduced at higher dosage **C**, i.e., "pop 2" conditions. Tolerance is most significantly associated in this regime to the presence of the public good.

Characterizing a novel phenotype: the subcellular localization of a bacterial public good

To further study the complexity that biological constraints introduce in public good dynamics, we selected one particular effect in a natural system, pyoverdin production in *P. fluorescens*. Pyoverdin is one of the most widely studied molecules with a social aspect, the intricacy of which is still being unraveled. It must be noted that while many of the studies concerning the social dynamics of pyoverdin are performed using *P. aeruginosa*, and there is a great diversity of pyoverdin-receptor pairs in this bacterial genus, comparative genomic analysis of *P. aeruginosa* and *P. fluorescens* enables careful translation of a great proportion of the conclusions across both strains [104]. Some observations challenge the assumed homogeneous distribution of pyoverdin in the medium, finding instead some evidence of personalization [30, 88]. We focused on a highly specific phenomenon that could be tied to this type of distribution: previous unpublished observations noticed an accumulation of the molecule in the cell pole of *P. fluorescens* cells but no systematic characterization or plausible mechanisms were available. What follows is an attempt to set the foundation for the rigorous description of this effect and its possible functional implications. In a more global perspective, this adds to the growing interest in thoroughly contextualizing a purported social interaction in its ecology and natural physiology, including subcellular localization processes [10].

Observed under epifluorescence microscope in the pyoverdin emission range (460 nm), microcolonies of *P. fluorescens* present fluorescence that is evenly distributed all over the cells with highest intensity in the cellular edges, reflecting the periplasmic localization of the molecule. In contrast, our phenomenon of interest manifests as an intensified fluorescence spot in the cell pole. We tracked the growth of microcolonies of *P. fluorescens* SBW25 on an agarose pad in succinate minimal medium, which is known to promote the production of pyoverdin (Pvd) [88], with an epifluorescence microscrope equipped to visualize the siderophore. Initial assessment revealed that the appearance of bright Pvd spots in cell poles (heretofore termed "polarization")(Fig. 2.8A) can be reproduced through extended culture of the cells, of at least an overnight ($\sim$ 16 - 18h) (Fig. 2.8B,C). Under these conditions polarization was clearly distinguishable in some of the cells forming part of smaller colonies, as longer culture increased the probability of obtaining large multilayered colonies where individual cells could not be properly visualized. A control experiment where nonproducing mutants (defective in one of the initial synthesis steps, the sigma factor PvdS) were grown in the same conditions confirmed that the observed bright spots were due to the presence of Pvd and not some artifact of the fluorescence measurement. Importantly, polarization is only present in nondividing cells, as it only appears once the microcolonies that have grown from an initial inoculated cell reach

a final, stable size. In all the analyzed samples this phenotype displayed great variability, appearing in some cells but not others; and then in some cells earlier and others later. Preliminary observations are consistent with polarization appearing within the first few hours after colony growth has halted (Fig. 2.8 C, where growth stops after 10h of culture and the first identifiable pyoverdin spots appear 1h 30 min later) and reaches a variable proportion of cells in the mature colony (30/58 cells in this colony).

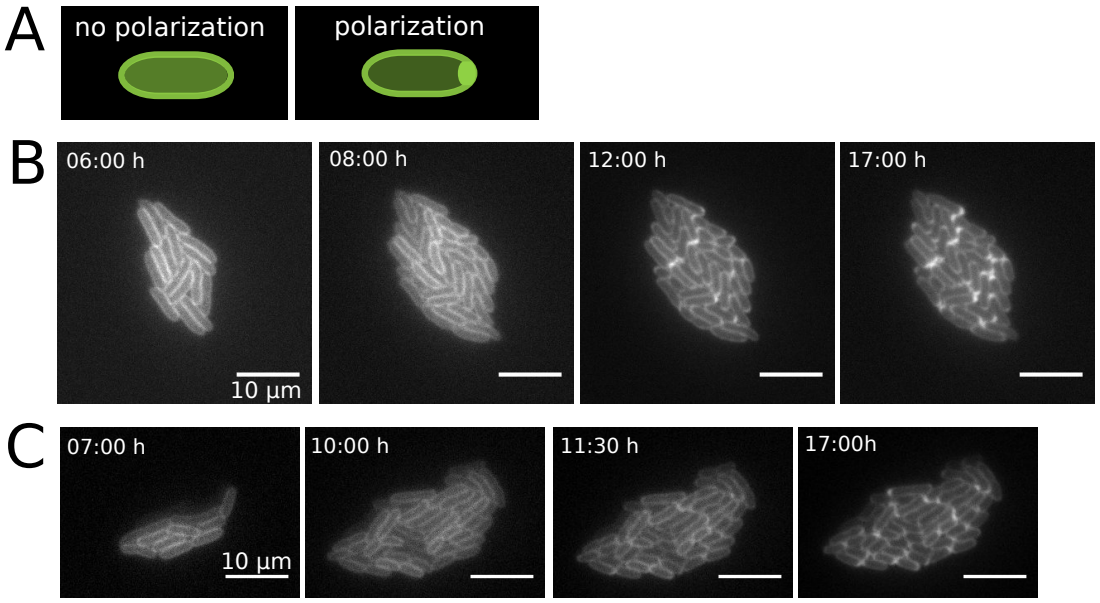

FIGURE 2.8: **Polarization appears as cells stop dividing**. **A**) Cartoon depicting the phenotypic characteristic of polarization i.e. a bright fluorescence spot in the cell pole. **B**) Selected time-lapse images from a growing microcolony of SBW25, reflecting points in which division is still taking place, final colony size and morphology, the appearance of pyoverdin polarization, and the state of the colony at the end of acquisition. **C**) Image sequence from an independent biological replicate in the same conditions as B.

The effect of spatial distribution on microbial social dynamics is well established (see above in this Chapter) and, specifically in the case of Pvd, contact among adjacent cells is responsible for non-uniform distribution of the public good in the related strain *P. aeruginosa* PAO1. To evaluate spatial effects on pyoverdin localization we tested two additional conditions: one where high initial inoculum density precluded division in the agarose pad, and another where cells were grown in liquid medium instead of on the solid agarose surface but in otherwise equivalent conditions. In both cases polarization reappears in a similar fashion to the standard conditions, indicating that spatial structure and cell-cell contacts are not necessary to induce polarization (Fig. 2.9). This suggests that polarization is tied to some individually-sensed signal inducing growth arrest, possibly the depletion of some essential nutrient. One

intriguing candidate is oxygen (of which we expect quick reduction given the preparation of the samples, see *Materials and Methods*), given that its has been previously described to affect pyoverdin social dynamics [30].

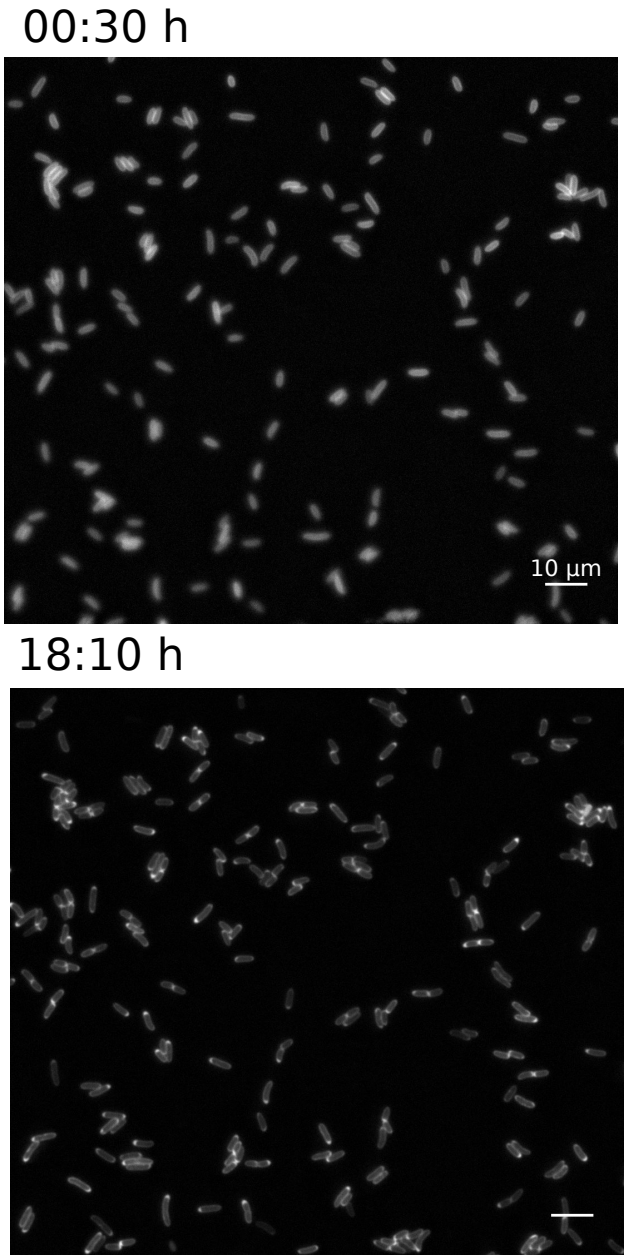

FIGURE 2.9: **Polarization is independent of spatial effects**. Selected time points in a time-lapse acquisition of an inoculum of SBW25 prepared with high cell density (standard density conditions were selected to observe $\sim$ 10 colonies per frame; these images reflect a cropped region of a photographic frame of equal size) at the beginning and at the end of acquisition time. Cell crowding prevents division in these conditions, allowing the direct observation of isolated bacteria.

Pyoverdin is transported across the periplasmic membrane of *P. fluorescens* by specific transporters, some of which participate in both extrusion of freshly synthesized molecules and their recycling after iron acquisition such as OpmQ-RT, but other unknown mobilization mechanisms exist [105]. Thus, the observed accumulation of Pvd at the cell poles could be attributed to recently synthesized pyoverdin that is failing to be exported to the medium after maturation, or to imported siderophores that are remaining in the periplasm after iron release. As a first approach to distinguish between these two scenarios, we co-cultured pyoverdin producing *wild type* SBW25 with the PvdS mutants (which we previously checked for an absence of any fluorescence signal in the Pvd wavelength). Nonproducers were tagged with red fluorescence to enable their identification (*Materials and Methods*). Presence of polarization in microcolonies of Pvd-defective mutants indicates that the uptake/recycling machinery is sufficient to produce this effect (Fig. 2.10); additional tests with cultures of pure nonproducers and Pvd from the filtered supernatant of *wild type* SBW25 confirmed this observation .

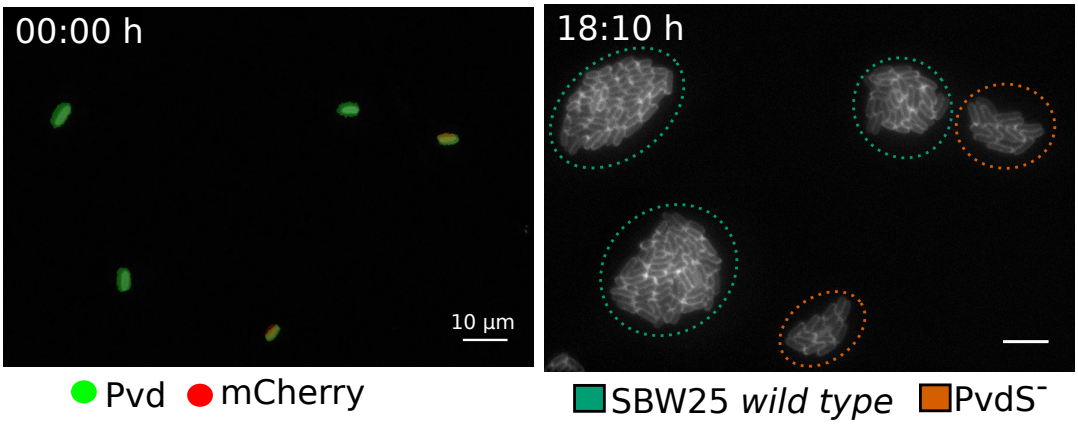

FIGURE 2.10: **Uptake/recycling machinery is sufficient for pyoverdin polarization**. Culture inoculated with a 50/50 mixture of SBW25 *wild type* (pyoverdin producers) and PvdS defective mutants tagged with red fluorescence (nonproducers). Producers and nonproducers are identified on the first frame of the acquisition time by their fluorescence signal. At the end of the acquisition the microcolonies result from the clonal expansion of the original cells, enabling us to establish their composition as producers (SBW25 *wild type*, green) or nonproducers (PvdS mutants, red)

Another feature of relevance regarding a possible functional role for pyoverdin polarization was reversibility, which would indicate that this process is part of the cellular repertoire of the bacteria rather than an artifactual marker for decaying or damaged individuals. To test this, we generated an initial inoculum of SBW25 cells in conditions where polarization was reliably obtained, with the added experimental design feature that we should be able to collect the final culture and re-inoculate

a fresh agarose pad (*Materials and Methods*). We monitored the ensuing inoculum in our standard conditions and we were able to capture the "depolarization" of some cells, corroborating reversibility and the association of polarization to an active cellular state. Furthermore, we observed pre-polarized cells as they again divided and acquired polarization towards the end of the culture time (Fig. 2.11). This suggests that polarization is part of the normal functioning of *P. fluorescens* SBW25 populations, reinforcing also the apparent incompatibility of the polarized phenotype with cellular division.

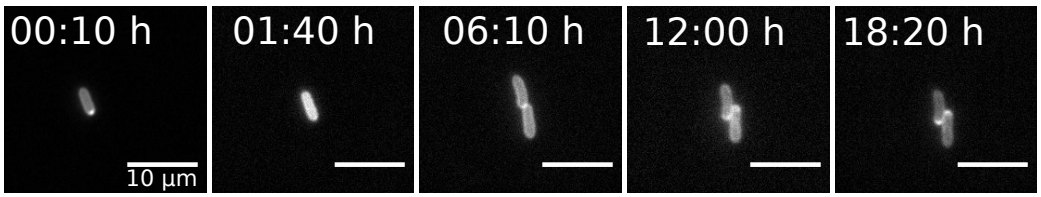

FIGURE 2.11: **Polarization is reversible**. Selected images from the time-lapse acquisition of a sample prepared by obtaining the inoculum from conditions in which cells are in the polarized state. (Aside from inoculum preparation, the experimental protocol remains equal). At the start of the acquisition time, some cells appear in a clearly polarized state (first frame). Within the first hours of incubation, the Pvd spot disappears from the pole and fluorescence is again evenly distributed (second frame). The cell is alive and able to undergo one cycle of division, maintaining the depolarized phenotype, after which polarization begins to reappear (third and fourth frames). At the end of the acquisition time both daughter cells again display polarization (fifth frame).

2.4 Discussion

With a combination of simulations and experiments, we demonstrated how feedback between evolutionary and ecological processes can determine the destiny of a microbial social community. This effect is mediated by specific attributes of the social system; in this case, essentiality of a public good. The final ingredient shaping the primary dynamics that we describe here is spatial structure. The interplay of eco-evolutionary phenomena with these additional features produces the counterintuitive preservation of cooperative behavior after cheater invasions. Here, exploitation by cheaters lead to a demographic collapse that, through spatial constraints, results in the assortment of cooperators and their eventual recovery. This type of dynamics had been explored theoretically [27] and experimentally, where the necessary inter-group variability was deliberately introduced (in order to clearly show an effect known as Simpson's Paradox [25]). Instead we explore conditions where this mechanism is endogenous.

The sustainability of cooperative behaviors is a subject of intense study, in which experiments with microbes have become both a tool and a subject of discussion [24, 72]. Indeed, impact of spatial structure on a social interaction was developed in social evolution theory and has been directly observed in growing colonies of microbes producing a public good, where the establishment of assorted subsections ensured protection of cooperators from cheaters [101]; and during range expansions [106, 107]. Frequency dependence is another well-known variable determining social outcomes [75, 78, 108]. However, the notion of integrating evolutionary and ecological dynamics is a recently proposed framework [6] that has only started to be explored experimentally in social microbial systems [8].

The use of a synthetic system eliminates some of the regulatory complexity of natural public goods [109] and allows us to specifically explore the combined role of essentiality and spatial structure in the stabilization of cooperation through eco-evolutionary feedbacks. We engineered a social interaction between two strains of *E. coli*, where cooperators constitutively synthesize a public good molecule that enables tolerance to an antibiotic stress (Fig. 2.3). Essentiality of the public good directly ties the abundance of cooperators to population size after exposure to stress (Fig. 2.5.) Spatial structure translates the lack of population resilience due to cheater invasions into assortment of cooperators, and thus recovery (Fig. 2.6. These basic properties of a biological system generate intrinsic eco-evolutionary dynamics that preserve cooperation (Fig. 2.2). Nevertheless, we recognized the ramifications of additional biological features and constraints on the cooperative interaction. Specifically, we evaluated how bacterial mechanisms to resist antibiotic stress that operate in tangential or even contradictory manners to our public good can influence the

dynamics. While in the conditions where cooperator recovery after cheater-induced collapse is strongest these effects are shallower (Fig. 2.7), we highlight the potential integration of multifaceted phenomena into a social interaction.

Recent discussions have also emphasized the need to properly contextualize purported microbial public goods, including approaching the natural living conditions of the organisms and biophysical and molecular-level processes. While we have focused on one particular microbial interaction, cooperation, the larger effort to understand the complex interplay of evolution and ecology modulated by molecular and biophysical constraints applies to other social behaviors such as competition [110]. We make an additional contribution to this research avenue by analyzing populations of bacteria involved in the production of a molecule with social aspect.

We were able to narrow down some of the characteristics of a previously undescribed phenotype for *P. fluorescens* SBW25 and the conditions under which it manifests: localization of the siderophore pyoverdin in the cellular poles, in contrast to its usually homogeneous periplasmic distribution. Polar localization is a pattern of molecular cellular distribution associated to important bacterial functions [111], such as cell division, flagellum motility and chemotaxis [112, 113]. Indeed, specific cues produce the active localization of proteins to the cell pole, such as membrane curvature (in the process of sporulation), membrane potential (in cell division) and membrane lipid composition (biofilm formation, protein secretion) [114]. Thus, precedent exists for an interest in localization to the cell poles and the exploration of a possible functional role.

Furthermore, polarization of pyoverdin in *P. fluorescens* could impact on the eco-evolutionary dynamics of this species, as siderophore production is a cellular behavior with social implications. Pyoverdin synthesis in the related species *P. aeruginosa* has long been used as a canonical model for public goods in microbes, a view whose generality has been challenged [30, 86]. Evidence exists of pyoverdin producers maintaining a fitness advantage over nonproducers in contexts where a social dilemma should be in full effect. In growing colonies of a *Pseudomonas* sp. pyoverdin is mostly transferred locally among adjacent cells [88]. A recent study showed that privatization can delineate competitive strategies between different siderophore-producing strains [86]. This again places an interest on the asymmetrical distribution of the siderophore that we describe here.

We observed that localization of pyoverdin to the poles was associated to one particular state: nondividing cells. As a preliminary study case, the colony displayed in Fig. 2.8C was analyzed with the segmentation package for Matlab SuperSegger (`http://mtshasta.phys.washington.edu/website/SuperSegger.php`), which tracks cell lineage as the microcolony develops. This

allows the identification of the old and new cell poles of each cell; in the cells presenting polarization slightly over 50% (57%) displayed it in the old pole as identified by the software. Alternatively, the cell tracked in Fig. 2.11 underwent one cycle of division, after which polarization reappeared in the new pole of both daughter cells. The only association between cellular poles and siderophore production described in the literature is the placement of siderosomes, protein complexes carrying the initial cytoplasmict steps of pyoverdin synthesis. Siderosomes cluster at cell poles (preferentially old, but also new) during early exponential phase, delocalizing in late exponential phase and stationary phase [105]. Because we are observing mature pyoverdin, which does not enter the cytoplasm, and polarization appears in the opposite stages of the cell cycle, it is unclear how both phenomena could be connected. While polarization is clearly linked to nondividing cells, there is great variability in terms of which individual cells display polarization and the timeline of its appearance. In the colony analyzed above (Fig. 2.8C), approximately 50% of the cells are polarized by the end of an overnight culture (18 h). This proportion is roughly consistent with other replicate colonies by ocular inspection, (when identification of individual cells and thus quantification is hindered by their overlap). Phenotypic variability in a clonal bacterial population could be tied to intrinsic noise in the underlying molecular process; it is also a marker for specific ecological strategies such as bet-hedging, a possibility that while unevidenced at this point regarding polarization cannot be entirely discounted [115].

Given that undergoing division is not a requirement for the development of polarization in a particular growth environment (Fig. 2.9) and that neither is cell-cell contact or a particular spatial distribution – de-emphasizing a possible connection of this phenomenon with the two well established social variables of space and kinship – one possible cause for intercellular variability lies in the individual sensibility to an environmental trigger for polarization. This signal could be related to growth arrest, such as the depletion of an essential nutrient. In our experimental samples we observed a clear gradient of colony growth from the oxygen source, making this gas a likely candidate (although not discounting scarcity of the carbon source as the defining variable) Oxygen is closely tied to siderophore dynamics, as its absence increases iron solubility and renders pyoverdin unnecessary, even maladaptive [30]. Shifts between oxygen rich, pyoverdin-requiring and oxygen poor, pyoverdin-redundant conditions could mediate a possible functional role for polarization in this strain.

Another aspect of the discussed sociality of pyoverdin production concerns the contrast between laboratory and ecological conditions i.e. is abundant siderophore production, with its associated social conflict, an artifact of experimental manipulation? [30]. As an exploratory depart from laboratory to more natural conditions, we cocultured *P. fluorescens* SBW25 with a cellulose-degrading *Bacillus* sp. strain from the

Rainey Lab collection, where this polymer was the only carbon source (which SBW25 is unable to process unaided). We were able to recover the polarized phenotype in these communal conditions, which suggests polarization is not entirely dependent on our particular experimental design.

Reversibility of the polarized state eliminates another possible artifactual explanation for this phenomenon: as an indirect marker for dying cells (Fig. 2.11). Elucidating the molecular mechanism behind polarization would reveal whether it is a specific and/or active phenomenon, the first clues of which are revealed by co-culturing SBW25 *wild type* and nonproducting mutants. Expression of pyoverdin localization in nonproducers suggests that the molecular recycling machinery is sufficient for the development of polarization (Fig. 2.10). Construction of the appropriate deletion mutants of the importers and exporters of the siderophore would be an essential next step in the rigorous understanding of this phenotype. Additionally, because pyoverdin is only visible in its unbound state, and there is evidence that most of the specific receptor (FpvA) sites are occupied by this molecule regardless of iron availability [116], we could be visualizing one possible stable siderophore distribution – of course, questions would remain regarding polar localization and intercellular variability.

In sum, while the phenotype described here is highly specific, its thorough characterization is tied to important aspects of the ecophysiology of *P. fluorescens* SBW25, from the integration of the nutrient-scarcity response of siderophore production with other environmental cues, to a potential role in community dynamics. Its description at all levels of complexity – molecular to eco-evolutionary – will ultimately add to the understanding and proper contextualization of microbial public goods [10].

Chapter 3

Evolutionary Interactions

3.1 Introduction

Antibiotic resistance is one of the greatest upcoming global health challenges [117], and one of the best documented real-time examples of evolution in motion [118]. The rapid spread of resistance has created the need to go beyond traditional clinical tools and tackle it with system-level approaches [16]. These approaches include the use of high-throughput technologies and *-omics* analyses for the surveillance and characterization of resistance; it also requires us to take an ever closer look at basic ecological and evolutionary processes [119]. Here the role of microbes as tools for experimentation reappears, as experimental evolution in controlled laboratory settings [19] provides clues into the evolutionary processes defining antibiotic resistance in the clinic. Again, it becomes fundamental to integrate system variables at different levels of complexity, from the molecular features of antibiotic resistance to the properties of genomic evolution and how they influence each other reciprocally.

Details matter: molecular mechanism of antibiotic action and acquired resistance

Antibiotics are small molecules that inhibit microbial cell growth by halting division (bacteriostatic) or actively killing cells (bactericidal). Some of them were discovered in the early 20th century as natural compounds secreted by microbes, and since many synthetic drugs have been developed based on their basic design and properties. Antibiotics interfere with the essential cell functions of DNA replication (eg. quinolones), translation (eg. rifamycins) and transcription (eg. aminoglycosides); with the structural integrity of the cell (eg. β-lactamases) and with its energy metabolism (eg. sulfonamides). While each antibiotic has a specific subcellular target (eg. kanamycin and other aminoglycosides bind the 16S rRNA component of the 30S ribosome subunit, promoting tRNA mismatching during translation which produces misfolded proteins), the cell damage caused by these drugs is tied to many

indirect effects (such as increased cell membrane permeability due to the insertion of misfolded proteins) and general cellular responses (such as the generation of cell-disrupting hydroxyl radicals due to the action of most bactericidal antibiotics, despite their differing molecular mechanisms of action) [120].

In a similar fashion, bacterial resistance to antibiotics is achieved through both specific and general mechanisms. Some taxa are equipped with intrinsic resistance to certain antimicrobial agents, due to their cellular architecture (Gram negative bacteria have an additional protective layer against β-lactams in their external membrane) and particular species characteristics (*Pseudomonas* spp. are resistant to many antibiotics due to their large repertoire of efflux pumps [121]). Indeed, antibiotic resistance genes are naturally present even in ancient environments [122]; it is acquired resistance by clinically relevant pathogens that is a global health concern. Antibiotic resistance or tolerance can be achieved by i) avoiding drug-target interaction, ii) altering the target, iii) disabling the drug. Avoiding drug-target interactions is usually achieved by nonspecific mechanisms that decrease the intracellular concentration of the antibiotic, such as a reduction cell permeability or augmented efflux through energy-dependent pumps. Resistance through these mechanisms has been described for a large proportion of antibiotics, such aminoglycosides, chloramphenicol, macrolides or tetracycline [103, 123, 124]. Specific mechanisms following this strategy also exist, as in the case of proteins protecting the molecular targets of quinolones, DNA gyrase and topoisomerase IV [124, 125]. The second strategy consists of modifying the antibiotic target to reduce the effectiveness of the drug against it. This can be achieved by direct mutation of the molecules involved, such as PBPs (Penicillin Binding Proteins) with reduced affinity for β-lactams, modified peptidoglycan precursors protected against glycopeptides, or mutations in the DNA binding surface in the genes for DNA gyrase and topoisomerase IV conferring resistance to quinolones [124]. Alternatively, the antibiotic target can be chemically modified by other enzymes to achieve the same result of reduced affinity for the drug; examples include methylation of different rRNAs protecting against ribosome-targeting antibiotics such as aminoglycosides and macrolides, lincosamide and streptogramin (targeting the 30S and 50S subunit, respectively). Finally, instead of protecting the cell against the toxic compound, resistance can be acquired by altering it. Antibiotic-modifying enzymes include a wide range of acetyltransferases acting against aminoglycosides, chloramphenicol or tetracycline, and antibiotic-degrading proteins act against β-lactams or fosfomycin [103, 123–126].

Fast acquisition of antibiotic resistance can occur through non-genomic mechanisms

The evolutionary features previously described would apply to *de novo* genomic evolution of antibiotic resistance. However, bacteria can acquire resistance through horizontal gene transfer (HGT). Antibiotic-modifying enzymes are frequently obtained by HGT, but other genes are amenable to this mode of transmission such as alternative versions of the drug target and efflux pumps. Mobile genetic elements conferring antibiotic resistance comprise DNA molecules of varying autonomy, such as plasmids (which are self-replicating), integrons, and transposons. These elements can be transmitted via conjugation (that requires bacterial contact with a specific molecular machinery) or transformation (where naked DNA molecules can be incorporated into a bacterial cells), and some can be shared among different species. Transduction via bacteriophages has also been described to spread antibiotic resistance genes. Like genomic resistance, HGT-acquired resistance carries associated fitness costs and is subject to compensatory mutations. Additional constraints apply, such as incompatibility between some plasmid classes and bacterial mechanisms to guard against foreign DNA such as the CRISPR/Cas system. HGT induces an incredibly rapid spread of resistance, with its instantaneous acquisition of one or multiple genes and inter-species promiscuity [123].

Evolution experiments in microbes allow us to directly observe evolutionary processes

Although there has been recent discussion about the integration of simultaneous evolutionary and ecological phenomena [6] evolution is typically thought to occur over long timescales. Consequently, its outcomes and processes are inferred indirectly in most cases. Microbes, however, present such short generation times that, when combined with new high-throughput technology such as whole genome sequencing, the direct observation of evolution has been enabled. Experimental evolution is a framework in which functional and evolutionary questions can be answered with molecular detail [127]. Briefly, it involves the prolonged culture of microorganisms under carefully designated selective pressures and the posterior analysis of evolved clones; with the possibility of storing intermediate time points akin to a "fossil record". A notable example is the Long Term Evolution Experiment (LTEE) where parallel populations of *Escherichia coli* have been evolving in glucose-limited medium for >50.000 generations, finding unexpected adaptation to a novel carbon source through potentiating mutations [11] in one of them. Data from the LTEE also allowed exploration on the prevalence of epistasis during evolutionary trajectories

of bacteria, finding a predominance of negative interactions that produce diminishing returns in fitness as adaptation progresses [13]. Experimental evolution has shed light on some basic characteristics of the evolution of antibiotic resistance. An evolution experiment were bacteria were under constant antibiotic selective pressure revealed that the shape of an adaptive trajectory depends on the size of the genomic mutational target, where smooth adaptation results from many possible mutations with cumulative effects whereas a sharp step-wise adaptation is tied to a small target with sequential mutations [36]. Adaptation of *Pseudomonas aeruginosa* to an antibiotic showed changes in distribution of fitness effects of beneficial mutations (DFBM) under increased drug doses: whereas at low concentrations the DFBM consists mainly of rare mutations of small effect, a higher antibiotic exposure can shift it towards many mutations of large effect [29]. Even as it simplifies the natural history defining every existing organism, experimental evolution is thus a powerful tool to explore the forces shaping microbial adaptation.

Molecular constraints shape the repeatability of evolutionary trajectories

One essential problem that can be addressed with evolution experiments is the repeatability of evolution: how similar are outcomes of parallel evolutionary trajectories under the same selection pressure? At a broad phenotypic level, repeated adaptation is quite clear, such as the reliable appearance of antibiotic resistance in different species and geographical locations, both in laboratory and clinical conditions. However, the mapping of phenotypic to genotypic changes in an evolutionary context is vastly more complex. Different studies have approached this topic experimentally in microbes, at the level of individual proteins and at the cellular level.

A few studies shed light on the constraints delineating the evolution of the the β-lactamase TEM. Variants of this enzyme, originally targeting ampicillin, can be obtained with activity against numerous β-lactams. Only 5 point mutations increase 100.000-fold its activity against cefotaxime. Assessment of all the possible mutation accumulation trajectories from one version to the other revealed that a majority of them were inaccessible mostly due to sign epistasis (that is, a mutation was only beneficial in combination with specific others, and ineffective or deleterious in the rest) [128]. Another study took a more open-ended approach to the same question, and performed *in vitro* evolution of this protein with the use of error-prone PCR as it measured its adaptation to degrade cefotaxime. While the predominant trajectory was the one previously described, researchers found that initial mutations could direct evolution toward alternative pathways through epistatic interactions [38]. Thus, even though individual protein evolution seems severely constrained by

sign epistatic interactions between mutations, historical chance allows an evolving system to explore different adaptive peaks.

One study assessed the ability of *E. coli* to recover an essential metabolic function lost due to a gene deletion [129]. Growth was recuperated by a combination of structural and, particularly, regulatory mutations in pathways close to the deleted gene, where the contribution of each type of mutation depended on the affected cellular subsystem. In a large number of *E. coli* populations adapting to temperature, an environmental variable with multifaceted effects, researchers found two exclusionary adaptive trajectories of equal fitness but different tradeoffs. Parallelism was clear at at the level of genes, with many beneficial mutations accumulating in a few functional units. At the mutation level, convergence varied by the type of mutation, higher for larger deletions and lower for point mutations (with some widely-shared exceptions) which showed the previously described pattern of negative epistasis within each gene [130, 131].

In general terms, the selective pressure will point towards phenotypic changes with different degrees of underlying molecular specificity. The particularities of this molecular target will shape the repeatability of evolutionary trajectories through differences its size and organization (that is, the availability of targets in which changes can readily be translated into the phenotype), the cost of associated pleiotropic effects, and epistatic interactions between subsequent mutations. Adaptation progresses through a complex interplay of constraints and contingency highly dependent on the genomic architecture of the evolving cellular system [132].

Interactions between bacterial adaptive histories are a promising framework to approach antibiotic resistance

New conceptual and experimental tools against antibiotic resistance incorporate a systems-level view and careful assessment of ecological and evolutionary processes. One such approximation involves tailoring antibiotic therapy to interactions between the drugs [133]. Physiological interactions between antibiotics refer to the masking or potentiating effects of one compound over another when they are co-administered. Synergistic combinations (where the effect of the two drugs is greater than the addition of the individual effects) are more effective at killing bacteria but promote the evolution of multiresistance. Antagonistic interactions (where one drug masks the effect of the other) have the opposite effect, as development of resistance against one uncovers the deleterious effect of the other [134].

Another systems-level approximation considers instead evolutionary interactions. An evolutionary interaction occurs when adaptation to a particular environmental

variable modifies fitness under another variable that the organism has never encountered before. Then, the development of resistance to a given antibiotic can either increase (cross-resistance) or decrease (cross-sensitivity) tolerance to a different drug. A few recent studies have explored this issue, finding that commonalities in responses at the molecular level often underlie the development of evolutionary interactions [33, 34, 135]. Despite the many challenges in translating basic studies into clinical applications, antibiotic interactions are a promising avenue to combat antibiotic resistance [32]. Indeed, success has recently been reported against one of the most resilient multiresistant pathogens, Methicillin-resistant *Staphylococcus aureus* (MRSA), using a combination of drugs exhibiting physiological synergy and evolutionary cross-sensitivity [136].

Our aim is to further understand some of the basic features of evolutionary interactions between antibiotics. We obtain a collection of clones adapted to a set of antibiotics through experimental evolution, and construct their evolutionary interaction networks with phenotypic measurements of resistance. Adaptation to antibiotics can occur through specific (constrained to a small region of the genome or set of genes) or general mutations, and in turn these can be acquired through genomic mutation or horizontal transfer. Genetic features of the resistance determinants, combined with the evolutionary context, can generate adaptive pathways that are more or less repeatable. We discuss how these fundamental evolutionary processes and the specific molecular mechanisms of each drug combine to produce the observed patterns of interactions. Crucially, the diversity of evolutionary pathways that enable adaptation to a particular drug introduces variability in these types of interactions; we specifically focus on the impact that this variability might have on the conclusions established by observing global patterns, which ultimately have implications for the development of clinical protocols.

3.2 Materials and Methods

Strains, culture media, and reagents

All strains are derivatives of *E.coli* MG1655. Overnight cultures for the evolution experiment and MIC measurements were performed in LB (casein peptone 10 $g.l^{-1}$, yeast extract 5 $g.l^{-1}$, sodium chloride 5 $g.l^{-1}$) (Affymetrix). Evolution experiments were performed in M9 minimal medium (M9 salts: Na_2HPO_4 6 $g.l^{-1}$, KH_2PO_4 3$g.l^{-1}$,NaCl 0.5 $g.l^{-1}$, NH_4Cl 1 $g.l^{-1}$; $MgSO_4$ 2mM, $CaCl_2$ 0.1 mM)(Panreac) adjusted to support growth in these experimental conditions following previous work [137], supplemented with 1% casamino acids (Bacto Casamino Acids)(Beckton, Dickinson and Co.) and 1% glucose (D(+)-Glucose)(Panreac). MIC (Minimum Inhibitory Concentration) measurements were performed in 12x12 mm square LB Agar plates (1.5% w/v) supplemented with the necessary antibiotics. All incubations were carried out at 37 °C in static conditions. The following antibiotics were used at the indicated concentrations. Amikacin (Normon), Cefotaxime (Normon), Colistin (Sigma-Aldrich), Fosfomycin (Normon), Imipenem (Sigma-Aldrich), Norfloxacin (Sigma-Aldrich) and Sulfamethoxazole/Trimethoprim 5:1 (Soltrim) (Normon)

Evolution experiment

For each antibiotic treatment, 48 parallel populations were propagated in increasing concentrations of the indicated antibiotics in a 96-wel deep-well multiwell plate (1.1 ml, Axygen) covered with a loose-fitting plastic lid in static conditions. Every 24 h 20 µL of each well was transfered to 1ml fresh medium. The wells were inoculated in a chessboard pattern to minimize contamination, the contamination rate was 1% . Antibiotic dosage was increased every 48 h in a gradient determined by the wild type strain's MIC, starting at 1/4 x MIC and finishing at 128 x MIC in 2^n x MIC steps. Starting with 2 transfer sin antibiotic-free medium, the evolution experiment continued for a total of 21 days. Survival of each well was monitored by visual inspection of turbidity. Clones from the last 6 surviving wells in each treatment were streaked to isolation and stored in glycerol 20% (v/v) at −80 °C. In cases where more than 6 wells were available for clone isolation they were selected randomly using the online random number generator https://www.random.org/. An additional evolution experiment was carried out in antibiotic-free medium for 19 days and the corresponding isolates were used as controls for adaptation to the medium. Intermediate time-points were also stored at −80 °C.

Antibiotic resistance measurements

To characterize the resistance of each clone to the antibiotic set, a standard MIC measurement protocol was chosen. All MIC measurements were performed following the Agar dilution method detailed in [138], using LB as the nutritive medium. Briefly, all 48 strains (7 antibiotics x 6 clones/antibiotic + 6 control clones) were grown overnight in LB without agitation, the concentration was adjusted to obtain roughly the same number of cells per well, and all wells were spotted on a set of LB Agar plates containing growing concentrations of one antibiotic using a pin replicator. The MIC value was considered the lowest concentration at which there was no visible growth of the isolates. 3 biological replicates of each measurement were collected.

Cross-resistance and Cross-sensitivity calculations

Evolutionary interactions between antibiotics were calculated for each clone by normalizing the median observed MIC value by the median MIC of the most representative control isolate. This normalization accounts for a possible interacting effect of adaptation to the M9 medium. Interaction networks were assembled using the log2-fold change of this calculated value, so that an interaction between a clone and an antibiotic is represented by the number of steps increased (positive values, cross-resistance) or decreased (negative values, cross-sensitivity) in a MIC gradient where concentrations vary in steps of 2^n (see [138]). Cross-resistance and cross-sensitivity interactions are considered reliable if they are ± 1, as changes below this threshold fall within the margin of error of the experimental technique. Individual clone networks were aggregated in a summary network depicting the frequency of evolutionary interactions between all clones in each set. To measure the variability within the clones adapted to each antibiotic, we compared the interaction networks of all clones in a given set. To do this, we represented each clone network as a vector where entries are the evolutionary interaction between the clone and each of the n antibiotics. We calculated the distance d between all possible pairs of networks (X and Y) for each clone set as $d = \sqrt{\sum_{i=1}^{n}(cloneX_i - cloneY_i)^2}$, and obtained the mean value.

3.3 Results

Genomic adaptation can generate significant levels of resistance

Starting from a common *wild type* strain (*E. coli* MG1655) we obtained a collection of evolved mutants by subjecting parallel bacterial populations to increasing concentrations of our set of antibiotics (Fig. 3.1, *Materials and Methods*). Antibiotics were chosen to represent a variety of targets and mechanisms, from different drug classes (Table 3.1; SMX and TMP used in combination in proportion 5:1). The antibiotic gradients were determined by the ancestor strain's MIC to the respective antibiotics (Table 3.2), so that the first drug dosage they encounter is $1/4$ of the MIC value and the maximum dosage to which they are exposed is 128xMIC (Fig 3.1).

During the evolution experiment we visually estimated the proportion of surviving parallel populations (Fig. 3.1A). For each antibiotic treatment we isolated 6 clones from the last 6 surviving populations, named after the compound used (Table 3.1) and numbered 1-6. The particular effect on population dynamics associated to each antibiotic provides some initial clues regarding the availability, number and diversity of resistance mutations, with large step-wise changes possibly indicating that mutations are constrained to narrow genomic regions, and smaller continuous changes suggesting a wider mutational target [36]. Differences between antibiotics and clones within a set are already evident from these trajectories, with some drugs inducing early and dramatic population decays (COL,IMP, SMX/TMP); others producing this effect in a gradual manner (CTX, NFX) and others maintaining growth in most parallel evolving populations until the end (AMK, FOS)(Fig 3.1). Consequently, some clones in the same antibiotic set were isolated at different points in the adaptive trajectory (particularly in the gradually decaying trajectories of CTX and NFX, and also SMX/TMP, detailed information is available in Table 3.2). Adaptation was compared not to the ancestor MG1655 MIC but to clones evolved with the same protocol without antibiotic, to control for any possible effects of the medium (*Materials and Methods)*. Clones isolated later in the evolutionary trajectories, and thus selected in larger antibiotic dosages, exhibit a greater increase in resistance (Table 3.2), ranging from an 8-fold increase in MIC for FOS clone 1 (Figure 3.1B, note that MIC increase is expressed in log2-fold, such that an 8-fold increase in MIC means resistance to an antibiotic concentration 256 times the original MIC) to clones that show no significant adaptation such as COL2, COL4 and S-T6. Except in the case of these unadapted clones, all isolates reached, and most significantly surpassed, the Epidemiological Cutoff points (ECOFFS,taken from `https://mic.eucast.org/Eucast2/`) for that antibiotic and *E.coli* (Table3.2).

TABLE 3.1: List of antibiotics used in these experiments.

Antibiotic	**Family**	**Effect**	**Mechanism**
Amikacin (AMK)	aminoglycoside	bactericidal	Binds the 16S rRNA of the 30S ribosomal subunit producing misfolded proteins [123].
Cefotaxime (CTX)	cephalosporin (β-lactam)	bactericidal	Inhibits bacterial cell wall synthesis by binding penicillin-binding proteins (PBPs) and interfering with production of peptidoglycan [137].
Colistin (COL)	polymyxin	bactericidal	Disrupts bacterial cell membrane by binding to LPS (Lipopolysaccharide) [139].
Fosfomycin (FOS)		bactericidal	Inhibits bacterial cell wall synthesis by binding MurA and interfering with production of peptidoglycan [126].
Imipenem (IMP)	carbapenem (β-lactam)	bactericidal	Inhibits cell wall synhesis by binding PBPs [123].
Norfloxacin (NFX)	fluoroquinolone	bactericidal	Inhibits replication by binding DNA gyrase and topoisomerase IV [125].
Sulfamethoxazole (SMX)	sulfonamide	bacteriostatic	Inhibits synthesis of folic acid by binding the enzyme DHPS (dihydropteroate synthetase). [123]
Trimethoprim (TMP)		bacteriostatic	Inhibits synthesis of folic acid by binding DHFR (dihydrofolate reductase) [123].

Acquiring levels of resistance of such clinical significance can usually be traced to the transfer of mobile genetic elements such as plasmids. These plasmids commonly carry antibiotic-modifying enzymes, such as aminoglycoside acetylases (AAC), nucleotidyl transferases (ANT) and phosphotranspherases (APH); and β-lactamases, an extensive range of proteins with different levels of activity against the β-lactam family of antibiotics from the earliest penicillins to fourth-generation cephalosporins and carbapenems. However, in this experimental setup completely *naive* bacteria are able to acquire substantial protection against the aminoglycoside AMK (5-6 MIC fold

increase) and the cephalosporin CTX (4-5 MIC fold increase). In both cases clones were isolated towards the end of the antibiotic dosage range, meaning that bacteria were able to survive 32-128 times their original MIC. On the other hand, the carbapenem IMP exhibited a very moderate increase in MIC (2 fold) and the evolving populations consistently went extinct at a dosage *ca.* 8 x MIC. This suggests that, even though CTX and IMP belong to the same broad antibiotic class, their particular biochemistry translates into different resistance determinants.

Specific genomic alterations conferring significant drug resistance are described for some of the antibiotics used here. Resistance to quinolones is commonly associated to mutations in the molecular targets gyrase and topoisomerase IV[123, 125], and clones evolved under NFX treatment reached notably higher MICS compared to control strains (6-7 fold).

Mutation or overexpression of the – unique for this antibiotic– drug target MurA has also been found to generate high levels of resistance to FOS [137] at a low fitness cost, which could explain the increase in MIC (up to 8-fold) and the large proportion of surviving populations. Resistance to FOS can also be acquired through mutation or downregulation of its transporters, which again are specific for this drug [126].

While a lot of attention has been placed on the plasmidic COL resistance gene *mcr-1* and its quickly spreading derivatives [140], genomic mechanisms to resist polymyxins have also been described. The cellular target LPS can be modified to reduce its negative charge, and thus the binding of colistin (which is a positively charged lipopeptide), by substituting the phosphate group with aminoarabinose or phosphoetanolamine [139]. The MIC increases of 3-5 fold observed in the endpoint isolates could be due to this mechanism.

In the case of the synergistic combination SMX/TMP, where each drug inhibits a different step in the same biochemical pathway, clones exhibited low levels of adaptation. The previously described genomic mechanisms to resist either of these drugs is the overexpression of their targets folA (dihydropholate reductase) in the case of TMP [141] and folP (dihydropteroate synthase) for SMX [123]. These mutations are likely to be insufficient unless combined, a more improbable event that could explain the moderate increase in MIC and the early extinction of evolving populations.

Although not conceived as the main resistance-conferring mutations, alteration of the cellular targets of aminoglycosides – by methylation of the 16S rRNA subunit — and β-lactams – mutating the PBPs to reduce drug affinity – have also been characterized and could give rise to the observed levels of acquired resistance [123].

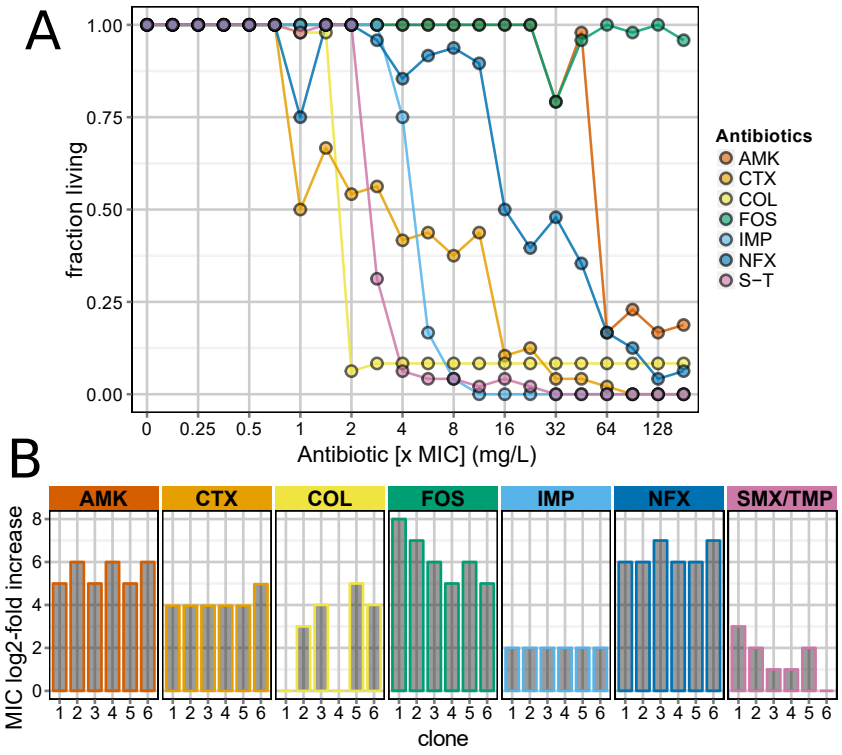

FIGURE 3.1: **Experimental evolution trajectories and acquired resistance of adapted clones. A)** Surviving parallel populations evolving under an antibiotic gradient. Every 24h, 48 parallel bacterial population are diluted into fresh medium. Starting from antibiotic-free medium, every 48h the antibiotic concentration is doubled following a gradient determined by the *wild type* MIC. The proportion of surviving wells in each time-step is estimated visually. Each dot is the proportion of populations with visible growth at the end of the 24h incubation period, colors represent the different antibiotics. **B)** Acquired resistance of evolved clones. A representative clone from the last 6 surviving populations of each treatment is isolated and MIC to the corresponding antibiotic is assessed. Bars indicate the median log2-fold increase in MIC for each isolate and treatment.

Nonspecific resistance mechanisms can explain some interaction patterns

In-pathway mutations that produce significant resistance have been described for most antibiotics, in some cases representing the main mechanism and sufficiently explaining the acquired MIC increases to the selection antibiotic in our isolate collection (detailed above) [123]. Survival to the high dosages to which the clones have evolved would *a priori* point towards these specific resistance mechanisms. However, because most of our antibiotics belong to different classes and thus represent an assortment of subcellular targets (Table 3.1), evolutionary interactions would likely arise from mutations associated to, instead, general mechanisms of resistance. Augmented tolerance (**cross-resistance**) or vulnerability (**cross-sensitivity**) to previously unencountered compounds will then indicate the selection of mutations with pleoiotropic effects, and tradeoffs.

To uncover evolutionary interactions between our set of antibiotics, the resistance of all clones to all antibiotics was measured and deviations from neutrality (i.e. a phenotype indistinguishable from unadapted controls) were assessed (*Materials and Methods*). A pattern of cross-resistance that is consistent and reciprocal across two or more clone sets could be a marker for a general resistance mechanism. The clearest case here is the interaction between CTX and NFX, where 4/6 CTX clones and all NFX clones exhibit cross resistance to each other (MIC fold increase mean=2.25 and 2.8, respectively)(Fig. 3.2). Mutations producing increased efflux and/or decreased cell permeability are strong candidates to explain these interactions. Indeed, down-regulation of the outer membrane porins of the Omp family (OmpF, OmpC) has been described in *E.coli* strains resistant to quinolones [142] and β-lactamases [143]. Another common reported resistance strategy is the overexpression of efflux pumps such as the AcrAB-TolC system [142, 144]. In the case of CTX-adapted clones, a broad mechanism of this kind could also account for their cross-resistance to SMX/TMP (eg.through up-regulation of efflux pumps [145], 2/6 clones interact with MIC fold increase mean=2.5, and reciprocally 3/6 SMX/TMP evolved clones are cross-resistant to CTX with MIC fold increase mean = 2.67). Coresistance to fluoroquinolones and sulphonamides has been observed in clinical isolates of cefotaximase-carrying *E. coli* [146]. This type of resistance mechanism is also coherent with the population dynamics during the evolution experiment, as these smooth trajectories have been associated to a large mutational target set with cumulative and broad effects, tied to the same molecular subsystem proposed here [36].

Previous studies analyzing evolutionary interactions in antibiotics identified a general pattern of increased sensitivity in aminoglycoside-evolved clones [33, 34]. This was attributed to conflicting effects of changes in the membrane potential: while a decrease in this potential reduces aminoglycoside uptake (which is dependent of

the proton-motive force), it also reduces the activity of the multidrug efflux system AcrAB. Hence, sensitivity to the antibiotics usually expelled by this pump is raised. Cross-sensitivity to these antibiotics is not present in our AMK-evolved set of clones, where the only notable decrease in MIC is obtained in FOS (2/6 mutants, MIC fold decrease mean = -2). Instead, significant levels of cross resistance are observed against IMP (4/6 clones,MIC fold increase mean = 2), with some reciprocity (2/6 IMP clones, MIC fold increase mean = 3). This, together with the single-direction cross-resistance of CTX clones to IMP (2/6 clones, MIC fold increase mean=2) creates an atypical interaction profile for both the carbapenem and the aminoglycoside.

The only antibiotic to present a predominance of cross-sensitivity is COL to SMX/TMP (2/6 clones, MIC fold decrease mean = -2.5). A moderate decrease in SMX/TMP MIC in colistin resistant isolates of *P. aeruginosa* has been observed in at least one study [147], with no further mechanistic discussion. Further analysis of these clones with increased susceptibility would reveal if this interaction could be of clinical importance, given the role of COL as a last-resort antibiotic against particularly multiresistant pathogens.

Another striking pattern is found in FOS clones, which exhibit the highest acquired resistance and survival during the evolution experiment, yet are dramatically lacking in interactions with other antibiotics. Specificity of the described genomic mechanism of resistance could explain this phenomenon.

Parallel evolutionary trajectories generate unique interactions

If there is a predominant mutational target to increase resistance, we expect a family of clones to present similar interaction profiles with different intensity (allowing for nonsignificance of some interactions under our measurements). This generates the global interaction patterns between antibiotics observed in this work and in previous studies [33, 34, 135]. On the other hand, chance can allow parallel evolving populations to explore similarly suited targets, generating particular interactions in some clones. Here, variability between individual clones' interaction networks (Fig.3.3) can again be related to the size and diversity of genomic resistance determinants for each antibiotic, and, further, hint at the prevalence of tradeoffs between general and specific resistance mechanisms.

Cohesive interaction patterns involving over half of the clones in a set include the cross-resistance of AMK-evolved strains to IMP, the reciprocal cross-resistance of CTX and NFX, and the overall non-interactivity of FOS clones (discussed above, Fig. 3.2). Some interactions do not rise to the level of significance but match the overall trend of the significant ones. Aggregated interactions match the general paradigm of a relationship between specificity of the resistance mechanism and evolutionary

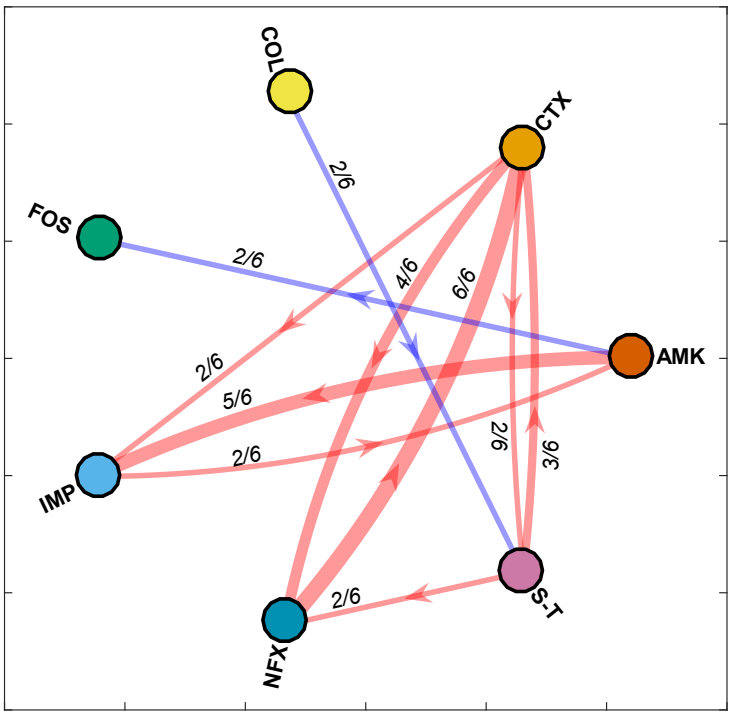

FIGURE 3.2: **Evolutionary interactions between antibiotics.** Network representing the general trends of the evolutionary interactions between antibiotics. Evolutionary interactions are defined as the log2-fold change in MIC of each clone adapted to a given antibiotic, to all other antibiotics, compared to control isolates. Nodes represent the different antibiotics. A directed edge from one antibiotic to another represents their interaction frequency, as the proportion of clones adapted to the first antibiotic that exhibit increased or decreased(respectively, *cross-resistance*, red lines and *cross-sensitivity*, blue lines) resistance to the second. Edge width represents interaction frequency; this value is also reflected above each edge for clarity. Unique interactions in a clone set are removed. This type of network is often used in evolutionary interaction studies, and presents the aggregated information of all clones adapted to the same antibiotic. Interactions of each individual clone are itemized in an ensuing figure.

TABLE 3.2: **Resistance and evolutionary interaction features of evolved isolates.** Clones are identified by the trajectory antibiotic and numbers 1-6. For each clone we include the *wild type* ancestor MIC to the selection antibiotic, the antibiotic dosage from which it was isolated (see Fig. 3.1), the acquired MIC in the selection antibiotic, and the number of evolutionary interactions with the remaining antibiotics.

Clone	Initial MIC (mg/L)	Isolation dose (mg/L)	Acquired MIC (mg/L)	No. interactions
FOS1	16	2048	4096	0
FOS2	16	2048	2048	0
FOS3	16	2048	1024	0
FOS4	16	2048	512	0
FOS5	16	2048	512	0
FOS6	16	2048	512	0
AMK1	8	1024	128	0
AMK2	8	1024	256	1
AMK3	8	1024	64	1
AMK4	8	1024	128	2
AMK5	8	1024	64	2
AMK6	8	1024	128	1
COL2	0.5	64	2	3
COL3	0.5	64	4	0
COL5	0.5	64	8	0
COL6	0.5	64	4	1
NFX1	0.125	16	8	3
NFX3	0.125	16	16	1
NFX6	0.125	16	16	2
CTX2	0.125	8	1	0
NFX2	0.125	8	8	1
NFX4	0.125	8	8	2
NFX5	0.125	8	8	2
S-T1	0.5	8	16	2
S-T2	0.5	8	8	2
CTX5	0.125	4	1	0
CTX1	0.125	2	1	1
CTX3	0.125	2	1	2
CTX4	0.125	2	1	3
CTX6	0.125	2	2	3
S-T3	0.5	2	4	0
S-T4	0.5	2	4	0
S-T5	0.5	2	8	0
S-T6	0.5	2	2	0
IMP1	0.25	1	1	2
IMP2	0.25	1	1	0
IMP3	0.25	1	1	0
IMP4	0.25	1	1	1
IMP5	0.25	1	1	0
IMP6	0.25	1	1	0
COL1	0.5	0.5	0.25	0
COL4	0.5	0.5	0.25	0

interactivity. However, in most clone sets there are low frequency interactions that could have relevant implications for evolutionary dynamics and clinical outcomes.

The pattern of interactions of CTX isolates exemplifies this increased complexity observed at the individual clone level. Their interaction pattern is largely coherent with pre-existing literature on antibiotic resistance: a predominance of cross-resistance to drugs against which the same general mechanisms (increased efflux, decreased permeability) have been described. This clone sets has the highest number of interactions per interacting clone (mean=2.25, details in Table 3.2), and most are to NFX, IMP, SMX/TMP fitting the strategy of decreasing intracellular antibiotic levels. Nevertheless, clone CTX6 presents an unusual, if moderate, resistance to AMK (MIC fold increase = 2; clones CTX1, 3 and 4 exhibit the same interaction below the threshold of significance). This, like the cross-resistance of AMK clones to IMP, seems to contradict other evolutionary interaction studies and should be further explored.

In SMX/TMP clones, the administered drug combination possibly shifted the main resistance determinant from highly specific to general, which could explain the diversification of interactions. 2 of the 3 clones that developed cross-resistance to CTX also acquired it against NFX. These are the two isolates obtained later in the evolution experiment, meaning they probably underwent a stronger selective process. Surprisingly, the other SMX/TMP interacting clone, S-T6, did not show an increase in SMX/TMP MIC. This would typically be interpreted as it not having undergone evolution, and yet it is cross-resistant to CTX. Perhaps the population went extinct before the nonspecific CTX cross-resistance-conferring mutation(s) could be adequately refined against SMX/TMP.

The IMP clone collection shows little interactivity, which is congruent with its early isolation (Fig. 3.2) and low levels of acquired IMP resistance (Fig. 3.1B). Nevertheless, clone IMP5 developed strong (MIC fold increase = 4) cross resistance to AMK. Yet another clone, IMP1, is very strongly resistant to FOS (MIC fold increase = 6). That is, in a population with moderate resistance against IMP there exists the potential for high tolerance of other antibiotic classes, which are of particular importance given that both fosfomycin and aminoglycosides have been suggested as last-line treatment against carbapenemase-carrying bacteria [148].

Because 2 of the 6 COL clones where isolated very early, it is trivial to explain their lack of resistance and interactions (Table 3.2). The other 4 clones tend towards increased sensitivity to SMX/TMP, as was previously detailed, but one particular clone (COL2) also developed cross-sensitivity to IMP (fold decrease = -2) and cross-resistance to CTX (fold increase = 2). This is the only COL clone with significant resistance to other antibiotics. Together these observations and the adaptation trajectory (Fig. 3.1) could be explained by a specific colistin resistance mechanism with

pleiotropic tradeoffs, which is nevertheless compatible with particular mutations that increase resistance to other drugs.

Although FOS clones did not acquire interactions with other antibiotic classes, selected clones from other sets do interact with this antibiotic. Two AMK clones (AMK4, AMK5) and one NFX clone (NFX1) show increased sensitivity to fosfomycin, while one IMP clone (IMP1) and another NFX clone (NFX6) developed cross-resistance. While cross-resistance to fosfomycin is rare, both interactions are among the strongest (MIC fold increase = 6) and the level of acquired resistance is comparable to FOS clones. That is, even though fosfomycin has an idiosyncratic uptake pathway-where commonalities usually lead to cross-resistance-, significant collateral resistance can be developed against it.

The NFX clone set is the most interactive (6/6 clones possess significant interactions, for a combined total of 11 interactions; both are the highest values in the whole clone collection, details in Table 3.2). It also exhibits the highest variability in terms of clones with unique interactions: aside from the global CTX resistance, clone NFX1 is sensitive to FOS and IMP (both with MIC decrease = -2), NFX4 is sensitive to AMK (MIC decrease = -2), NFX5 is resistant to COL (MIC increase = 3), and NFX6 is highly resistant to FOS (MIC increase = 6). Notably, the interaction of NFX5 is the only instance of collateral resistance to colistin. Furthermore, this clone shows evidence that in parallel trajectories of adaptation to antibiotic it is possible to acquire both cross-sensitivity and cross-resistance to the same drug (FOS, in this case). One explanation is the acquisition of specific mutations along or within a large predominant mutational target (producing in this case generalized CTX resistance), such as compensatory mutations, or combinations that are only available to selection through epistasis. These low probability events could translate into vastly different outcomes.

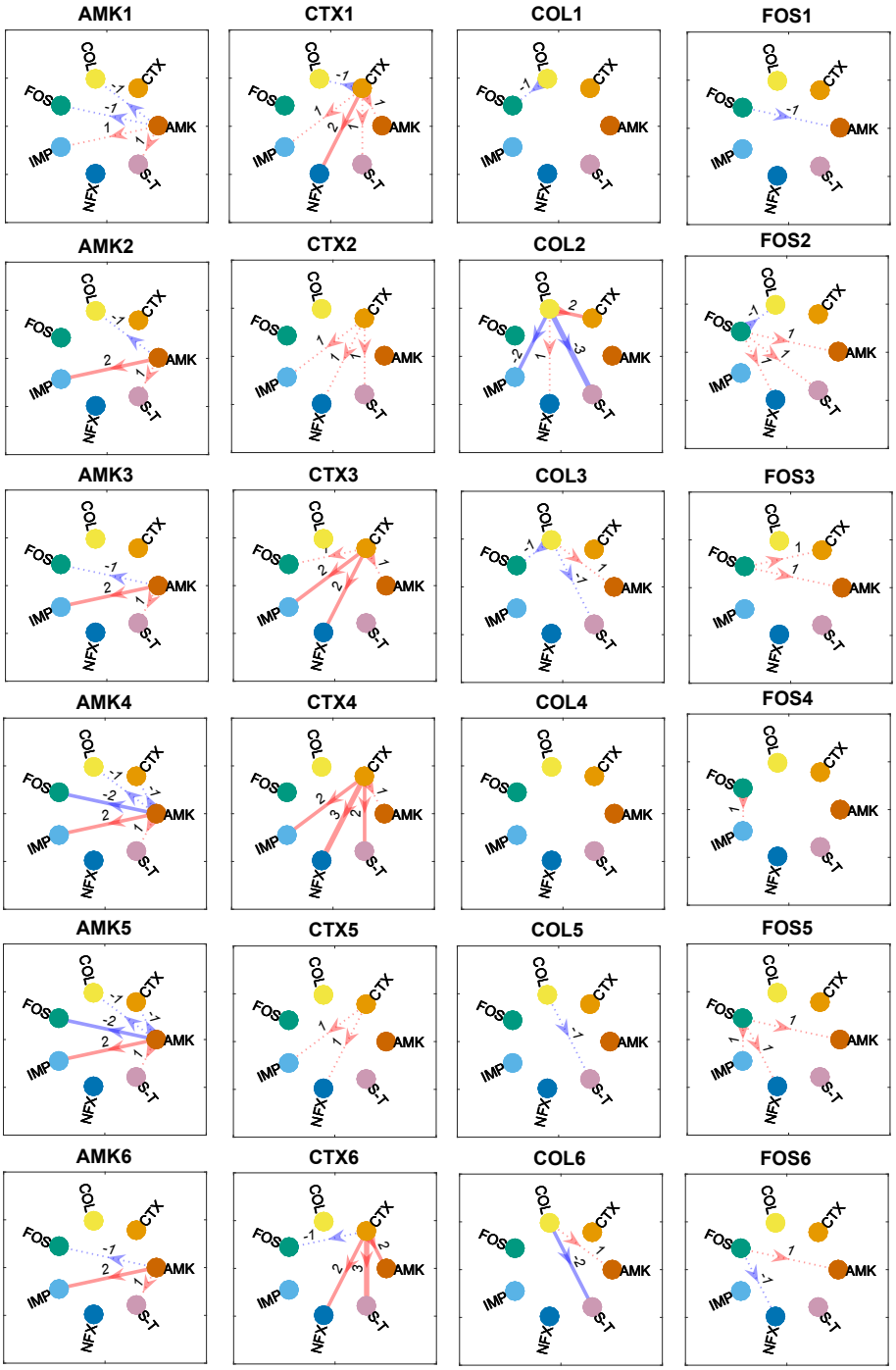

FIGURE 3.3: **Evolutionary interaction networks of individual clones.** (continues in next page)

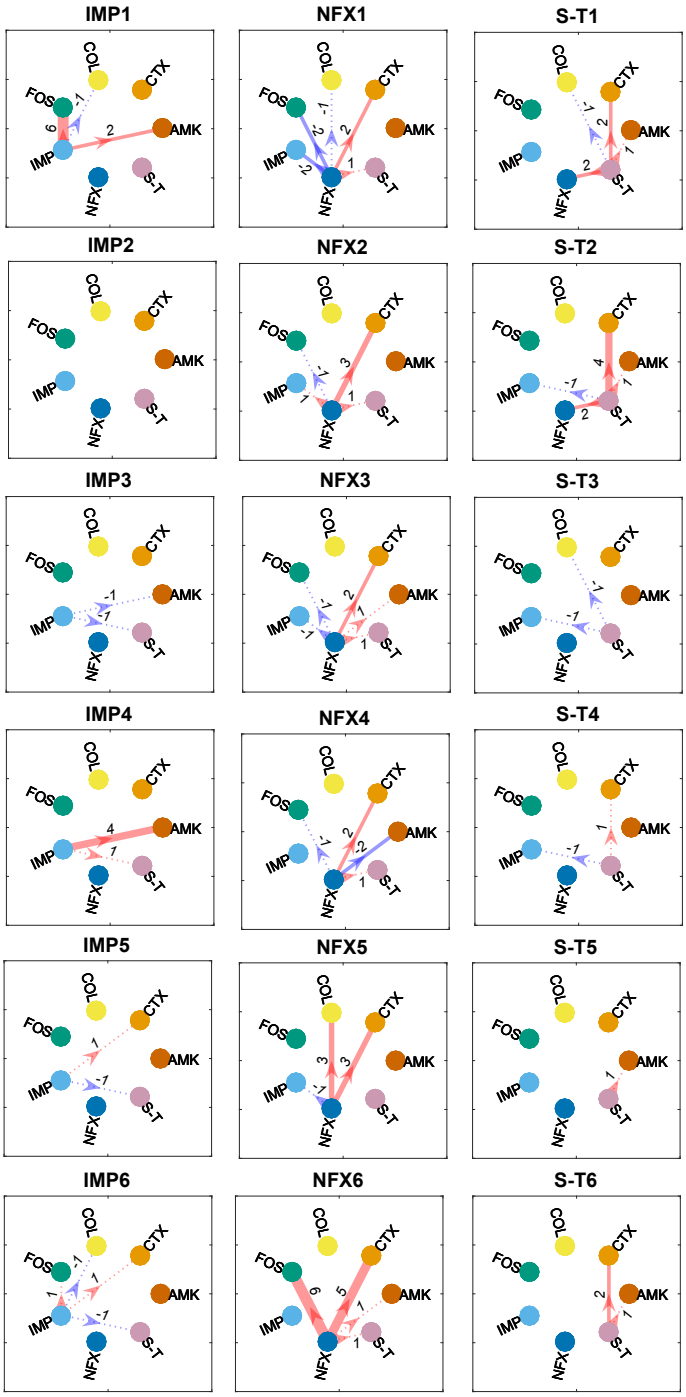

FIGURE 3.3: **Evolutionary interaction networks of individual clones.** Cross-resistance (red lines) and cross-sensitivity (blue lines) of each individual isolate to the remaining antibiotics. Nodes represent antibiotics, and edges represent interactions between the clone named above each network and all the antibiotics. Edges represent interaction strength (i.e. the log2-fold change in MIC to each drug), and this value is also reflected above each edge; negative values represent a decrease in resistance. Solid edges represent interactions considered significant (MIC log2-fold change of at least 2 in either direction) and dotted edges represent interactions within the experimental error of the measurement, added because of their possible biological entity given interaction trends.

3.4 Discussion

The analysis of these interaction networks built with standard phenotypic measurements of antibiotic resistance allows us to delineate some preliminary conclusions about adaptation to our set of antibiotics, which bear on the question of interaction variability: AMK probably developed an atypical general resistance mechanism (producing cross-resistance to IMP). Both CTX and NFX acquired a general mechanism related to permeability/efflux, more efficient in CTX (producing more interactions with antibiotics tied to this resistance strategy) and accompanied by more specific mutations in NFX producing unique interactions. Resistance in COL is probably due to a specific resistance mechanism with broad tradeoffs that induce cross-sensitivity to other drugs. FOS acquired a highly specific mechanism with few tradeoffs. Mutations in IMP are probably associated to a mechanism of low effectiveness (with some relation to the mechanism of AMP, deviating from previous studies). Finally, SMX/TMP probably developed resistance through a general mechanism similar to CTX and NFX but of lower effectiveness, due to the exclusion of the specific and effective mutations for each drug in isolation.

Interestingly, higher adaptation to the initial antibiotic – measured by a greater increase in MIC – does not necessarily lead to higher interactivity. This was recently remarked in other studies [34]. Further, we wanted to explore how similar are the interaction patterns resulting from adaptation to each antibiotic, and the potential connection to other relevant adaptive properties. We measured interaction variability among a collection of isolates by comparing whole networks (that is, considering both the antibiotics to which sensitivity might be altered and its degree, see *Materials and Methods*) and we additionally observe that acquired resistance is not strongly tied to interaction diversity (Fig. 3.4). FOS and NFX produced some of the most highly adapted clones, and yet they represent the two extremes in the interactivity distribution, with a total of 0 and 11 interactions respectively (Table 3.2) and, again, both extremes in terms of interaction network variability (Fig. 3.4). Furthermore, clone families with consistent levels of acquired resistance, such as AMK, CTX, IMP, and NFX (Fig.3.1) nevertheless encompassed substantial interaction variability. Parallel evolution at the broad phenotypic level, then, was not necessarily a predictor of underlying diversity at the molecular level.

Instead, interactivity seems more closely tied with the specificity of the main resistance mechanism under the particular selection pressure conditions: FOS is characterized by an uptake pathway and molecular target that are unique among the different antibiotic classes, where a small number of mutations dramatically increases tolerance with little fitness cost. On the other hand, protection against NFX and

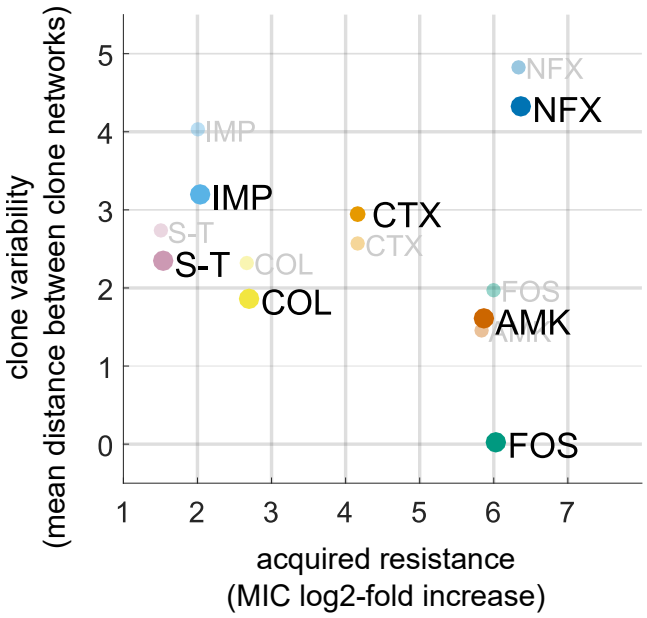

FIGURE 3.4: **Variability in clone interaction networks.** Variability within each antibiotic-adapted clone set is measured by comparing the interaction network of all isolates, considered as vectors where each entry represents the collateral resistance/sensitivity of the isolate against each antibiotic. Variability is then computed as the mean euclidean distance between the interaction networks of all clones in a specific set (*Materials and Methods*). This variability is plotted as a function of the mean level of acquired resistance to the trajectory antibiotic, as another relevant feature of each clone set. The relationship between these two variables is discussed in the main text. Distances are calculated excluding interactions with strength below a log2-fold change of ± 2 (black letters), and including them for comparison (gray)

its main interacting partner CTX can be acquired through the same multidrug resistance determinants, based on generalized reduction of intracellular concentration of toxic compounds. Plausible commonality of this general resistance mechanism, in turn, does not necessarily lead to the same diversity among a family of clones (Fig. 3.4). Here, NFX is again in the lead with multiple unique interactions comprising almost all the remaining antibiotics and in both directions (cross-resistance and cross-sensitivity). This crucial difference can only be discovered by assessing individual clone networks, as these low-frequency but, in some cases, strong interactions are lost in the aggregate networks typically assembled in this type of studies (Fig. 3.2).

Not unexpectedly, most evolutionary interactions are associated to smaller MIC increases than direct adaptation to a given antibiotic (typically 2-fold as opposed to 4-fold, respectively). However, cross-resistance of comparable magnitude to the strongest direct adaptation has been obtained in specific clones: to AMK (in clone

IMP4), CTX (S-T2), and FOS (IMP1 and NFX6) (Fig. 3.3). Remarkably, these individual interactions appeared in clones that showed low levels of adaptation (IMP and S-T), and with an antibiotic with strong interactive isolation (FOS). This could indicate that these interactions are due to chance events, again highlighting the great evolutionary potential hidden in clone diversity.

Evolutionary interactions between antibiotics is a topic of very recent interest. Previous studies [33, 135] found both cross-sensitivity and cross-resistance were frequent, but the first was largely constrained to one antibiotic class, the aminoglycosides (the mechanistic reasons are discussed in *Results*). Mutational similarities, a proportion of which affected the cellular subsystems discussed here involving cell permeability, underlied a substantial part of the observed cross-resistance patterns. In [34], evolutionary interaction networks obtained under weak and strong selection pressures were compared, observing greater interactivity in the latter. Antibiotics inducing more evolutionary interactions were associated to an enrichment in what we term here both specific and nonspecfic mutations (referred therein as "in-pathway" and "off-pathway", respectively). On the other hand, antibiotics exhibiting little cross-resistance lacked these off-pathway mutations. These studies by design focus on the shared mutations and have been tremendously useful in identifying common mechanisms and mutational profiles that lead to cross resistance and, crucially, cross sensitivity. Both [33, 34] report an increased susceptibility to many other antibiotic classes after adaptation to aminoglycosides, and another study [32] successfully applied this effect to avoid the development of concerning resistance by administering these drugs cyclically.

The authors in [33, 135] note that antibiotic adaptation seems to generally proceed through a diverse set of mutations in a set of functional units shared among many antibiotics. These results are reinforced in [34] and our discussion of the interactions of NFX and CTX follows the same logic. Some details concerning specific drug classes are worth mentioning. In [135] they also encounter that adaptation to fluoroquinolones (ciprofloxacin and nalixidic acid in their case) produced some of the highest degrees of cross-resistance; these antibiotics have available highly efficacious specific (eg.*gyrA*) and nonspecific (eg. *acrAB*) resistance mutations. Alternatively, in [34] they classify the folic acid synthesis inhibitors sulfamonomethoxine, sulfamethoxazole and trimethoprim in the low interaction category; by applying them in combination we possibly forced evolution through a more general mechanism that increases interactivity. In [32] colistin exhibits an interaction pattern largely composed of cross-sensitivities, matching our observations; and fosfomycin presents low levels of cross-resistance overall, which combined with the high adaptation and low interactivity described here provides an interesting alternative type of trajectory. These authors specifically notice that antibiotics belonging to the same

class can nevertheless interact in remarkably different ways, as is the case of CTX and IMP here.

Our main interest, however, is a preliminary evaluation of the variability of evolutionary interactions beneath the class-level assessments previously discussed. While the two studies covering evolutionary interactions most directly [34, 135] do not address this issue, both comment on the related question of parallel evolution in antibiotic resistance. Authors in [135] report high parallelism at the level of sites, genes, and functional units, with many mutations shared across different antibiotics. For instance, one specific aminoacid change in acrB (part of the AcrAB-TolC complex) was found in four lines adapted to chloramphenicol, ampicillin and cefoxitin; and as many as 66% of the genes mutated in parallel were observed in lines adapted to different drugs. The proportion of shared mutations diverged between different antibiotic-adapted lines, where overlap correlated with the described levels of cross-resistance. In [34], in turn, authors highlight the greater diversity of drug-specific mutations in lines evolved under strong selection pressure. They note that mutations found in two populations adapted to the same antibiotic do not necessarily coincide, where repeatability again varies among drug classes being highest for quinolones and folic acid inhibitors. Because many antibiotics, despite differences in the molecular mechanism, converge in the subcellular systems damaged and activated as a response, it is not surprising that there exists substantial convergent evolution. However, substantial parallel evolution is not at odds with the appearance of particular mutations that accompany the shared ones. We specifically explore how these unlikely or chance-driven events can introduce functional diversity in a bacterial population that analyses of aggregate networks cannot capture.

A very recent study explored the influence of alternative adaptation trajectories on the development of evolutionary interactions between antibiotics in *P. aeruginosa* [35]. Not insignificantly, they do not report the generalized aminoglycoside-evolved cross-sensitivity that the studies done in *E.coli* showed. Instead, they obtain some instances of cross-resistance and cross-sensitivity only against penicillins. Some of the contrasting interactions in clones adapted to the same antibiotic that we describe here (e.g. cross-resistance and cross-sensitivity to FOS in NFX lines) were observed here as well; for instance, in 10 populations adapted to cefsulodin (a cephalosporin) 3 acquired resistance to gentamicin while other 5 acquired sensitivity. Using a clustering approach on phenotypic interaction patterns and genotypic changes the authors were able to tie specific mutations to both resistance to the antibiotic on which they arose and collateral sensitivity to others. These mutations appeared in genes related to the regulation of efflux and other membrane organization processes and mediated cross-sensitivity between the aminoglycosides gentamicin and streptomycin and the

penicillins carbenicillin and piperacillin-tazobactam. Nevertheless, this highly specific association was only described for a small number of gene variants and the study acknowledges that much of the variability remains to be explained.

A combination of evolutionary processes could account for the observed diversity and patterns of interaction. One of the effects mentioned above alludes to the size and fitness effects of resistance determinants: general resistance mechanisms can emerge from a variety of combinations of mutations of small effect in broad genomic regions [36]; this explains both the smooth shape of the adaptive trajectory of CTX and NFX and their interactivity. The underlying diversity of mutations that produce this beneficial phenotype could in turn be tied to the diversity of evolutionary interactions in a clone set. Many factors shape this variability, including the genomic architecture of the mutational target and epistatic interactions between mutations. Genomic architecture of the target pathway will determine the availability of mutations that are easily transformed into phenotypic changes, following a hierarchy atop which are loss-of-function mutations [37, 149]. Epistasis, in turn, will introduce constraints in evolutionary trajectories [13] and make them contingent upon the initial mutational steps [14, 38]. Alternative pathways of equal levels of adaptation can be found, which nevertheless can have different tradeoffs in other conditions [131].

An alternative genetic explanation for mutational diversity is the appearance of hypermutator genotypes (which carry errors in the DNA repair machinery that increase their mutation rate), frequently described in antibiotic resistance [137, 150]. However, because the level of interaction variability is somewhat consistent within a clone family, hypermutators do not seem the most likely candidates to explain it.

The extracellular medium plays a role too: combining an evolution experiment with *in silico* metabolic modeling, researchers found that resistance to antibiotics arose more readily in glucose than in acetate medium, due to the greater plasticity of respiro-fermentative metabolism in the former [151]. Of note,this study also finds increased sensitivity to fosfomycin only in ampicillin-glucose evolved clones, suggesting metabolic rewiring as another relevant factor shaping evolutionary interactions between antibiotics.

Then, the size and fitness effects of genomic resistance determinants; the availability of beneficial mutations; epistasis between them and between compensatory mutations, and metabolic tradeoffs all combine to produce this complex landscape of interactions.

Our work deviates from the three studies of evolutionary interactions in *E. coli* discussed above in one important way: we did not observe cross-sensitivity in aminoglycoside-evolved clones (all three studies, and ours, include amikacin); instead we find cross-resistance to a carbapenem. Differences between our study and

others can be attributed to the selection of specific drugs in a class (discussed in [32]), the effect of the culture medium [151, 152], differences in the genetic background of the bacterial ancestor [15] (even when the same strain is used as in [32, 34]; in [33, 135] another *E. coli* strain was chosen) and the particular features of the evolution protocol such as the size of the dilution bottleneck [153] and selection strength [34]. Indeed, a recent study evaluating the effect of previous antibiotic exposure history on further adaptation during drug cycling protocols in *P. aeruginosa* failed to find collateral sensitivity after evolution to the aminoglycoside chosen, tobramycin [154].

We observed that clones isolated in a given antibiotic concentration do not necessarily exhibit MICs matching that value (Table 3.2). Populations can subsist in a high-dosage environment through physiological plasticity, by dedicating a subpopulation of cells to a protective state of dormancy (this phenomenon is know as persistence). Persistence is associated in non-trivial ways to specific antibiotic biochemistry; for instance, it can be activated via the SOS response by fluoroquinolones [155], or inactivated by carbon sources in a way that makes bacterial cells again susceptible to aminoglycosides [152]. Survival to antibiotic can also be achieved by indirect tolerance mechanisms such as adapting the lag phase to exposition time [28] and other adaptive mechanisms with quick reversibility [156].

The experimental technique chosen to measure antibiotic resistance also influences to some extent the obtained interaction network. Phenotypic resistance is typically measured with MIC assays, based on observable bacterial growth in an antibiotic gradient. Other evolutionary interaction studies specifically discuss choosing an alternative, more sensitive method based on optical density to measure resistance [33, 135]. We utilized a standard MIC assay because it is the most widespread technique, with well-defined protocols [138] and substantial data to make rough comparisons across studies (see EUCAST). However, it must be noted that the sensitivity of the technique combined with differences in the ecological context in which resistance is measured means that some portion of the evolutionary interaction network might remain cryptic.

In sum, the full scope of evolutionary interactions between antibiotics is far from being elucidated, and this preliminary work and the recent study in *P. aeruginosa* discussed above [35] emphasize the fundamental importance of parallelism and variability in these evolutionary processes. Just one mutation, or a more complex but equally low-frequency event, can define the nature of an evolutionary interaction -resistance or sensitivity- and thus alter the landscape for the design of rational drug treatments.

Future directions

The results presented here reflect a work in progress where the logical next step is the sequencing of all evolved clones. The smaller sample size compared to other work (which nonetheless captures both global trends and significant variability) allows the direct, itemized comparison of mutations. It also makes feasible individualized phenotypic tests to elucidate the molecular underpinnings of interactions, in terms of pleiotropy and tradeoffs. Tests include assessment of changes in membrane integrity and potential (as in [33]), competition assays (eg. between clones that exhibit the same MIC to a certain antibiotic, one by direct adaptation and the other through cross-resistance), and alternative resistance measurements that consider the influence of the culture medium and cellular growth stage. The role of epistasis in shaping adaptive trajectories is frequently discussed regarding the causes of parallel evolution (see *Introduction*). Presumably, some of the variability in the interactions observed here could be explained by this phenomenon. Our clone set makes feasible the reconstruction of epistatic constraints through the analysis of: 1)frozen timepoints during the evolution experiment, 2)synthetic combination of mutations in endpoint isolates. Broadening the picture, these evolutionary interactions do not only depend on the molecular characteristics of each particular antibiotic but also on the genetic background of the adapted strain. Again, in a clinical context, one genetic component of particular importance is the acquisition of plasmidic antibiotic resistance genes by lateral gene transfer. The existence of this highly specific antibiotic resistance mechanism could bias adaptation to the antibiotic so that the final evolutionary interaction network is altered. Nonspecific genomic resistance mechanisms have been described in coexistence with plasmidic resistance genes in clinical isolates. Consistent application of the conceptual framework of evolutionary interactions would require the incorporation of HGT and phage transduction as modulating forces of natural adaptive trajectories of bacteria.

Discussion

We explore three levels of complexity tied to fundamental questions on biological systems: genotype-phenotype mapping (Chapter 1), eco-evolutionary feedbacks (Chapter 2), and parallel evolutionary processes (Chapter 3). In each we select a type of interaction tightly connected to the broad conceptual question: epistatic interactions between metabolic genes, a social interaction mediated by the production of a bacterial public good, and evolutionary interactions arising from bacterial adaptation to different antibiotics.

We aim to understand general aspects of the fundamental biological process and, crucially, how the understanding of these basic questions is inextricably linked to details of the biological system under study – which again ties to another fundamental biological question: historical contingency. Both lenses, the theoretical concept and the molecular detail, are absolutely indispensable to explain existing biological phenomena. At each level, in turn, the multi-layered features of the biological system interact ultimately shaping its full complexity.

Aside from the overarching theme of understanding essential conceptual questions through interactions at different levels of biological complexity (genetic, ecological, evolutionary), the three projects in this thesis are connected by particular aspects. Epistasis appears as both a tool in defining the genotype to phenotype map and its potentiality for change under genetic perturbation (Chapter 1) and as a force shaping the variability of evolutionary trajectories e.g. through diminishing returns in beneficial mutations [13] as organisms become better suited to an antibiotic pressure, or constraining the paths to more efficient antibiotic- resistance enzymes [38] (Chapter 3).

We explore antibiotic resistance as a property of individuals in the form of selected clones after experimental evolution (Chapter 3), but resistance can be social [157] and in turn social dynamics might help fight infections [158]. Likewise, antibiotic resistance (Chapter 3) can mediated by the metabolic versatility (a concept from Chapter 1) of the evolving species [151]), and metabolism can in turn define the dynamics of a social interaction [159] (such as metabolic prudence in swarming [109]).

Furthermore, throughout this thesis we have focused on microbial organisms – *Saccharomyces cerevisiae* (Chapter1), *Escherichia coli*, (Chapter 2, Chapter 3) *Pseudomonas*

fluorescens (Chapter 2)- but these intertwined basic ecological-evolutionary processes are of equal importance in multicellular organisms and might even provide novel clinical applications against cancer [160]. Microbes appear here both as a model system for these global questions and as subjects of interest in their own right, as the complexity of their impact in human lives, beyond their traditional conception as disease-causing antagonists, is increasingly being recognized in the microbiome [71]. Here, too, aspects of the conceptual framework of this thesis impart valuable insights such as the social relationships (Chapter 2) between gut microbiota [161].

Together, these projects highlight how the study of an interaction in a carefully selected context can manifest properties of the organization of each level of complexity and their interconnection. The dependence on the genetic background of genetic interaction revealed the distributed robustness of catabolism. In a context that combines essentiality and spatial structure, eco-evolutionary feedbacks can turn cheaters of a social interaction into part of the mechanism that preserves cooperation. Social interactions are further contextualized by their molecular implementation, which introduces additional constraints at biophysical and physiological levels. Evolutionary interactions analyzed in the context of a specific type of selection pressures, that is, under a set of specific antimicrobials, exposes how the architecture of genomic resistance determinants introduces varying diversity. This if anything strengthens the motivation for this multidisciplinary thesis, as emphasis on the interrelations between all aspects and layers of biological processes.

Conclusions

1. In an *in silico* reconstruction of *Saccharomyces cerevisiae* metabolism, epistatic interaction networks change in response to single deletions of active genes by rewiring predominantly weak, positive interactions connecting different functional modules. This pattern reflects the distributed robustness of catabolism.

2. Accumulation of neutral deletions in the yeast metabolic model results in an increase in negative interactions and essential genes as well as reduced environmental plasticity. This reveals a reduction in buffering mechanisms and the functional connection between genetic and environmental robustness.

3. In a microbial social community studied combining simulations and experiments on a synthetic interaction implemented in *Escherichia coli*, eco-evolutionary feedbacks mediated by essentiality of the public good and spatial structure translate population collapse induced by cheater invasions into the recovery of cooperators.

4. Features of the experimental system concerning the growth stage of bacterial cells and the emergence of spontaneous mutants introduce interacting secondary effects on the population dynamics.

5. Single-cell imaging of populations of *Pseudomonas fluorescens* SBW25 identified a novel phenotype regarding the subcellular distribution of a molecule that can behave as a public good: polar localization of the siderophore pyoverdin, which entails potential implications for the social dynamics of the bacteria.

6. Assessment of collateral resistance and sensitivity between evolutionary trajectories in the adaptation of *Escherichia coli* to a variety of antibiotics showed substantial interaction diversity unequally distributed among drug classes, including opposite trends within the same selection conditions. This highlights the importance of parallel evolutionary processes in the design of next-generation clinical protocols against the challenge of global antibiotic resistance.

Conclusiones

1. En un modelo *in silico* del metabolismo de *Saccharomyces cerevisiae*, las redes de interacción epistática se modificaron en fondos genéticos generados por deleción de genes metabólicamente activos. Los cambios ocurrieron predominantemente en interacciones débiles y positivas, que conectan diferentes módulos funcionales, reflejando la robustez distribuida del catabolismo.

2. En fondos genéticos generados por la acumulación de deleciones neutrales se observó un incremento de las interacciones negativas y el número de genes esenciales, así como una reducción en la plasticidad ambiental del modelo metabólico. Estos cambios revelan una reducción en los mecanismos de amortiguamiento, y a su vez manifiesta la relación funcional entre robustez genética y ambiental.

3. En una comunidad microbiana social, estudiada mediante una comibinación de simulaciones y experimentos que implementan una interacción sintética en *Escherichia coli*, la retroalimentación entre procesos ecológicos y evolutivos mediada por la esencialidad del bien común y la estructura espacial produjo un efecto contraintuitivo: la invasión de células egoístas indujo un colapso poblacional que se convirtió en parte del mecanismo que preserva el comportamiento cooperativo en dicha comunidad.

4. Características adicionales del sistema experimental, relacionadas con el estado de cremiento de las bacterias y la emergencia de mutantes espontáneos, introducen efectos secundarios en la dinámica de la población.

5. La visualización de células individuales en una población de *Pseudmonas fluorescens* SBW25 permitió la identificación de un nuevo fenotipo definido por la distribución subcelular de una molécula que puede comportarse como un bien común. Se describió la localización en los polos célulares del sideróforo pioverdina, lo cual podría conllevar efectos sustanciales sobre la dinámica social de esta bacteria.

6. La comparación de las resistencias y sensibilidades colaterales desarrolladas tras la adaptación de *E. coli* a un conjunto de antibióticos mostró una importante diversidad. La variabilidad en las interacciones evolutivas es diferente

entre distintas clases de drogas, apareciendo en algunos casos tendencias opuestas dentro del mismo tratamiento selectivo. Estos resultados enfatizan la importancia de considerar procesos evolutivos paralelos en el diseño de protocolos clínicos de nueva generación que se enfrenten al reto global de la aparición de resistencias a antibióticos.

Bibliography

1. Phillips, P. C. Epistasis–the essential role of gene interactions in the structure and evolution of genetic systems. *Nature Reviews Genetics* **9,** 855–67 (2008).
2. Wagner, A. Robustness and evolvability: a paradox resolved. *Proceedings of the Royal Society B: Biological Sciences* **275,** 91–100 (2008).
3. Masel, J. & Trotter, M. V. *Robustness and evolvability* 2010.
4. Lawrence, D. *et al.* Species interactions alter evolutionary responses to a novel environment. *PLoS Biology* **10,** e1001330 (2012).
5. Guantes, R., Benedetti, I., Silva-Rocha, R. & de Lorenzo, V. Transcription factor levels enable metabolic diversification of single cells of environmental bacteria. *The ISME Journal,* 1–12 (2015).
6. Schoener, T. W. The newest synthesis: understanding the interplay of evolutionary and ecological dynamics. *Science* **331,** 426–9 (2011).
7. Smallegange, I. M. & Coulson, T. Towards a general, population-level understanding of eco-evolutionary change. *Trends in Ecology & Evolution* **28,** 143–148 (2013).
8. Sánchez, A. & Gore, J. Feedback between population and evolutionary dynamics determines the fate of social microbial populations. *PLoS Biology* **11,** e1001547 (2013).
9. Hardin, G. The tragedy of the commons. *Science (New York, N.Y.)* **162,** 1243–8 (1968).
10. Tarnita, C. E. The ecology and evolution of social behavior in microbes. *Journal of Experimental Biology* **220** (2017).
11. Blount, Z. D., Borland, C. Z. & Lenski, R. E. Historical contingency and the evolution of a key innovation in an experimental population of Escherichia coli. *Proceedings of the National Academy of Sciences of the United States of America* **105,** 7899–906 (2008).
12. Gravel, D. *et al.* Experimental niche evolution alters the strength of the diversity–productivity relationship. *Nature* **469,** 89–92 (2011).
13. Khan, A. I., Dinh, D. M., Schneider, D., Lenski, R. E. & Cooper, T. F. Negative epistasis between beneficial mutations in an evolving bacterial population. *Science* **332** (2011).

14. Jerison, E. R. & Desai, M. M. Genomic investigations of evolutionary dynamics and epistasis in microbial evolution experiments. *Current Opinion in Genetics & Development* **35,** 33–39 (2015).
15. Vogwill, T., Kojadinovic, M. & MacLean, R. C. Epistasis between antibiotic resistance mutations and genetic background shape the fitness effect of resistance across species of Pseudomonas. *Proceedings of the Royal Society B: Biological Sciences* (2016).
16. Kitano, H. Systems Biology: A Brief Overview. *Science* **295** (2002).
17. Oberhardt, M. A., Palsson, B. Ø. & Papin, J. A. Applications of genome-scale metabolic reconstructions. *Molecular Systems Biology* **5** (2009).
18. Kawecki, T. J. *et al.* Experimental evolution. *Trends in Ecology & Evolution* **27,** 547–560 (2012).
19. Orgogozo, V. Replaying the tape of life in the twenty-first century. *Interface Focus* **5** (2015).
20. Costanzo, M. *et al.* The genetic landscape of a cell. *Science* **327,** 425–431 (2010).
21. Chandler, C. H., Chari, S. & Dworkin, I. Does your gene need a background check? How genetic background impacts the analysis of mutations, genes, and evolution. *Trends in Genetics* **29,** 358–366 (2013).
22. Lewis, N. E., Nagarajan, H. & Palsson, B. O. Constraining the metabolic genotype–phenotype relationship using a phylogeny of in silico methods. *Nature Reviews Microbiology* (2012).
23. Duarte, N. C., Herrgård, M. J. & Palsson, B. Ø. Reconstruction and validation of Saccharomyces cerevisiae iND750, a fully compartmentalized genome-scale metabolic model. *Genome Research* **14,** 1298–1309 (2004).
24. Xavier, J. B. Social interaction in synthetic and natural microbial communities. en. *Molecular Systems Biology* **7,** 483 (2011).
25. Chuang, J. S., Rivoire, O. & Leibler, S. Simpson's paradox in a synthetic microbial system. *Science* **323,** 272–5 (2009).
26. Cavaliere, M. & Poyatos, J. F. Plasticity facilitates sustainable growth in the commons. *Journal of the Royal Society, Interface / the Royal Society* **10,** 20121006 (2013).
27. Waite, A. J., Cannistra, C. & Shou, W. Defectors can create conditions that rescue cooperation. *PLoS Computational Biology* **11,** e1004645 (2015).
28. Fridman, O., Goldberg, A., Ronin, I., Shoresh, N. & Balaban, N. Q. Optimization of lag time underlies antibiotic tolerance in evolved bacterial populations. *Nature* **513,** 418–21 (2014).
29. MacLean, R. C. & Buckling, A. The distribution of fitness effects of beneficial mutations in Pseudomonas aeruginosa. *PLoS genetics* **5,** e1000406 (2009).
30. Zhang, X.-X. & Rainey, P. B. Exploring the sociobiology of pyoverdin-producing Pseudomonas. *Evolution* **67,** 3161–3174 (2013).

31. Pál, C., Papp, B. & Lázár, V. Collateral sensitivity of antibiotic-resistant microbes. *Trends in Microbiology* **23,** 401–407 (2015).
32. Imamovic, L. & Sommer, M. O. A. Use of collateral sensitivity networks to design drug cycling protocols that avoid resistance development. *Science Translational Medicine* **5,** 204ra132 (2013).
33. Lázár, V. *et al.* Bacterial evolution of antibiotic hypersensitivity. en. *Molecular Systems Biology* **9,** 700 (2013).
34. Oz, T. *et al.* Strength of selection pressure is an important parameter contributing to the complexity of antibiotic resistance evolution. *Molecular Biology and Evolution* **31,** 2387–401 (2014).
35. Barbosa, C. *et al.* Alternative Evolutionary Paths to Bacterial Antibiotic Resistance Cause Distinct Collateral Effects. *Molecular Biology and Evolution* **25,** 2865–2871 (2017).
36. Toprak, E. *et al.* Evolutionary paths to antibiotic resistance under dynamically sustained drug selection. *Nature Genetics* **44** (2011).
37. Lind, P. A., Farr, A. D. & Rainey, P. B. Experimental evolution reveals hidden diversity in evolutionary pathways. *eLife* **4** (2015).
38. Salverda, M. L. M. *et al.* Initial mutations direct alternative pathways of protein evolution. *PLoS Genetics* **7,** e1001321 (2011).
39. Junker, J. P. & Van Oudenaarden, A. Every cell is special: Genome-wide studies add a new dimension to single-cell biology. *Cell* **157,** 8–11 (2014).
40. Liberali, P., Snijder, B. & Pelkmans, L. Single-cell and multivariate approaches in genetic perturbation screens. *Nature Reviews Genetics* **16,** 18–32 (2014).
41. Ghosh, S., Matsuoka, Y., Asai, Y., Hsin, K.-Y. & Kitano, H. Software for systems biology: from tools to integrated platforms. *Nature Reviews Genetics* (2011).
42. Alon, U. Network motifs: theory and experimental approaches. *Nature Reviews Genetics* **8,** 450–461 (2007).
43. Estrada, J. & Guantes, R. Dynamic and structural constraints in signal propagation by regulatory networks. *Molecular BioSystems* **9,** 268–284 (2013).
44. Wagner, A. The role of robustness in phenotypic adaptation and innovation. *Proceedings of the Royal Society B: Biological Sciences* **279,** 1249–1258 (2012).
45. Tong, A. H. Y. *et al.* Systematic Genetic Analysis with Ordered Arrays of Yeast Deletion Mutants. *Science* **294** (2001).
46. Lehner, B., Crombie, C., Tischler, J., Fortunato, A. & Fraser, A. G. Systematic mapping of genetic interactions in Caenorhabditis elegans identifies common modifiers of diverse signaling pathways. *Nature Genetics* **38,** 896–903 (2006).
47. Poyatos, J. F. The balance of weak and strong interactions in genetic networks. *PLoS ONE* **6** (2011).

48. Feist, A. M., Herrgård, M. J., Thiele, I., Reed, J. L. & Palsson, B. Ø. Reconstruction of biochemical networks in microorganisms. *Nature Reviews Microbiology* **7,** 129–143 (2008).
49. Orth, J. D., Thiele, I. & Palsson, B. Ø. What is flux balance analysis? *Nature Biotechnology* **28,** 245–8 (2010).
50. Sánchez, B. J. *et al.* Improving the phenotype predictions of a yeast genome-scale metabolic model by incorporating enzymatic constraints. *Molecular Systems Biology* **13,** 935 (2017).
51. Mori, M., Hwa, T., Martin, O. C., De Martino, A. & Marinari, E. Constrained Allocation Flux Balance Analysis. *PLoS Computational Biology* **12** (2016).
52. Snitkin, E. S. & Segrè, D. Optimality criteria for the prediction of metabolic fluxes in yeast mutants. *Genome informatics. International Conference on Genome Informatics* **20,** 123–34 (2008).
53. Wang, Z. & Zhang, J. Abundant Indispensable Redundancies in Cellular Metabolic Networks. *Genome Biology and Evolution* **1,** 23–33 (2009).
54. Segrè, D., DeLuna, A., Church, G. M. & Kishony, R. Modular epistasis in yeast metabolism. *Nature Genetics* (2004).
55. Szappanos, B. *et al.* An integrated approach to characterize genetic interaction networks in yeast metabolism. *Nature Genetics* **43,** 656–662 (2011).
56. You, L. & Yin, J. Dependence of Epistasis on Environment and Mutation Severity as Revealed by in Silico Mutagenesis of Phage T7. *Genetics* **160** (2002).
57. Onge, R. P. S. *et al.* Systematic pathway analysis using high-resolution fitness profiling of combinatorial gene deletions. *Nature Genetics* **39,** 199–206 (2007).
58. Bandyopadhyay, S. *et al.* Rewiring of Genetic Networks in Response to DNA Damage. *Science* **330** (2010).
59. Guénolé, A. *et al.* Dissection of DNA Damage Responses Using Multiconditional Genetic Interaction Maps. *Molecular Cell* **49,** 346–358 (2013).
60. Dixon, S. J. *et al.* Significant conservation of synthetic lethal genetic interaction networks between distantly related eukaryotes. *Proceedings of the National Academy of Sciences of the United States of America* **105,** 16653–8 (2008).
61. Roguev, A. *et al.* Conservation and Rewiring of Functional Modules Revealed by an Epistasis Map in Fission Yeast. *Science* **322,** 405–410 (2008).
62. Ryan, C. J. *et al.* Hierarchical modularity and the evolution of genetic interactomes across species. *Molecular Cell* **46,** 691–704 (2012).
63. Frost, A. *et al.* Functional repurposing revealed by comparing S. pombe and S. cerevisiae genetic interactions. *Cell* **149,** 1339–52 (2012).
64. Greenspan, R. J. *Selection, gene interaction, and flexible gene networks* in *Cold Spring Harbor Symposia on Quantitative Biology* **74** (2009), 131–138.
65. Pál, C. *et al.* Chance and necessity in the evolution of minimal metabolic networks. *Nature* **440,** 667–670 (2006).

66. Deutscher, D., Meilijson, I., Kupiec, M. & Ruppin, E. Multiple knockout analysis of genetic robustness in the yeast metabolic network. *Nature Genetics* **38,** 993–998 (2006).
67. Pedrós-Alió, C. & Manrubia, S. The vast unknown microbial biosphere. *Proceedings of the National Academy of Sciences of the United States of America* **113,** 6585–7 (2016).
68. Gilbert, J. A. & Dupont, C. L. Microbial metagenomics: beyond the genome. *Annual Review of Marine Science* **3,** 347–371 (2011).
69. Ghiglione, J.-F. *et al.* Pole-to-pole biogeography of surface and deep marine bacterial communities. *Proceedings of the National Academy of Sciences* **109,** 17633–17638 (2012).
70. Mira, A., Simon-Soro, A. & Curtis, M. A. Role of microbial communities in the pathogenesis of periodontal diseases and caries. *Journal of Clinical Periodontology* **44,** S23–S38 (2017).
71. Rakoff-Nahoum, S., Coyne, M. J. & Comstock, L. E. An ecological network of polysaccharide utilization among human intestinal symbionts. *Current Biology* **24,** 40–49 (2014).
72. West, S. A., Diggle, S. P., Buckling, A., Gardner, A. & Griffin, A. S. The Social Lives of Microbes. *Annual Review of Ecology, Evolution, and Systematics* **38,** 53–77 (2007).
73. Cavaliere, M., Feng, S., Soyer, O. S. & Jiménez, J. I. Cooperation in microbial communities and their biotechnological applications. *Environmental Microbiology* **19,** 2949–2963 (2017).
74. Waters, C. M. & Bassler, B. L. Quorum sensing: cell-to-cell communication in bacteria. *Annual Review of Cell and Developmental Biology* **21,** 319–46 (2005).
75. Gore, J., Youk, H. & van Oudenaarden, A. Snowdrift game dynamics and facultative cheating in yeast. *Nature* **459,** 253–6 (2009).
76. Cordero, O. X., Ventouras, L.-A., DeLong, E. F. & Polz, M. F. Public good dynamics drive evolution of iron acquisition strategies in natural bacterioplankton populations. *Proceedings of the National Academy of Sciences of the United States of America* **109,** 20059–64 (2012).
77. Branda, S. S., Vik, Å., Friedman, L. & Kolter, R. Biofilms: the matrix revisited. *Trends in Microbiology* **13,** 20–26 (2005).
78. Rainey, P. B. & Rainey, K. Evolution of cooperation and conflict in experimental bacterial populations. *Nature* **425,** 72–4 (2003).
79. Diard, M. *et al.* Stabilization of cooperative virulence by the expression of an avirulent phenotype. *Nature* **494,** 353–356 (2013).
80. Nowak, M. A. Five rules for the evolution of cooperation. *Science* **314,** 1560–3 (2006).

81. Travisano, M. & Velicer, G. J. Strategies of microbial cheater control. *Trends in Microbiology* **12,** 72–78 (2004).
82. Mitri, S. & Foster, K. R. Pleiotropy and the low cost of individual traits promote cooperation. *Evolution* **70,** 488–494 (2016).
83. Wolf, J. B. *et al.* Fitness Trade-offs Result in the Illusion of Social Success. *Current Biology* **25,** 1086–1090 (2015).
84. Schalk, I. J. & Guillon, L. Pyoverdine biosynthesis and secretion in Pseudomonas aeruginosa : implications for metal homeostasis. *Environmental Microbiology* **15,** 1661–1673 (2013).
85. Hannauer, M. *et al.* The PvdRT-OpmQ efflux pump controls the metal selectivity of the iron uptake pathway mediated by the siderophore pyoverdine in Pseudomonas aeruginosa. *Environmental Microbiology* **14,** 1696–1708 (2012).
86. Niehus, R., Picot, A., Oliveira, N. M., Mitri, S. & Foster, K. R. The evolution of siderophore production as a competitive trait. *Evolution* **71,** 1443–1455 (2017).
87. Rainey, P. B., Desprat, N., Driscoll, W. W. & Zhang, X. X. Microbes are not bound by sociobiology: Response to Kümmerli and Ross-Gillespie (2013). *Evolution* **68,** 3344–3355 (2014).
88. Julou, T. *et al.* Cell-cell contacts confine public goods diffusion inside Pseudomonas aeruginosa clonal microcolonies. *Proceedings of the National Academy of Sciences* **110,** 12577–12582 (2013).
89. Koch, H., Frickel, J., Valiadi, M. & Becks, L. Why rapid, adaptive evolution matters for community dynamics. English. *Frontiers in Ecology and Evolution* **2** (2014).
90. Bell, G. & Gonzalez, A. Evolutionary rescue can prevent extinction following environmental change. *Ecology Letters* **12,** 942–948 (2009).
91. Lindsey, H. A., Gallie, J., Taylor, S. & Kerr, B. Evolutionary rescue from extinction is contingent on a lower rate of environmental change. *Nature* **494,** 463–468 (2013).
92. Andrade-Domínguez, A., Salazar, E., del Carmen Vargas-Lagunas, M., Kolter, R. & Encarnación, S. Eco-evolutionary feedbacks drive species interactions. *The ISME Journal* **8,** 1041–1054 (2014).
93. Cavaliere, M. & Poyatos, J. F. Plasticity facilitates sustainable growth in the commons. *Journal of The Royal Society Interface* **10,** 20121006–20121006 (2013).
94. Hammerschmidt, K., Rose, C. J., Kerr, B. & Rainey, P. B. Life cycles, fitness decoupling and the evolution of multicellularity. *Nature* **515,** 75–9 (2014).
95. Diederich, L, Rasmussen, L. J. & Messer, W. New cloning vectors for integration in the lambda attachment site attB of the Escherichia coli chromosome. *Plasmid* **28,** 14–24 (1992).

96. Lutz, R. Independent and tight regulation of transcriptional units in Escherichia coli via the LacR/O, the TetR/O and AraC/I1-I2 regulatory elements. *Nucleic Acids Research* **25,** 1203–1210 (1997).
97. Silva-Rocha, R. *et al.* The Standard European Vector Architecture (SEVA): a coherent platform for the analysis and deployment of complex prokaryotic phenotypes. *Nucleic Acids Research* **41,** D666–75 (2013).
98. Archetti, M. & Scheuring, I. Review: Game theory of public goods in one-shot social dilemmas without assortment. *Journal of Theoretical Biology* **299,** 9–20 (2012).
99. Foster, P. L. Methods for determining spontaneous mutation rates. *Methods in Enzymology* **409,** 195–213 (2006).
100. Edelstein, A., Amodaj, N., Hoover, K., Vale, R. & Stuurman, N. Computer Control of Microscopes Using μManager. *Current Protocols in Molecular Biology* **92,** 14.20.1–14.20.17 (2010).
101. Van Dyken, J. D. *et al.* Spatial Population Expansion Promotes the Evolution of Cooperation in an Experimental Prisoner's Dilemma. *Current Biology* **23,** 919–923 (2013).
102. Byers, J. T., Lucas, C., Salmond, G. P. C. & Welch, M. Nonenzymatic turnover of an Erwinia carotovora quorum-sensing signaling molecule. *Journal of Bacteriology* **184,** 1163–71 (2002).
103. Garneau-Tsodikova, S. & Labby, K. J. Mechanisms of resistance to aminoglycoside antibiotics: overview and perspectives. *MedChemComm* **7,** 11–27 (2016).
104. Moon, C. D. *et al.* Genomic, genetic and structural analysis of pyoverdine-mediated iron acquisition in the plant growth-promoting bacterium Pseudomonas fluorescens SBW25. *BMC Microbiology* **8,** 7 (2008).
105. Gasser, V., Guillon, L., Cunrath, O. & Schalk, I. Cellular organization of siderophore biosynthesis in Pseudomonas aeruginosa: Evidence for siderosomes. *Journal of Inorganic Biochemistry* **148,** 27–34 (2015).
106. Datta, M. S., Korolev, K. S., Cvijovic, I., Dudley, C. & Gore, J. Range expansion promotes cooperation in an experimental microbial metapopulation. *Proceedings of the National Academy of Sciences of the United States of America* **110,** 7354–9 (2013).
107. Kerr, B., Neuhauser, C., Bohannan, B. J. M. & Dean, A. M. Local migration promotes competitive restraint in a host–pathogen 'tragedy of the commons'. *Nature* **442,** 75–78 (2006).
108. Turner, P. E. & Chao, L. Escape from Prisoner's Dilemma in RNA Phage Φ6. *The American Naturalist* **161,** 497–505 (2003).
109. Xavier, J. B., Kim, W. & Foster, K. R. A molecular mechanism that stabilizes cooperative secretions in Pseudomonas aeruginosa. *Molecular Microbiology* **79,** 166–79 (2011).

110. Ghoul, M. & Mitri, S. The Ecology and Evolution of Microbial Competition. *Trends in microbiology* **24,** 833–45 (2016).
111. Davis, B. M. & Waldor, M. K. Establishing polar identity in gram-negative rods. *Current Opinion in Microbiology* **16,** 752–759 (2013).
112. Güvener, Z. T., Tifrea, D. F. & Harwood, C. S. Two different Pseudomonas aeruginosa chemosensory signal transduction complexes localize to cell poles and form and remould in stationary phase. *Molecular Microbiology* **61,** 106–118 (2006).
113. Laloux, G. & Jacobs-Wagner, C. How do bacteria localize proteins to the cell pole? *Journal of Cell Science* **127** (2013).
114. Govindarajan, S., Nevo-Dinur, K. & Amster-Choder, O. Compartmentalization and spatiotemporal organization of macromolecules in bacteria. *FEMS Microbiology Reviews* **36,** 1005–1022 (2012).
115. Eldar, A. & Elowitz, M. B. Functional roles for noise in genetic circuits. *Nature* **467,** 167–173 (2010).
116. Schalk, I. J. *et al.* Iron-free pyoverdin binds to its outer membrane receptor FpvA in Pseudomonas aeruginosa: a new mechanism for membrane iron transport. *Molecular Microbiology* **39,** 351–361 (2001).
117. Bush, K. *et al.* Tackling antibiotic resistance. *Nature Reviews Microbiology* **9,** 894–896 (2011).
118. MacLean, R. C., Hall, A. R., Perron, G. G. & Buckling, A. The population genetics of antibiotic resistance: integrating molecular mechanisms and treatment contexts. *Nature Reviews Genetics* **11,** 405–414 (2010).
119. Crofts, T. S., Gasparrini, A. J. & Dantas, G. Next-generation approaches to understand and combat the antibiotic resistome. *Nature Reviews Microbiology* **15,** 422–434 (2017).
120. Kohanski, M. A., Dwyer, D. J. & Collins, J. J. How antibiotics kill bacteria: from targets to networks. *Nature reviews. Microbiology* **8,** 423–35 (2010).
121. Breidenstein, E. B. M., de la Fuente-Núñez, C. & Hancock, R. E. W. Pseudomonas aeruginosa: all roads lead to resistance. *Trends in Microbiology* **19,** 419–26 (2011).
122. D'Costa, V. M. *et al.* Antibiotic resistance is ancient. *Nature* **477,** 457–61 (2011).
123. Van Hoek, A. H.A. M. *et al.* Acquired antibiotic resistance genes: An overview. *Frontiers in Microbiology* **2,** 203 (2011).
124. A Blair, J. M., Webber, M. A., Baylay, A. J., Ogbolu, D. O. & V Piddock, L. J. Molecular mechanisms of antibiotic resistance. *Nature Publishing Group* **13** (2014).
125. Hooper, D. C. Mechanisms of Action and Resistance of Older and Newer Fluoroquinolones. *Clinical Infectious Diseases* **31,** S24–S28 (2000).

126. Castañeda-García, A., Blázquez, J. & Rodríguez-Rojas, A. Molecular mechanisms and clinical impact of acquired and intrinsic fosfomycin resistance. *Antibiotics* **2,** 217–36 (2013).
127. Adams, J. & Rosenzweig, F. Experimental microbial evolution: history and conceptual underpinnings. *Genomics* **104,** 393–398 (2014).
128. Weinreich, D. M., Delaney, N. F., DePristo, M. A. & Hartl, D. L. Darwinian Evolution Can Follow Only Very Few Mutational Paths to Fitter Proteins. *Science* **312** (2006).
129. Blank, D., Wolf, L., Ackermann, M. & Silander, O. K. The predictability of molecular evolution during functional innovation. *Proceedings of the National Academy of Sciences of the United States of America* **111,** 3044–9 (2014).
130. Tenaillon, O. *et al.* The Molecular diversity of adaptive convergence. *Science* **335,** 457–461 (2012).
131. Rodríguez-Verdugo, A., Carrillo-Cisneros, D., González-González, A., Gaut, B. S. & Bennett, A. F. Different tradeoffs result from alternate genetic adaptations to a common environment. *Proceedings of the National Academy of Sciences of the United States of America* **111,** 12121–6 (2014).
132. Gompel, N. & Prud'homme, B. The causes of repeated genetic evolution. *Developmental Biology* **332,** 36–47 (2009).
133. Baym, M., Stone, L. K. & Kishony, R. Multidrug evolutionary strategies to reverse antibiotic resistance. *Science* **351** (2015).
134. Yeh, P. J., Hegreness, M. J., Aiden, A. P. & Kishony, R. Drug interactions and the evolution of antibiotic resistance. *Nature Reviews Microbiology* **7,** 460–466 (2009).
135. Lázár, V. *et al.* Genome-wide analysis captures the determinants of the antibiotic cross-resistance interaction network. en. *Nature Communications* **5,** 4352 (2014).
136. Gonzales, P. R. *et al.* Synergistic, collaterally sensitive β-lactam combinations suppress resistance in MRSA. *Nature Chemical Biology* **11,** 855–861 (2015).
137. Couce, A., Rodríguez-Rojas, A. & Blázquez, J. Bypass of genetic constraints during mutator evolution to antibiotic resistance. *Proceedings. Biological sciences / The Royal Society* **282,** 20142698– (2015).
138. Wiegand, I., Hilpert, K. & Hancock, R. E. W. Agar and broth dilution methods to determine the minimal inhibitory concentration (MIC) of antimicrobial substances. *Nature Protocols* **3,** 163–175 (2008).
139. Olaitan, A. O., Morand, S. & Rolain, J.-M. Mechanisms of polymyxin resistance: acquired and intrinsic resistance in bacteria. *Frontiers in Microbiology* **5,** 643 (2014).
140. Yin, W. *et al.* Novel Plasmid-Mediated Colistin Resistance Gene mcr-3 in Escherichia coli. *mBio* **8,** e00543–17 (2017).

141. Soo, V. W. C., Hanson-Manful, P. & Patrick, W. M. Artificial gene amplification reveals an abundance of promiscuous resistance determinants in Escherichia coli. *Proceedings of the National Academy of Sciences of the United States of America* **108,** 1484–9 (2011).
142. Jacoby, G. A. Mechanisms of Resistance to Quinolones. *Clinical Infectious Diseases* **41,** S120–S126 (2005).
143. Masi, M. Structure, Function and Regulation of Outer Membrane Proteins Involved in Drug Transport in Enterobactericeae: the OmpF/C – TolC Case. *The Open Microbiology Journal* **7,** 22–33 (2013).
144. Nikaido, H. & Takatsuka, Y. Mechanisms of RND multidrug efflux pumps. *Biochimica et Biophysica Acta* **1794,** 769–81 (2009).
145. Phetsang, W. *et al.* Fluorescent trimethoprim conjugate probes to assess drug accumulation in wild type and mutant Escherichia coli. *ACS Infectious Diseases* **2,** 688–701 (2016).
146. Cassier, P. *et al.* Cephalosporin and fluoroquinolone combinations are highly associated with CTX-M β-lactamase-producing Escherichia coli: a case–control study in a French teaching hospital. *Clinical Microbiology and Infection* **17,** 1746–1751 (2011).
147. Vidaillac, C., Benichou, L. & Duval, R. E. In vitro synergy of colistin combinations against colistin-resistant Acinetobacter baumannii, Pseudomonas aeruginosa, and Klebsiella pneumoniae isolates. *Antimicrobial Agents and Chemotherapy* **56,** 4856–61 (2012).
148. Morrill, H. J., Pogue, J. M., Kaye, K. S. & LaPlante, K. L. Treatment options for carbapenem-resistant Enterobacteriaceae infections. *Open Forum Infectious Diseases* **2,** ofv050 (2015).
149. Chevereau, G. *et al.* Quantifying the determinants of evolutionary dynamics leading to drug resistance. *PLOS Biology* **13,** e1002299 (2015).
150. Woodford, N. & Ellington, M. The emergence of antibiotic resistance by mutation. *Clinical Microbiology and Infection* **13,** 5–18 (2007).
151. Zampieri, M. *et al.* Metabolic constraints on the evolution of antibiotic resistance. *Molecular Systems Biology* **7,** 500–500 (2017).
152. Allison, K. R., Brynildsen, M. P. & Collins, J. J. Metabolite-enabled eradication of bacterial persisters by aminoglycosides. *Nature* **473,** 216–20 (2011).
153. Rozen, D. E., Habets, M. G.J. L., Handel, A. & de Visser, J. A.G. M. Heterogeneous Adaptive Trajectories of Small Populations on Complex Fitness Landscapes. *PLoS ONE* **3,** e1715 (2008).
154. Yen, P. *et al.* History of antibiotic adaptation influences microbial evolutionary dynamics during subsequent treatment. *PLOS Biology* **15,** e2001586 (2017).
155. Dörr, T., Lewis, K. & Vulić, M. SOS response induces persistence to fluoroquinolones in Escherichia coli. *PLoS Genetics* **5,** e1000760 (2009).

156. Motta, S. S., Cluzel, P., Aldana, M., Nikaido, H & Hearst, J. Adaptive resistance in bacteria requires epigenetic inheritance, genetic noise, and cost of efflux pumps. *PLOS ONE* **10,** e0118464 (2015).
157. Lee, H. H., Molla, M. N., Cantor, C. R. & Collins, J. J. Bacterial charity work leads to population-wide resistance. *Nature* **467,** 82–5 (2010).
158. Leggett, H. C., Brown, S. P. & Reece, S. E. War and peace: social interactions in infections. *Philosophical transactions of the Royal Society of London. Series B, Biological sciences* **369,** 20130365 (2014).
159. Boyle, K. E. *et al.* Metabolism and the evolution of social behavior. *Molecular Biology and Evolution* (2017).
160. Korolev, K. S., Xavier, J. B. & Gore, J. Turning ecology and evolution against cancer. *Nature Reviews Cancer* **14,** 371–380 (2014).
161. Rakoff-Nahoum, S., Foster, K. R. & Comstock, L. E. The evolution of cooperation within the gut microbiota. *Nature* **533,** 255–259 (2016).

Appendix A

Appendix - Publication corresponding to Chapter 1

Content available under the following reference:

Djordje Bajić, Clara Moreno-Fenoll, Juan F. Poyatos. Rewiring of Genetic Networks in Response to Modification of Genetic Background. *Genome Biology and Evolution* **6** 12 3267–3280 (2014)

https://doi.org/10.1093/gbe/evu255

Appendix B

Appendix - Publication corresponding to Chapter 2

Content available under the following reference:

Clara Moreno-Fenoll, Matteo Cavaliere, Esteban Martínez-García & Juan F. Poyatos. Eco-evolutionary feedbacks can rescue cooperation in microbial populations. *Scientific Reports*, **7** 42561 (2017)

doi:10.1038/srep42561